CoA. REPORT Aero. No. 192

THE COLLEGE OF AERONAUTICS
CRANFIELD

FURTHER TESTS OF A LAMINAR FLOW SWEPT WING WITH BOUNDARY LAYER CONTROL BY SUCTION

by

R. R. Landeryou and P. G. Porter

CoA Report Aero. No. 192

May, 1966

THE COLLEGE OF AERONAUTICS

CRANFIELD

Further tests of a laminar flow swept wing with boundary layer control by suction

- by -

R.R. Landeryou and P.G. Porter

SUMMARY

Further flight tests have been performed on the Handley Page swept fin having slitted suction surfaces for laminar flow control.

The main object of the tests was to achieve full chord laminar flow at and slightly above a unit Reynolds number of 1.5×10^6 per foot.

Laminar flow was obtained, at the instrumentation position (90% chord) up to a unit Reynolds number of 1.87×10^6 per foot. It was also demonstrated that it was possible to achieve 99% laminarisation of the laminarisable area forward of 90% chord at a unit Reynolds number of 1.58×10^6 per foot.

Complete suppression of leading edge contamination has been demonstrated up to 1.47 times the theoretical critical Reynolds number based on the attachment line momentum thickness.

Investigations have been carried out into the effect of changes in incidence, suction quantity and unit Reynolds number on the chordwise position of transition.

Experimental and calculated boundary layer profiles at the same conditions have been compared and a good correlation between them has been obtained.

A qualitative assessment of environmental and production difficulties likely to be encountered on an aircraft using this system, has also been made.

Prepared under Ministry of Aviation Contract No. KD/18/09/CB63(a)

Footnote: R.R. Landeryou is a member of the Research Department, Handley Page Ltd.
P.G. Porter is a member of the Department of Flight, The College of Aeronautics.

Contents

Notation

C_{D_s}	Equivalent suction pump drag coefficient
C_{D_w}	Wake drag coefficient
C_{D_T}	Total drag coefficient
C_{L_L}	Lift coefficient for station 50 span
C_p	Pressure coefficient
C_Q	Suction quantity coefficient
ΔC_{pi}	Correction to the pressure coefficient
h	Height from the surface - inches
R_c	Chord Reynolds number
Rc	Resistance of Hot Film - ohms
Rcable	Resistance of Hot Film's cable - ohms
U/ν	Unit Reynolds number per ft.
u/U	Velocity ratio in the boundary layer
V_R	Equivalent air speed corrected for instrument correction
ΔV_R	Pressure error correction to be applied to V_R
V_∞	Free-stream speed
x/c	Position - chord ratio
α	Nominal incidence - degrees
y	Overheating ratio for the hot films
Mx/DMF_x	Ratio of mass flow of zone x to the design mass flow of zone x

1. Introduction

When the flight tests of the laminar flow swept fin using the Lancaster aircraft described in reference (1) had been completed, the fin was tested in the 13ft. x 9ft. wind tunnel at R.A.E. Bedford. The main object of these tests was to achieve full chord laminar flow at a unit Reynolds number of 1.5×10^6 per foot at mid-span. For a full description of this work see ref. (2) or ref. (7).

The main objective of the flight test programme, described in this report, was to repeat the wind tunnel results in flight at the same or at higher Reynolds number with the wing in, as far as possible, the same condition as it was in the wind tunnel tests. The secondary objective was to investigate any environmental or operational differences between flight and wind tunnel tests.

The original requirements for the overall flight test programme were as follows:-

1. To demonstrate the suppression of two dimensional and three dimensional instabilities of the laminar boundary layer over the full chord or nearly the full chord of the wing, and to establish the residual wake drag, the overall suction flow rate and the suction distribution required.

2. To investigate the tolerance of the laminar flow fin to incidence changes.

3. To determine the efficiency of a practical slitted surface.

4. To bring to light and, if possible, to investigate any unknown difficulties associated with boundary layer control on such a wing with the type of slitted suction surface adopted.

5. To study the effects of excrescences and surface waviness.

6. To determine the validity of the design methods including theoretical methods for calculating the laminar boundary layer development and stability.

7. To determine the success of the manufacturing techniques and materials and the design features embodied in the wing to influence their further evolution.

8. To investigate the influence of acoustic disturbances on laminar flow.

All the above requirements have been investigated except for the influence of acoustic disturbances on laminar flow. Some of these investigations have been described in the reports of the earlier tests, see ref. (1), (2) and (7).

2. Description of the aircraft, suction system, instrumentation and other equipment used

The laminar flow fin, suction system and ancillary equipment were originally installed on Lancaster PA 474[1]. When this aircraft was grounded, due to the expiration of its engine life, the complete installation was transferred to the Lincoln RF 342. This installation was completed after the Fin was returned from the wind tunnel at R.A.E. Bedford[2]. The internal layout is shown in figure 2.

2.1 The aircraft

The Lincoln RF 342 (see figure 3) was a four engined ex-World War II bomber of larger wing span and fuselage length than the Lancaster. The Lincoln was ideally suited for conversion, as it had been used for de-icing research and already had a facility for the mounting of a dorsal fin.

With the fin installed, the Lincoln could be flown at speeds up to 210 kts. EAS., in level flight, and 240 kts. EAS. in a shallow dive. It was normally flown for test purposes at an altitude of 10,000 ft.

2.2 The fin and suction system

The fin and suction system were not altered between the tests on the Lancaster and on the Lincoln, apart from work on the fin surface and root fence geometry described below. To aid flow visualisation, in the wind tunnel, the surface of the fin was painted black. The first paint finish was replaced, for the second series of wind tunnel tests, by a coat of black "chrome etch" paint. This paint did not readily peel or chip as it had a very good bond with the surface and was only 0.0003" thick. The amount of fin surface waviness was substantially reduced between the two wind tunnel test series. During the course of the second series of wind tunnel tests it was also found that a large amount of separated flow was occurring over the leading edge of the fin root fence. This was prevented by extending the leading edge of the fence and by giving it a small amount of droop. A conical fillet was also added to the fin root leading edge (see reference 2).

As detailed in reference (1), the fin was divided into seven suction zones. The leading edge, forward of 7 per cent chord, formed one zone and, aft of the leading edge, the suction surfaces were divided into inboard, middle and outboard zones on both port and starboard sides. The inboard zones were from station 0 to 40, the middle zones from 40 to 70 and the outboard zones from 70 to 100. These zones were labelled respectively A, B and C (Fig. 1).

The flow was first drawn into the wing through a series of 0.005 inch wide spanwise slits and then into small channels situated beneath the slits. To ensure a more uniform distribution of inflow, the air then passed through throttling holes, into a low velocity compartment. It then passed through the compartment's needle valve, into the zone collector duct. In each of zones A, B and C there were 13 needle valves, the aftmost two valves being ganged together. These needle valves were installed in line, spanwise and were operated by means of 13 sets per side of three concentric tubes. The outer tube of each set operated a valve in zone A, the middle tube operated a valve in zone B and the centre tube operated the zone C valve. Thus it was possible to reduce the number of needle valve actuators to 12 and to situate the actuators in the fin root where they were accessible. They could then be coupled to the valves in any zone to provide fin control of inflow distribution across the chord. Each needle valve was provided with pressure tappings from which the mass flow through each compartment could be measured. The total flow from each zone was passed through a venturi meter, so that the zone mass flow could be measured. The zone mass flows were controlled by hand-operated butterfly valves, fig. 4, situated downstream of the venturi meters.

The flow passed from the butterfly valves into the plenum chambers of the suction engines. Two sets of butterfly valves were installed, so that suction could be applied from either or both of the suction engines. An automatic anti-surge valve was also

installed to prevent the suction engines overheating when the mass flow was reduced too far. This valve admitted air direct, from outside the aircraft, and the engines were started with it open.

The two suction engines were Budworth Mark 1 Gas Turbine units, modified to permit running with a large inlet depression. The Budworth operator's control panel is shown in fig. 5.

2.3 The instrumentation

2.3.1 Manometer and photographic recording system

The 150 tube manometer bank, fig. 6, described in detail in reference 1, was used to set up and monitor zone and compartment mass flows, to give the chordwise pressure distribution at 50% span and to display the readings of total pressure obtained from the pitot combs.

The manometer bank and the observer's A.S.I. and altimeter readings could be photographed, via a mirror, by a remotely controlled camera. Best results were obtained when the camera shutter speed was set at 1/200 sec. with the lens set at f4 and 6.5 ft. range.

2.3.2 Hot film traverse

A system with a carriage carrying a hot film, and capable of traversing in both a chordwise and a spanwise direction on the fin surface, was designed and manufactured by Handley Page Ltd. (Fig. 7). Development of the carriage continued during the second series of wind tunnel tests.

By traversing the carriage in a spanwise direction at a series of constant chord positions it was possible to determine the position of turbulent wedges and transition fronts. This method was used extensively in the subsequent flying programme.

Movement in the chordwise direction was obtained by means of the existing chordwise traversing mechanism, described in reference 1. Chordwise position was displayed inside the aircraft, on a milliameter which was connected to a helical potentiometer located at the mid span trailing edges. (Fig. 8).

The single wedge-type hot film carried on the carriage was sprung onto the surface (Fig. 9). The carriage was attached to and sprung onto the surface by a wire cable running across the span of the fin. To cut down carriage friction drag and to prevent the possibility of surface scratching, a small amount of Polytetrafluorethylene tape was wound around the two points of the carriage in contact with the surface.

At the tip end, the cable was fed through a pulley system to a Tensator motor located at the tip trailing edge. At the root end, the cable was fed through a similar pulley system to a winding handle situated inside the aircraft. The Tensator motor gave a constant tension of 60 lb. on the cable. Spanwise position of the carriage, for a given chordwise position, was determined from a simple digital rev-counter connected to the winding handle. Having calibrated the system, allowing for air loads on the carriage, the hot film could be quickly placed, within an accuracy of 0.50", at any

position between 20% and 60% chord and 20% and 95% span of the surface.

2.3.3 Hot film system

The main type of hot film used in this programme was the glass wedge type with a bevelled tip coated with a film of platinum paint (Fig. 10). The method of manufacture of this type of hot film was detailed in reference 1.

As in reference 1, they were balanced in a Wheatstone bridge to an overheating ratio of 1.30, fig. 11, which was sufficient to give a turbulent signal output of between 2 and 8 mv. peak to peak amplitude, depending on the boundary layer thickness. By using a fairly sensitive oscilloscope, no further amplification was needed. The oscilloscope used was a Balanced Input, Twin Beam type, manufactured by Telequipment Ltd., incorporating two type 43B amplifiers, giving a minimum y - scale of 1 mv/cm. It was normally used at a y - scale of 2 mv/cm and at 10m sec/cm.

The normal hot film operating circuit is shown in detail in figure 12.

Towards the end of the programme the operation of a second type of hot film was investigated. This was the flush hot film, manufactured by R.A.E. Farnborough. Details are shown in figure 13. Three of these films were let into the surface of the fin in the following positions: (1) at the tip of the attachment line, (2) just forward of the porous inspection panel on the starboard surface and (3) at 90% chord, 32% span on the starboard surface. These positions were chosen so that any disturbances arising from faulty installation, or from the leads, would not affect the results obtained from the rest of the instrumentation.

Being flush with the surface, the turbulent input to this type of film was much lower than that to the glass wedge type. Because of this the signals were amplified, using a Tektronix type 122 pre-amplifier, before entering the oscilloscope (see Fig. 14). Details of tests made on a flush hot film of this type are given in Appendix I.

2.3.4 Pitot combs

The results of the R.A.E. Bedford wind tunnel tests[2] indicated that the momentum thickness for a boundary layer, reaching local freestream velocity not more than 0.40" from the surface, could be accurately determined from readings of u/U taken at 0.030" and 0.090" from the surface. The method of determining the boundary layer momentum thickness from these two readings is discussed in section 6.1.2.

The required heights were obtained by soldering together two $1\frac{1}{2}$ mm. hyperdermic tubes, one on top of the other, the lower one being in contact with the surface (Fig. 15a). Fourteen twin pitots were made in this fashion and used at 90% chord during the flying programme.

A further two tubes were added to six combs, at 0.20" and 0.40" from the surface (Fig. 15b), and these were used when manometer space permitted.

2.3.5 Pitot traverse

Towards the end of the programme a pitot, which could be traversed through the boundary layer, was designed and manufactured by Handley Page, and installed at 54% span, 90% chord, on the starboard surface (Fig. 17).

The pitot head was moved by a small geared down electric motor by means of a scimitar-shaped cam, so that the movement rate decreased as the head approached the surface.

The distance of the head from the surface was determined from the output of a helical potentiometer, the wiper of which was geared to the motor. An Avometer was used to read the resistance output. Using the ohms scale of the Avometer it was possible to determine the height of the pitot head from the surface to within 0.0005" when close to the surface and to within 0.0075" when it was about 0.50" from the surface.

2.4 Other equipment

2.4.1 Leading edge bump

The leading edge bump was a simple device, developed by Dr. M. Gaster, to prevent the occurrence of attachment line contamination. A full account of this phenomenum is given in references 1, 2 and 3. It was used successfully in the R.A.E. wind tunnel test (2) up to a theoretical laminar attachment line momentum thickness Reynolds number, $R_{\theta_{a.1}} = 113$, equivalent to a unit Reynolds number, $R = 1.63 \times 10^6$ per foot.

Made of cast araldite, the bump was attached astride the leading edge at 5% span, as shown in figure 18. The bump did not work as well during the initial flights as it had done in the wind tunnel experiment. This was due mainly to the reduced pressure at altitude, causing blow holes to appear in the bump surface. After the surface of the bump was cut back, refilled and polished, it was possible to maintain a stable attachment line up to a theoretical $R_{\theta_{a.1}} = 126$, or at a unit Reynolds number of 2.15×10^6 per foot, without having reached the limit. The incidence tolerance for this device was found to be about $\pm 2\frac{1}{2}^o$ throughout the speed range of the tests.

2.4.2 Leading edge protection against fly and dust deposits

A method of protecting the fin leading edge from fly and dust deposits during take-off and initial climb, was developed from the system used in reference 1.

Basically protection was provided by wrapping a thin piece of Melanex plastic, of 0.002" thickness and cut to shape, around the leading edge zone. Melanex is a polyester film made by Imperial Chemical Industries Ltd. This plastic sheet was then removed, by some means, at a convenient altitude.

On fitting the sheet it was necessary to ensure that there were no leaks at either end. The presence of instrumentation at the tip end and the "Gaster bump" at the root end of the attachment line made it difficult to cover the leading edge slits in these two areas. Hence it was necessary to locally blank off the slits with heavy adhesive tape to prevent leakage. The melanex sheet was tailored so that it fitted with not more than 1/16" margin beyond the aft-most slit covered. If this margin was exceeded, it was possible for the edge of the sheet to lift during taxiing of the aircraft.

Before the main aircraft engines were started, suction was supplied from a small external suction pump connected to the leading edge suction zone via a two-way cock. On starting the port inboard aircraft engine it was possible, by switching over the two-way cock, to obtain suction from the pumps which serve as an emergency supply to the aircraft instrumentation. These normally gave a pressure reduction of 2.25 lb/in^2 below ambient. In some cases it would have been possible for the depression to exceed this value but for a relief valve fitted in the system. The maximum fluorube height available on the manometer was equivalent to 2.4 lb/in^2. The pumps had a low mass flow rating and hence their effectiveness depended upon the degree of leakage that they had to be capable of overcoming. It was found that if the melanex lifted at all when the aircraft was taxiing out to the end of the runway, most of the depression was lost and this lead to the complete loss of the sheet. Because of this, low adhesion masking tape was used to attach the edges of the inboard two-thirds of the sheet to the fin surface. A small amount of tape was also used at the tip end of the melanex. The tape, with the exception of the pieces placed at the tip, was removed by hand after lining-up the aircraft into wind at the end of the runway. Any residue remaining on the fin surface was cleaned off with a cloth soaked in carbon tetrachloride.

Suction was applied continuously during take-off and initial climb, it was generally turned off at about 6,000 ft. which was considered to be above the expected fly and dust zone, or higher depending on the amount and height of the cloud cover.

The Melanex then shredded up on yawing the aircraft alternately to port and starboard. However, a small piece of Melanex often remained covering the leading edge bump. It was also observed, after landing, that small pieces of Melanex were occasionally finding their way into the leading edge slits and causing turbulent wedges and it was thought that this could be prevented if the sheet was shed more quickly, and in larger pieces.

Lengths of rigging chord were therefore attached to the outside face of the Melanex sheet, at the root end and about 50% span on one side. On turning off the suction it was now possible to completely and quickly remove the Melanex by pulling on the cords whilst yawing the aircraft as before.

Although this system worked satisfactorily, it was hoped to develop a fly protection system which would be more suitable in routine operation. With this in mind, a sheet was made up from two pieces of Melanex attached together with "medium tack" double sided adhesive tape along a spanwise lap joint. The lap joint was made to one side of the attachment line with the smaller width panel uppermost. A nylon cord ran along the length of the joint between the adhesive tape and the lower panel. This was then taken through a hole in the root fence, along the top of the fuselage and into the cabin so that when pulled it tended to peel off the outermost panel (see fig. 19).

Shortly after the suction was turned off, the cord was pulled. The uppermost panel was shed immediately, rolling up towards the tip. On yawing the aircraft in the other direction the second panel also shed in the same fashion.

Although more difficult to make than the simple sheet, it was felt that this system was a more commercially viable arrangement.

3. Preliminary flying tests

Before the main flying programme started, tests were carried out to determine the flow field characteristics over the top of the Lincoln fuselage in the plane of the fin and the pressure error correction to be applied to the observer's air speed indicator. After some unsatisfactory laminar flow tests at the start of the main programme with the fin installed, an investigation was also carried out on the flow aft of the cabin canopy at a number of speeds.

3.1 Flow field tests

Reference 6 gives the details of similar flow field tests carried out on the Lancaster PA 474. However these results were of doubtful value due to the short distance between the pressure holes and the leading edge of the supporting pole (a distance to pole chord ratio of 1:1). For the Lincoln tests this ratio was increased to 3:1.

3.1.1 Pressure pole

The pressure pole consisted basically of a 2.50" diameter tube which extended normal to, and passed through, the mid-upper fuselage skin of the aircraft. Inside the fuselage it was attached to the top of the adjacent frame and ended at a splayed foot which was bolted to the fuselage floor. This method of attachment gave a very rigid structure and external bracing was not required. Outside the fuselage the tube was enclosed by an aerodynamic fairing of 6" chord. Five sets of pitot/static probes were attached to the leading edge of the fairing at a pitch of 15". The reference plane of the pitot/static holes was 18" in front of the pole leading edge and 3' 6" aft of the root 25% chord station of the Handley Page Laminar Flow Fin when installed. Neoprene tubing of 5/32" bore was attached to the probes and it was routed down the space between the leading edge fairing and the tube to the manometer bank. The pole can be seen in position in figure 20.

3.1.2 Pressure error correction

Freestream static pressure was recorded by using a trailing static "bomb" suspended from the rear door. At first a standard RAE 7lb. bomb was used. However, it was found that the large dome beneath the fuselage, which housed the Palouste engine used in previous de-icing tests, caused turbulence which caused the cable to whip. This was overcome by replacing the 7lb. bomb by a high-speed type weighing 16lb. The difference between instrument static and freestream static was recorded on a differential pressure gauge. Freestream static pressure was also recorded on the manometer bank.

Freestream total pressure was sensed directly from a pitot-in-venturi situated at the nose of the aircraft. As negligible error is experienced from a source of this type when installed in a conventional manner, no correction was necessary. This reading was also displayed on the manometer bank.

3.1.3 Flow field results

The variation of C_p with height normal to the upper fuselage is given in figure 22. It can be seen that the measured values were very small and that in general the pressure

gradient was negative, although there was a tendency towards a very small positive gradient, of the order of $\partial C_{p/\partial_x} = .001/\text{inch}$, at distances greater than 70" from the skin datum.

The variation in velocity ratio with height normal to the upper fuselage is given in figure 23. It can be seen that in general the velocity distribution varied as little as $\pm$ 1% from the freestream value. A 200 kts. EAS. the total variation was still within 2%, being $\pm \frac{2}{0}$%.

It was also noted that the velocity tended to peak, although to a very small value, at a station 70" away from the skin datum. As the total pressure remained constant at all stations it was felt that this might have been due to the flow from the top of the cabin canopy rather than a propellor slipstream effect.

From figure 21 it is seen that the pressure error correction to be applied to the observer's air speed indicator was very small, varying from zero at 100 kts. EAS. to + 2 kts. at 200 kts. EAS. A check was made on the effect of operating the Budworth suction engines, and no effect was observed. From reference 6 it was inferred that the effect of fin incidence would be negligible.

3.2 Flow aft of cabin canopy

When the fin was initially installed it was not possible to obtain stable flow along the attachment line at any speed. This, combined with the velocity peak observed at 70" from the upper fuselage skin when the pressure pole was installed, led to the belief that turbulent air aft of the cabin canopy was not being contained sufficiently by the fin root fence. It was noticed that there were three whip aerials present just aft of the cabin canopy. Repositioning these aerials aft of the fin increased the attachment line stability speed substantially. However, there remained a lower limit speed of 115 kts. EAS. below which attachment line instability still occurred. This limitation was investigated using a flow visualisation technique.

A paint solution was made up using a suspension of Poster colours in paraffin. Using flexible bottles, as dispensers, different coloured solutions were sprayed from the port, centre and starboard sides of the cabin canopy about half way along its length. This was done at 110 kts. EAS. and 130 kts. EAS. on separate flights. From observations made in flight and after landing it was clearly indicated that the cabin shed two vortices, one from each side. The propellers, rotating in a clockwise direction when looking forward, tended to reinforce the port vortex and reduce the strength of the starboard vortex so that they wound around each other, in the same sense as the propeller rotation. Because of this, the paint shed from the port side of the canopy passed by the starboard fin surface and vice versa. The paint ejected on the cabin centre line tended to remain in contact with the surface and was swept to starboard as it progessed aft.

At 110 kts. EAS. the disturbed flow from the cabin definitely covered the leading edge bump, paint deposits being present up to 10 inches above the root fence on both surfaces. However at 130 kts. EAS., and consequently with the aircraft at a reduced angle of attack, the port and starboard paint solutions remained closer to the fuselage and there was less tendency for them to cross over. Although a few paint specks were evident in the region of the bump, 5 inches above the root fence, they were thought to be due to the natural dispersion of the spray. In this case the majority of the paint was deposited below the bump.

Hence it was concluded that the failure to obtain satisfactory results below a speed of 115 kts. EAS. was due to the inability of the fin root fence to contain vortices shed from the cabin canopy.

4. Experimental flight procedure

4.1 General

Immediately prior to each flight the fin surface was inspected and the Melanex fly and dust protection sheet fitted to the leading edge. With suction applied to the leading edge zone from the instrument pump, the aircraft was taxied out and lined-up into wind at the end of the runway. The "medium tack" masking tape was stripped by hand from the edges of the Melanex sheet and any gummy deposits removed with a cloth dipped in carbon-tetrachloride.

After the aircraft had climbed to about 6,000 ft., or above the cloud level, the leading edge suction was turned off and the Melanex shed by one of the methods described in section 3.4.2.

According to test requirements one or both Budworth suction engines were then started. Only one engine was needed to set up the mass flow for a single surface of the fin. Simultaneously the hot film was switched first to 'preheat', and then to 'run'. If any new films had been installed prior to the flight they were balanced in a Wheatstone bridge to an overheating ratio of 1.30 (see fig. 11). Once set up in this way, it was not necessary to rebalance films on subsequent flights.

With the fin incidence nominally set at zero, i.e. lined up with the centre line of the fuselage, it was necessary for the aircraft to be slightly yawed, nose to port, in order to give a true zero fin incidence. It was possible to determine when the fin incidence was aerodynamically zero by equalising the respective port and starboard flush static pressures, displayed on the manometer bank. A wind vane (fig. 24), was used to display a reading of yaw angle on a microammeter in front of the pilot. After setting up the conditions to give zero aerodynamic fin incidence, the pilot reset the needle of the microammeter to zero using the calibration knob. As the yaw angle needed to set up this condition was very small, it was fairly easy for the pilot to maintain it with reference to the zero setting of the microammeter. Once the microammeter had been set to zero in this way it was usually unnecessary to reset it for subsequent flights.

If reference to the tip hot films showed that the attachment line flow was stable, it was possible to proceed with the planned tests.

4.2 Use of the hot film traverse

The hot film traverse, described in section 2.3.2, was used in the manner described below.

With the fin at zero incidence the aircraft was flown at a constant speed, usually 150 kts. EAS. The zone suction was set up for the surface to be traversed, by means of the butterfly valves, and using the C_Q values found to give the best results in the wind tunnel tests. The compartment needle valves were generally kept at the positions finalised in the tunnel tests.

The carriage was put at a particular chordwise position near the tip. It was then traversed slowly towards the root whilst the hot film signal was monitored using the oscilloscope. Segments of turbulence were marked on a perspex covered plan of the surface being investigated. The plan had a calibration grid drawn on it (see Fig. 25), enabling the tip of the hot film to be located from the readings of the chordwise and spanwise indicators. Having completed one traverse, the carriage was repositioned at another chordwise station and again traversed spanwise. After three or four traverses it was possible to join up the boundaries of the turbulent segments drawn on the plan, so as to define any turbulent wakes. By extrapolating these boundaries forward until they crossed, it was possible to accurately predict the position of the source of turbulence.

After landing, these predicted positions were investigated and the cause of turbulence was eliminated before the next flight.

After minimising the occurrence of turbulent sources on the starboard surface over a number of flights, the traverse was transferred to the port surface and finally removed altogether.

This system helped immensely in the initial tracking down of blocked slits and other imperfections on both surfaces and it would, almost certainly, have been impossible to proceed without its use.

4.3 Instrumentation at 90% chord

As the film at the tip of the hot film carriage could not be traversed aft of about 60% chord, it was necessary to use fixed instrumentation behind this position. This instrumentation comprised twin and four-tube pitot combs (see section 3.3.4), and wedge-type hot films spread along the 90% chord line at about 5" intervals (e.g. see figures 26 and 35). It was felt that this was far enough aft to permit basic conclusions. Further aft the pressure gradient was increasingly affected by the presence of the struts which carried the hot film cables and the pressure tubing for the pitot combs. For reference purposes the static pressure was also measured at the tip and root end of the 90% chord instrumentation.

The pitot comb measurements displayed on the manometer were used for an initial assessment and when a significant area of laminar flow was indicated the hot film outputs were observed and utilised to form a more complete picture. The procedures used are detailed in the following sub-sections.

4.3.1 Minimum boundary layer thickness

Each zone suction was adjusted using the butterfly valves whilst observing changes in the pitot comb pressures on the manometer. A minimum thickness boundary layer was indicated by the pitot pressures approaching to the freestream value. This procedure was usually carried out at zero fin incidence.

4.3.2 Mass flow tolerance

Following the determination of the suction needed for a minimum boundary layer thickness at a particular speed, it was usual to observe the effect of increasing and decreasing the zone mass flow. The simplest way to do this was to change the RPM of the Budworth engines in steps of 100 RPM.

Photographs of the manometer bank were taken for each condition. On analysis these yielded the zone mass flows and the momentum thickness at each of the pitot positions.

The effect of altering the leading edge suction alone was also studied.

4.3.3 Incidence or C_L tolerance

For a particular test speed, the fin was set at zero incidence and the zone suction set up to give the mass flows suggested by the wind tunnel tests. After photographing the manometer bank at this condition the fin incidence was altered via the mechanism shown in figure 27 which was remotely controlled by the pilot. Manometer photographs were taken for 1^{o} increments up to a maximum of 3^{o} either side of zero incidence.

On analysis of the photographs it was possible to determine the zone mass flows and the momentum thickness at each of the pitch positions. The local C_L at 50% span, was obtained from the flush statics at this station. Figure 28 shows the variation of C_L with indicated incidence.

4.3.4 Speed tolerance

The effect of changes in speed, or unit Reynolds number, were studied for two cases. These were (i) constant suction setting and (ii) constant mass flow co-efficient C_Q.

4.3.5 Other investigations

It was noticed that flying near clouds or haze had an effect on the hot film results and this was investigated by flying through clouds and between cloud layers. However, time did not permit a full investigation into this phenomenon and the results obtained were purely of a qualitative nature (see section 7.9).

The operation of the flush hot films (see section 2.3.3) was also investigated in flight.

5. Maintenance

During the flight tests, the surface and slits of the fin suffered from various types of defects. These defects and the methods used to overcome them are detailed below.

5.1 The "Salvage Joints" and the stainless steel to glasscloth joints of the leading edge

The joints referred to as "salvage joints" were butt joints that occurred when sections of the glasscloth leading edge were cut out and reset during initial manufacture. This was necessary due to the de-lamination that occurred during the cutting of the channels for the steel tubes. The stainless steel to glasscloth joints occurred between the stainless steel tube inserts and the fibreglass.

It was found that the adhesive in these joints rose above and fell below the general contour by + 0.001 inches and - 0.004 inches. Greater rises would have occurred if the joints had not been rubbed down when they were proud of the surface. The changes

seemed to be associated with variations in humidity. At times of high humidity the joints rose, and at times of low humidity they fell. The relative humidity change had to be extreme and had to persist for about two days before a noticeable change occurred in the joint lines. After the relative humidity had returned to normal, the joints took about two days to return to the usual contour. If, the fin was left for a long period in the hot sun the joints sank below the surface due to the rapid drying action. Hence the aircraft was not left out on the tarmac any longer than was necessary.

This sensitivity to humidity was thought to be due to the proportions of the araldite mix used to glue the joints. The mix used was 18 parts of 125 Versamid hardener to 10 parts of MY 750 Araldite. At the time of manufacture this was the usual Araldite mixture used in the workshops. However, the proportion of hardener used was higher than the minimum required. This was in order to lower the curing time and make the mixture easier to brush. This procedure is normally quite satisfactory but as the hardener was hygroscopic it absorbed water and hence increased in volume when placed in a high humidity environment. It was found that by keeping the fin out of the sun as much as possible and applying heat to the surface in the hangar, when the relative humidity exceeded 85% for long periods, the changes in contour were minimised and kept within acceptable limits.

5.2 The joint at the attachment of the glasscloth leading edge to the fin

When the fin was manufactured a gap, of approximately 0.1 inches wide and 0.2 inches deep, existed between the leading edge section and the main fin surface. The gap was filled with a conventional cellulose filler and then painted. Unfortunately, this joint required continual maintenance. Before most flights it was necessary to refill sections of the joint. At best the fault would appear as a hair line crack, which still required rubbing down before flying.

It was finally decided to completely refill the joint line on both the port and starboard side of the fin. On removing the old filler it was found that the bottom of the gap contained a non-drying jointing compound. This meant that the filler had no firm foundation to key it. All jointing compound was cleaned out of the gap which was refilled with a two part resin filler. The joint line was then painted over with a two part polyurethane paint. Very little further breaking up of the joint line occurred after the joint was refilled in this manner.

5.3 Slivers in the slits

"Slivers" were originally noticed on the earlier flight tests and, later, in the tunnel tests. They originated from the method of manufacture. When the slits were cut in the panels, it was possible for swarf to be left in the channels under the slits and for small burrs to be left on the underside of the slits. These could subsequently break loose and could then move about inside the channel, eventually getting drawn into the slits, either blocking them or sticking up proud, and triggering off turbulence in the boundary layer.

During the wind tunnel tests this problem was overcome, once the slits were cleared of the slivers, by using a special "run-up" technique. This was to start the tunnel and begin sucking through the slits before a tunnel speed of approximately 40 ft./sec. had been achieved. On occasions when this was not done, slivers appeared in the slits.

In flight this technique could not be used, as it was not permissible to start the Budworth Suction Engines before or during take-off. The procedure was, therefore, to remove slivers when they appeared, and to vacuum slits at stations where a large number of slivers appeared on more than one flight.

The majority of the slivers appeared in the leading edge zone and in the first three slits of the main fin section.

5.4 Slits blocked or partially blocked

On some occasions the slits became locally blocked or partially blocked by a grey powdery substance. Microscopic examinations suggested that this deposit was a mixture containing aluminium dust and carborundum. This was presumably generated by the rubbing down, carried out to reduce the surface waviness during the period between the two wind tunnel test series. A set of specially shaped feelers were used, in conjunction with a vacuum cleaner, to clear the blockages.

5.5 Decrease in slit width

At the commencement of the flight programme a 0.004 inch feeler could be made to pass through all the slits, but during the course of the programme a .0035 inch feeler was found to be tight in some places. These tight slits coincided with turbulent wakes and, after easing the slits to 0.004 inches, the wakes disappeared. On the leading edge, humidity changes appeared to effect the slit width, the slits tending to close up during periods of high humidity.

5.6 Surface defects at countersunk bolt heads

The slight movement of the surface that was noted in the wind tunnel test (2) was not so noticeable during the flight tests. However, on the aft part of the surface a fine crack appeared on the aft side of some bolt heads. The cracks were filled with a two part polyurethane paint.

5.7 Repainting

After having cleared the blockage from a slit, the slit edges were lightly rubbed down and the slit vacuum cleaned. The paint on the slit edge was sometimes chipped, making it necessary to repaint over the slit in order to build up the edges. To help obtain a well defined edge, a length of shim steel was coated with a releasing agent and placed in the slit. It was left standing proud by approximately $1/8$" and the paint was then sprayed onto the chipped slit edges.

When it was necessary to repaint between the slits, e.g. to fill the bolt heads, or build up the 7% joint line, the slits were protected by inserting strips of waxed drawing linen into them. The linen was sufficiently stiff to remain erect so that it did not interfere with the painting of the surface. This technique differed from that used prior to the last series of wind tunnel tests when the complete fin was sprayed black. In the latter case slit protection was obtained by blowing air through the slits.

6. Analysis techniques

6.1 Determination of the momentum thickness of the boundary layer

A simple method was developed for rapidly determining the momentum thickness of the boundary layer from a minimum number of pitot readings. The justification

of the method and its application is outlined below.

6.1.1 Derivation

Consider boundary layer profiles plotted using a log scale for the distance from the surface i.e. log h versus u/U (Fig. 31). This method of presentation has the effect of distinguishing between laminar and turbulent boundary layer profiles. The basis of the method lies in a property of this log plot. Consider the profiles of two similar boundary layers of different thickness, i.e.

$$\left(\frac{u}{U}\right)_1 = f_1\left(\frac{h_1}{\Delta_1}\right) \text{ and } \left(\frac{u}{U}\right)_2 = f_1\left(\frac{h_2}{\Delta_2}\right)$$

When plotted in the above manner the shapes of the profiles remain identical, but one will be displaced, with respect to the other, parallel to the h-axis. Conversely it is possible to establish the existence of similarity by being able to match the two profiles. (Ref. 4).

The momentum thickness $\theta = \int_0^{h=\Delta} \frac{u}{U}\left(1 - \frac{u}{U}\right)dh$ (1)

For similar boundary layer profiles, this yields

$$\frac{\Delta_1}{\theta_1} = \frac{\Delta_2}{\theta_2} \text{ and } \frac{h_1^*}{\theta_1} = \frac{h_2^*}{\theta_2} \quad (2)$$

where h^* is the height for a given value of u/U.

Assume now that there is a standard boundary layer profile whose momentum thickness θ_1, is known, and also that there is a profile whose similarity has been established. It is then possible by choosing a convenient value of u/U to obtain h_1^*, and h_2^* and, using equation (2), to ascertain θ_2.

It is convenient to have the standard velocity profile plotted in non-dimensional form, i.e.

$$\log\left(\frac{h}{\theta}\right) \text{ vs } \frac{u}{U}.$$

The action of dividing by θ has no effect on the profile shape, but, as was the case with similar profiles, merely shifts the plot bodily. A comparison of the non-dimensional standard profile with the second profile will still show if similarity exists, but, in addition, for a convenient value of $\frac{h_1^*}{\theta_1}$ will yield the corresponding value of h_2^*. Hence θ_2 can be found as before.

6.1.2 The method in practice

As the method relies on a comparison between similar profiles, a sufficient number of standard profiles must be determined and should include as many variables as are likely to be encountered in the experiment, such as pressure gradient, suction conditions, laminar or turbulent state. The values of θ for these profiles must be

obtained and the graphs of $(\frac{h}{\theta})$ vs $\frac{u}{U}$ plotted on a log versus linear graph. The result is a standard profile comparison chart as shown in figure 32a.

The experimental points of the profile whose momentum thickness is to be determined are plotted on a transparent overlay to the same scales as fig. 32a. An example of the overlay is shown in fig. 32b. Two points are sufficient if the highest pitot tube can be placed where u/U = 0.9 to 0.95 and the lower tube at 1/3 to 1/2 of the height of the upper tube. The overlayed experimental points are aligned with the standard profile which gives the best correlation. When making the correlation the overlay is moved in the direction of the log h axis, with the velocity ratios of u/U = 1 on both graphs coincident. For the example given the correlation occurs when the lines marked A-A coincide. A convenient height on the overlay is taken, for example $h_2 = .090$, and the corresponding value of h_1/θ_1 is read off, through the overlay on the standard profile plot, i.e. $h_1/\theta_1 = 2.25$.

Thus since $\frac{h_2}{\theta_2} = \frac{h_1}{\theta_1}$

$\theta_2 = .040''$

The advantages of the method are that the time required to determine the momentum thickness is reduced by an order of magnitude, and moreover it can be determined by 2 - 4 pitot tubes instead of the usual 8 - 12 tubes.

6.2 Estimation of transition position from 90% chord instrumentation

In order that the maximum amount of information could be obtained from the instrumentation at 90% chord, it was convenient to have a method for estimating the position of transition when it occurred further forward.

This was achieved by obtaining the momentum thickness from the pitot readings as described in section 6.1 using it as described below. In earlier wind tunnel and flight results some momentum thickness of turbulent boundary layers on the fin had been measured. These results were plotted but were to sparse to permit curves to be drawn with confidence. However, some computed curves of the growth of turbulent boundary layers on a wing having a similar roof top type of velocity distribution were available. These were used as a guide in drawing the family of curves depicted in fig. 33a.

From results obtained on a flight on which the traversing hot film and pitots at the 90% chord position were installed, it was possible to compare the estimated transition positions with the actual positions obtained from the traversing hot film. The flight result for both the estimated and actual transition position is shown in figure 33. It can be seen that the methods agree with each other fairly well.

6.3 Comparison between a calculated and an experimental boundary layer profile

The design of the suction surface was based on a boundary layer calculation which was made using a desk calculator. The calculation traced the development of the boundary layer step by step and was approximate, involving chart reading and iterative procedures at each step. This meant that the effect of small changes of, say, the suction distribution could not be confidently predicted because there was always some doubt

whether all the predicted change was genuine or due to the accumulated effect of the approximations involved. The time involved in doing the calculation also meant that no calculation was undertaken unless it was absolutely necessary.

However, soon after completion of the experimental flight programme an improved method of boundary layer calculation, developed and programmed for a digital computer by Mr. M.P. Carr of the Handley Page Research Department (ref. 5), became available.

The basic idea of this method is to take the differential equations representing the flow in the boundary layer and convert them into finite difference equations. This involves obtaining solutions of the equations at a finite number of points, both in a chordwise direction and also through the boundary layer.

The other main point regarding the calculations is that a continuous suction distribution has to be assumed instead of suction taking place through discrete slits. Since this method used a computer program the result was repeatable and quickly obtainable.

The results obtained with the pitot traversing instrument on the last flight were used to compare an experimental boundary layer profile with a calculated one. In the calculations, 20 points were taken through the boundary layer and 758 steps from the leading edge to 90% chord. The measured velocity distribution around the aerofoil and the measured suction quantities were used in the calculation. Both the calculated and experimental results are shown in figure 37c. It can be seen that there is a good correlation between the two. The experimental results at the higher Reynolds number near the surface are not quite as close to the calculated results but this may be due to the measurements being taken when the manometer water heights were not entirely steady.

It should be noted that the calculated profile for the highest Reynolds number lies between the other two profiles. This is because the suction quantities did not correspond to exactly the same suction coefficient C_Q.

It appears from the good correlation between the calculated and measured results that the computer program calculation adequately predicted the development of the boundary despite the fact that the calculation was performed as if the suction was continuously distributed.

7. Results

7.1 Introduction

After successful wind tunnel tests at R.A.E. Bedford, the fin was transferred to the Lincoln installation, and it was hoped to repeat the wind tunnel results fairly quickly. However, various difficulties had to be overcome before the wind tunnel results could be repeated in flight; these are enumerated in sections 3 and 5.

The Lincoln tests could be considered as two distinct series. The first series of tests was primarily occupied with investigating and rectifying various defects that developed on the surface and exploring the environment e.g. the leading edge to fin joint and the vortices behind the canopy. After this, progress was much more rapid.

This marked what was called the second series and flights in this series are designated 2/N, where N is the flight number in the second series.

The effect of the defects in the first test series was to mask any other turbulent sources that were present. After these had been attended to, it was fairly easy to track down other sources of turbulence by means of the hot film traverse. However, several flights were still needed to reduce these causes to a minimum. When a satisfactorily low occurrence rate was achieved the traverse was removed and results were obtained purely from the instrumentation placed at 90% chord.

Effort was concentrated on the starboard surface which was more conservatively designed, having more slits, and therefore most of the results obtained relate to this surface. Work on the port surface was only started about half way through the second series of tests and consistent results were just being obtained on this surface at the end of the flying programme.

Most of the results are shown in the form of 90% chord momentum thickness plots versus various parameter changes. Where possible these plots are associated with diagrams showing how the transition "contours" moved over the fin surface. It should be noted that the transition "contours" were drawn by joining transition positions predicted from pitot comb results. They may not correspond closely with the actual transition front. In some cases, therefore, they may give a pessimistic indication of the transition front, whilst in others they may be slightly optimistic. The "contour" presentation of results were adopted where insufficient measurements were available to reliably infer an actual transition front. The hot film measurements could augment the pitot reading only when some of the fin was laminar at the 90% chord position and it was then possible to draw the transition fronts with confidence. However, it was felt that this presentation gave a reasonable indication of the effect of the various tolerance parameters.

Momentum thickness variations have not been plotted for stations where there is obviously a turbulent source near to the leading edge. All results quoted are for zero incidence conditions unless otherwise stated.

7.2 Chordwise pressure distribution

The variation of the 50% span chordwise pressure distribution with nominal incidence is shown in figure 29. From these plots it was possible to construct the C_{L_L} vs. α curve shown in figure 28.

A comparison between the theoretical sucked distribution and the wind tunnel and flight results, for zero incidence, is shown in figure 30. It can be seen that, forward of 50% chord, the flight results follow the theoretical distribution much more closely than the wind tunnel results. This difference is due mainly to wind tunnel blockage. However, aft of 50% chord, the adverse pressure gradient is increased in flight by the presence of the trailing edge instrumentation and supporting structure.

Without the trailing edge equipment, the in-flight pressure distribution closely follows that predicted by theory.

7.3 Operational repeatability

Repeatable results were not obtained until the latter half of the second test series. Figure 34 shows the percentgae laminarisation of the laminarisable area forward of 90% chord, for both the port and starboard surfaces during this period. These results were all obtained at a unit Reynolds number of 1.48×10^6 per foot.

It can be seen that once a figure of about 60% laminarisation has been achieved it is fairly easy to maintain the surface at between 60 and 80% laminarisation. This is evident from the starboard surface results but the results obtained from the port surface are not as consistent. This is mainly because investigations were only started on the port surface after flight 2/5 whereas about forty flights on the Lincoln had already been completed in relation to the starboard surface up to that time.

Figures 35 and 36a give the best results at a unit Reynolds number of 1.48×10^6 per foot for the port and starboard surfaces respectively.

Figure 36a is the first of a series of high percentage laminarisation results obtained on the starboard surface during the last flight of the programme.

7.4 Reynolds number tolerance

The effect of changing the unit Reynolds number was investigated in two ways. Firstly, the effect of increasing the unit Reynolds number above 1.48×10^6 per foot was observed with the suction increased to maintain approximately constant C_Q. The second method used was to investigate the effect of increasing the unit Reynolds number without increasing the suction.

The effects of increasing both suction and unit Reynolds number on the starboard surface are shown in figures 36a to 36e inclusive. As only one suction engine was working on this flight, zone A suction was reduced at the higher Reynolds numbers in order to give the correct amount of suction in zones B and C. Taking this into account it can be seen that an extremely high degree of laminarisation was obtained even at the highest unit Reynolds number of 1.86×10^6 per foot.

During this exercise the traversing pitot was used, at 90% chord, to obtain accurate boundary layer profiles. These results are shown in figure 37a. The resulting $\frac{u}{U}(1 - \frac{u}{U}) \sim h$ plot, shown in figure 37b, gives values of momentum thickness ranging from 0.0077 inches at a unit Reynolds number of 1.67×10^6, increasing to 0.0094 inches at a unit Reynolds number of 1.86×10^6. The actual results compare very favourably with the prediction based on the method outlined in section 6.3 (see figure 37c).

With the suction adjusted to give the best boundary layer conditions at 90% chord at a unit Reynolds number of 1.48×10^6 per foot it was found that the unit Reynolds number could be increased by 15% without any significant change occurring on the starboard surface. However, increasing the unit Reynolds number more than 7% caused a rapid forward movement of the transition contour on the port surface. Figures 44 and 45 give θ plots and transition contours for the starboard and port surfaces respectively.

7.5 Zone mass flow tolerance

Thinnest boundary layers were obtained, at 90% chord, when using between 95% and 105% of the design mass flows in zones A, B and C[1]. A typical example of this result is shown in figure 38.

7.6 Leading edge mass flow tolerance

In most cases, the plot of momentum thickness versus the percentage of leading edge design mass flow (D.M.F.) display a distinctive shape. At values below 30% D.M.F. the momentum thickness decreases rapidly with increase in suction, at between 30% and 70% D.M.F. the momentum thickness decreases with suction at a moderate rate and between 70% and 100% D.M.F. increases in suction have no detectable effect on the momentum thickness of the boundary layer.

Typical results, obtained on the starboard surface, are shown in figure 39. Corresponding results are shown in figure 40 for the port surface. In figures 40a and 40b the curves for stations 52P and 83P do not show the typical shape. This effect was due to the intermittent occurrence of turbulent sources as shown by the transition contours in figure 40c.

7.7 Drag coefficient variation with suction quantity coefficient, C_Q, and chord Reynolds number, R_C

Estimates of the wake drag coefficient were made from the momentum thicknesses obtained at 90% chord, using the Jones method and its extensions, outlined in reference 8.

Figure 47a shows the variation of C_D with suction coefficient C_Q at zero lift. It also shows that there is no marked dependence on unit Reynolds number within the range 1.67×10^6 per foot. The flight curves are based on results at station 78 on the starboard side, the result for $C_Q = 0.00067$ being interpolated from the results plotted in figure 43b. It can be seen that the flight results compare very favourably with the results obtained during the wind tunnel tests (reference 7). The results were obtained at approximately the same unit Reynolds number.

Three discrete points are also shown for unit Reynolds number 1.67×10^6, 1.76×10^6 and 1.86×10^6 per foot. These were obtained from the traversing pitot results at station 54 on the starboard side and were also used to plot the variation of wake drag coefficient with chord Reynolds number with constant C_Q as shown in figure 47b. Although the C_Q values obtained in flight were not absolutely identical, the curve indicates that the wake drag coefficient increases less rapidly in flight than in the wind tunnel with increase in chord Reynolds number.

The rapid increase of wake drag coefficient C_{DW} in the wind tunnel at the highest wind tunnel Reynolds numbers may be attributed to blockage and high frequency stream turbulence effects.

The total drag coefficient C_{DT} was obtained by adding the suction pump drag coefficient to the wake drag coefficient. The suction pump drag coefficient has been

set equal to the suction coefficient C_Q, which has been shown by detailed project studies to be a reasonable approximation.

Hence $C_{DT} = C_{DW} + C_Q$

Comparing the measured total drag coefficient at a unit Reynolds number of 1.67×10^6 per foot for the turbulent unsucked condition with that for the best laminar condition the following is obtained

Turbulent unsucked drag coefficient = 28.6×10^{-4} per surface

Laminarised drag coefficient = $1.7 \times 10^{-4} + 5.5 \times 10^{-4}$

$= 7.20 \times 10^{-4}$ per surface.

Hence the laminarised drag coefficient including pump drag is only 25% of the turbulent unsucked drag coefficient.

7.8 Lift coefficient tolerance

The fin surface under investigation was assumed to be equivalent to the top surface of a conventional horizontal wing. Hence, when investigating the starboard surface, C_L is positive when the fin nose was deflected to starboard.

In the time available it was only possible to investigate the effects of C_L changes on the starboard surface. Figures 41, 42 and 43 give typical results obtained at unit Reynolds numbers of 1.48×10^6, 1.58×10^6 and 1.67×10^6 per foot respectively.

Figure 46 gives the collected results of several flights for a unit Reynolds number of 1.48×10^6 per foot. The curve is drawn for the minimum recorded values of momentum thickness at 90% chord. Apart from some of the results obtained on flight 2/10 it can be seen that there is fairly good agreement.

From consideration of all these figures the starboard surface of the fin displays a negative critical C_L of between -0.075 and -0.10. There is no clearly defined positive critical C_L but the initial rate of increase of momentum thickness with positive increment of C_L is greater on the outboard part of the wing than on the inboard part.

7.9 The effect of water vapour

Flying near or through clouds caused the hot film signals to become unstable. On approaching a cloud downward pointing spikes were observed on the oscilloscope signal. The signal changed to a large amplitude turbulent signal as the cloud was entered.

Spiky signals were normally associated with contamination of the attachment line boundary layer, but in this case the spikes always pointed upwards (1).

The downward pointing spikes observed when flying near clouds or haze may be due to latent heat transfer between the hot film and the water vapour and not necessarily due to boundary layer transition. The large amplitude turbulent signals, however, correlated with the manometer results as being a function of the boundary layer state.

8. Conclusions

a) The results obtained in the wind tunnel tests were repeated and, subsequently, improved upon.

b) The experimental and calculated laminar boundary layer profiles at 90% chord, compared over a range of unit Reynolds numbers from 1.67×10^6 per foot to 1.86×10^6 per foot, showed a very good correlation.

c) Boundary layer profiles reaching freestream velocity within 0.10 inches from the surface were recorded at 90% chord up to a unit Reynolds number of 1.86×10^6 per foot.

d) Laminar boundary layers of 0.008 inch momentum thickness were repeatedly obtained at 90% chord in all zones.

e) Thinnest boundary layers at 90% chord were obtained with between 95% and 105% of the design mass flows in zones A, B and C throughout the speed range covered.

f) It was observed that the leading edge suction can be reduced to 70% of the design mass flow without significantly increasing the boundary layer thickness at 90% chord. A reduction to 30% D.M.F. was required to move the transition front well forward.

g) Varying the incidence without changing the suction mass flow or its distribution did not move the transition front forward by more than 5% of the chord as long as C_L remained between approximately - 0.1 and + 0.05.

h) Increasing the unit Reynolds number by up to 15% from a specific design condition, without altering the suction rate, did not have a significant effect on the results on the starboard surface. However, increases above 7% in unit Reynolds number were significant on the port surface.

i) At a unit Reynolds number of 1.67×10^6 per foot the estimated laminarised drag coefficient, including pump drag was only 25% of the value of the turbulent unsucked drag coefficient.

j) The starboard surface gave better results than the port surface. This may have been due to the smaller slit pitch on the starboard surface. However, it was thought that the port surface results could have been improved if it had received as much attention as the starboard side.

k) Some maintenance difficulties were encountered and were overcome by special measures. Awareness of these problems can lead to their avoidance by the adoption of better methods of construction and manufacture.

l) It is probable that some form of equipment for preventing contamination of the leading edge will be required in the commercial application of laminar flow control. A disposable system was developed during the programme, which might be used for this purpose.

m) The results achieved vindicate the basic aerodynamic design of the laminar flow

control system which, with the exception of the leading edge, was finalised as long ago as 1960.

n) During the flight programme methods for observing and measuring this boundary layers in flight and for the definative evaluation of the results have been developed.

9. Acknowledgements

The authors wish to acknowledge the enthusiastic participation during this programme of Mr. B.F. Russell, Lincoln pilot; Mr. N. Cook, Flight engineer; Mr. J. Cropp, Budworth operator; Mr. R. Wills, for his perserverance in maintaining the fin surface; Dr. M. Gaster for his useful comments and practical assistance and all other members of the Flight and Design Departments at The College of Aeronautics who were involved.

Similar acknowledgement is due to Mr. M. Knott of Handley Page Ltd., who assisted as an observer and with the analysis of results; and to Messrs. L.E. Hutchins and J. Jell for their assiduous efforts to achieve the initial overall high standard of surface finish. Acknowledgement is also made to the other members of Handley Page Limited who were responsible for the design and construction of the fin, and especially to Dr. G.V. Lachmann, Mr. J.B. Edwards and Mr. A.A. Blythe who also contributed to the success of the flight experiments by their continued assistance.

The authors also wish to acknowledge the services of Mr. M. Firmin and other members of R.A.E. Farnborough involved in manufacturing and supplying the flush hot films.

Finally, the authors would like to pay tribute to Mr. R.A. Shaw of the Ministry of Aviation for his steadfast encouragement throughout the programme.

References

1. Landeryou, R.R. and Trayford, R.S. — Flight tests of a laminar flow swept wing with boundary layer control by suction. Report Aero. No. 174 The College of Aeronautics. June, 1964.

2. Wyatt, L.A. — Low speed wind tunnel tests of a laminar flow swept wing. Technical Report No. 66046 Royal Aircraft Establishment February, 1966.

3. Gaster, M. — A simple device for preventing turbulent contamination on swept leading edges. p. 788. Journal of the Royal Aeronautical Society. November, 1965.

4. Edwards, J.B. — Identification of boundary layer profiles. Handley Page Technical Note No. 20, May, 1963.

5. Carr, M.P. — The calculation of laminar boundary layers on wings. Handley Page Research Report No. 81. May, 1966.

6. Burrows, F.M. — Characteristics of the flow field over the mid upper fuselage of Lancaster PA 474. Note No. 36, The College of Aeronautics, June, 1956.

7. Landeryou, R.R. — Wind tunnel test with the laminar flow swept wing at R.A.E. Bedford - 13' x 9' tunnel - Autumn, 1964.

8. Schilchting, H. — Boundary layer theory, page 510 - 514. Pergamon Press, 1955.

Appendix 1

Flush hot film tests

1. Introduction

A test was conducted, under simulated flight conditions, to obtain a comparison between the characteristics of a flush hot film and a wedge hot film of similar cold resistance.

The flush hot film used in the test was designed and manufactured by R.A.E. Farnborough. Details are shown in figure 13. The cold resistance of the flush hot film was 14.2Ω and that of the wedge hot film was 15.9Ω. The cable gave an extra resistance of 1.6Ω in both cases.

2. Method

The turbulent air flow was produced by aiming a blast of high pressure air at an angle of about 45° to the fin surface and at a distance of 6" ahead of the films. The air jet was obtained by coupling a spray gun nozzle into a compressed air supply.

The flush hot film was tested using the circuit shown in figure 14. The current was increased in increments of 10 mA from 100 mA up to 290 mA. The voltage across the film was noted, using a Avometer. The signal output was amplified by a type 122 Tektronix pre-amplifier, set at x 1000 gain, before being fed to the oscilloscope. The time scale of the oscilloscope was set at 50 m.sec./cm giving a total sweep time of 400 m.sec. Using a triggering switch it was possible to photograph a single sweep of the beam. With increased current the signal increased and it was necessary to alter the y-scale of the oscilloscope in the following manner. A y-scale of 200 mV/cm was used between 100 mA and 190 mA, 500 mV/cm between 190 mA and 270 mA and 1000 mV/cm between 270 mA and 290 mA. It should be remembered, when quoting these figures, that the y-scale was subject to a factor of $\frac{1}{1000}$.

The wedge type hot film was tested using the same operating circuit except that, due to the different characteristics of this type of film, it was necessary for a further 95Ω to be placed in series with the other controlling resistances.

In this case the output signal passed directly into the oscilloscope without going through the pre-amplifier. The current was increased in increments of 10 mA from 80 mA up to 180 mA. The y-scale used was 2mV/cm between 80 mA and 100 mA, 5mV/cm between 100 mA and 130 mA and 10 mV/cm between 130 mA and 180 mA. As before, a single 400 m.sec. trace was recorded with the aid of a camera.

As expected, the output obtained from both films was in the form of a random high frequency signal. It was decided that the best parameter to use for comparison purposes was the maximum change in signal level over a fixed time period. In flight the signal was normally observed by using a time scale of 10 m.sec/cm., giving a total sweep of 80 m.sec. on this oscilloscope. The 400 m.sec. traces, obtained during the comparison tests, were conveniently cut up into seven overlapping 100 m.sec. lengths and it was thought that this length was fairly representative of the normally observed signal. Hence seven values of maximum signal level change, for a time period of 100 m.sec., were obtained for each case. These values were

averaged out and the figure obtained was used to indicate the signal output level.

3. Results

The final results are shown in figures I(1) and I(2).

Figure I(1) shows the voltage obtained across the flush hot film for a particular current setting. As expected, the curve blends into the cold resistance slope at the lower current settings. The curve for the wedge type hot film is also drawn and shows a similar tendency. The deviation from the cold resistance slope gives a guide to the overheating ratio of the film. The overheating ratio is the ratio of the hot to cold film resistance and is sometimes used to indicate the sensitivity expected.

From figure I(1) it can be seen that the rate of change of voltage with current is much greater for the wedge film than the flush film. As a consequence, the wedge film reaches a particular value of overheating ratio at a much lower current than the flush hot film.

Figure I(2) compares the signal output for the two films against the power consumed in watts. The two curves display the same characteristic shape. However, the amplitude of the wedge hot film output is about twenty times that of the flush hot film at the same power rating. The wedge hot film output is also larger than that obtained from the flush hot film when compared on a constant overheating ratio basis.

Figure I(3) shows photographs of output signals. Figure I(3)a shows the output obtained from the wedge film when used at an overheating ratio of 1.40 and a power rating of 0.30 watts. This may be compared with figure I(3)b, the output obtained from the flush hot film at about the same power rating and I(3)c, the output from the flush hot film at the same overheating ratio. The oscilloscope grid is made up of 1 cm squares. When comparing the three signals due account must be taken of the particular y-scale used in each case.

4. Conclusions

1) For a given power rating the wedge type of hot film has a turbulent flow signal strength of about twenty times that of the flush type of film.

2) The maximum signal strength obtainable from the flush hot film is of the order of 3 mV peak to peak, whereas that from the wedge type film is of the order of 35 mV peak to peak.

3) For flush hot film applications, some form of pre-amplification is necessary in order to obtain a reasonable signal strength.

Appendix II

The measurement of the pressure field caused by the pitot traversing instrument

1. Introduction

At the design stage of the traversing instrument it was decided to do some wind tunnel tests. The tests were to determine the instrument's effect on wing circulation and to check that the proposed pitot tube length would give an acceptable pressure field interference. The tests were made in the Handley Page low speed wind tunnel.

2. Model and tests

A half scale wooden mock-up of the proposed instrument was made and mounted on a symmetrical two dimensional aerofoil whose chord was approximately half that of the fin. The aerofoil had been used for previous work and had a row of pressure orifices at its mid-span. The surface pressures were recorded on a multi-tube water manometer set to read pressure coefficiently directly. The accuracy of reading was estimated to be $\pm$ 0.001 in terms of C_p. Transition was fixed at 7% chord. The aerofoil was set to zero incidence and the test wind speed was 125 ft/sec. giving a chord Reynolds number of 2.6×10^6.

3. Results

During the test an attempt was made to measure the change in fin circulation due to the instrument. This was achieved by mounting the model on the opposite aerofoil surface to that which had the pressure tubes in it. The pressures measured with the instrument installed were compared with pressures obtained from the basic aerofoil. The results of these observations showed that the differences were negligible when compared with the expected experimental error.

The C_p distribution along the centre line of the instrument is shown in figure II(1). It can be seen that a pitot head, 2.0" forward of the instrument base plate on the half scale model, will experience a ΔC_p of + 0.015. This value is within acceptable limits and, while a longer pitot tube would decrease the ΔC_p at the head, it would lead to a less rigid tube and a greater distance travelled per revolution of the measuring potentiometer.

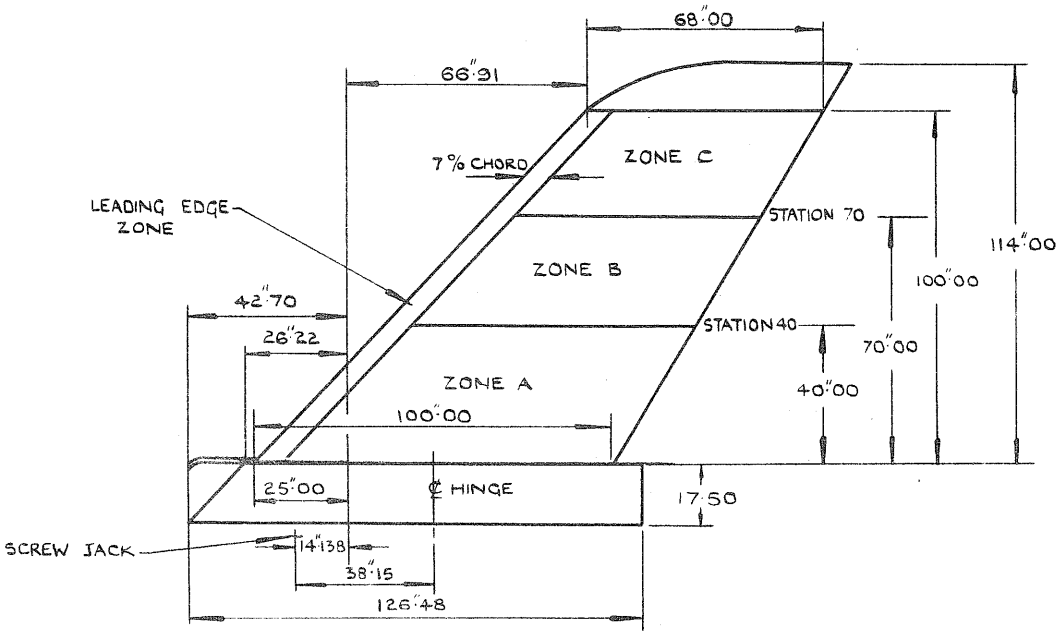

FIG. 1 SUCTION ZONES AND FIN DIMENSIONS

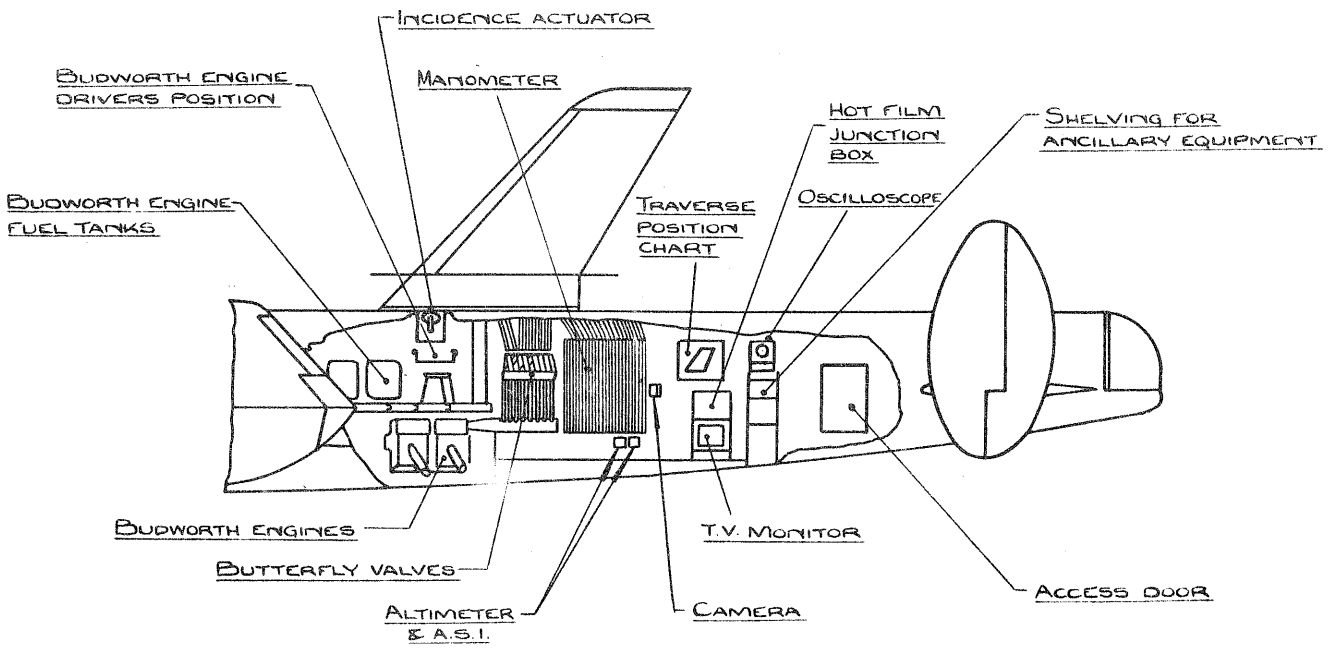

FIG. 2 INTERNAL EXPERIMENTAL EQUIPMENT

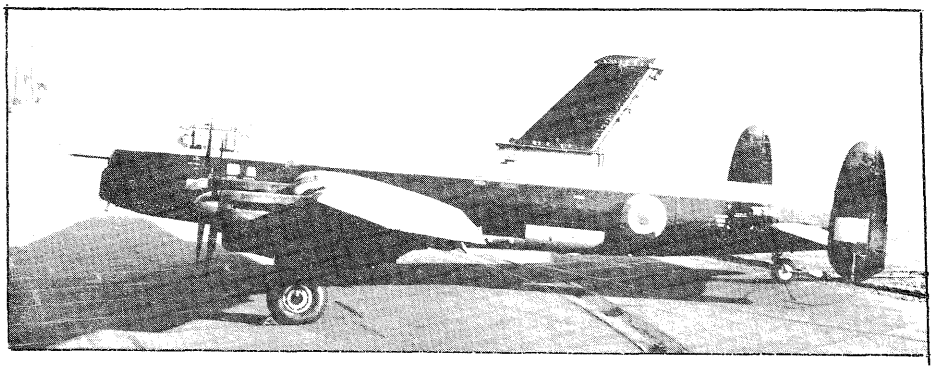

FIG. 3 EXTERNAL VIEW OF INSTALLATION

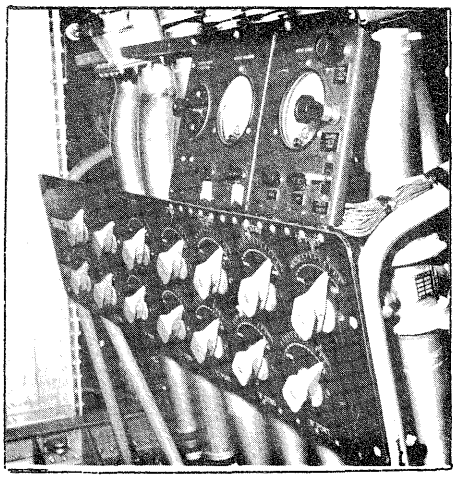

FIG. 4 BUTTERFLY VALVES

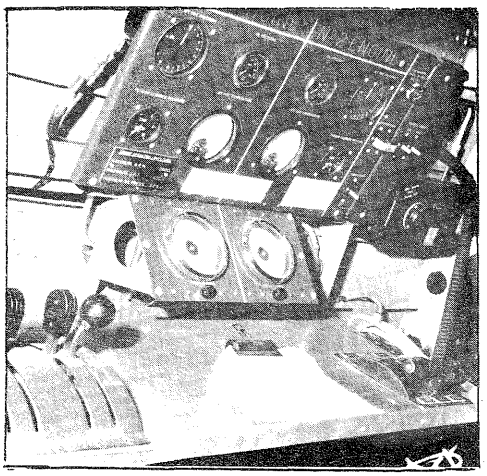

FIG. 5 BUDWORTH OPERATORS CONTROL PANEL

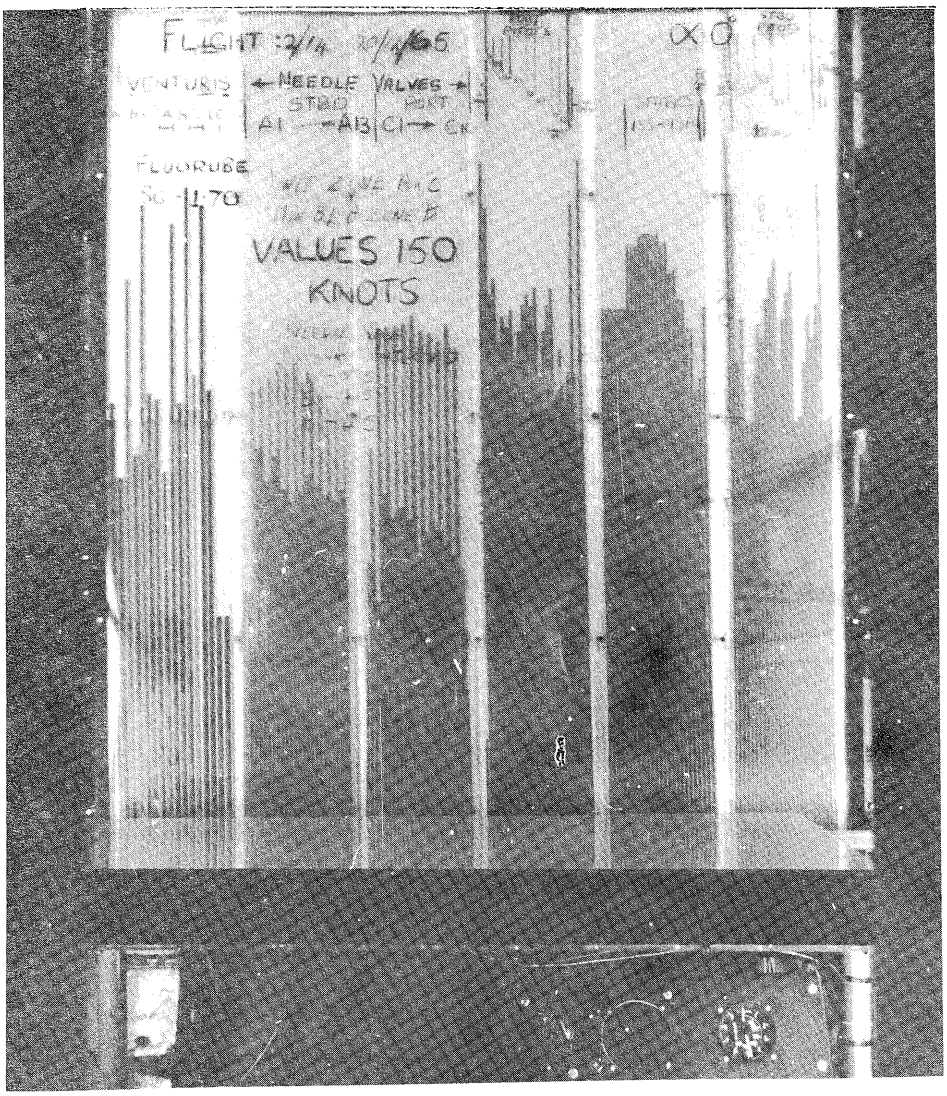

FIG. 6 MANOMETER BANK

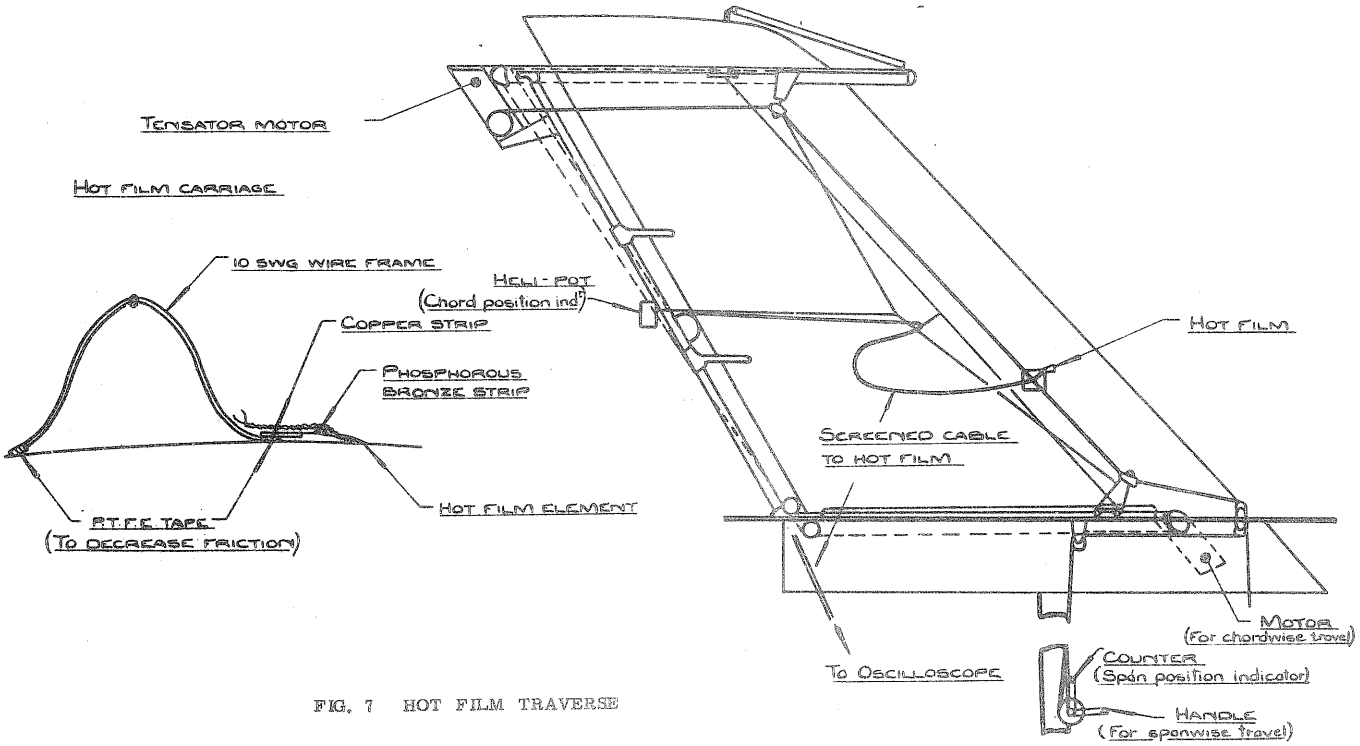

FIG. 7 HOT FILM TRAVERSE

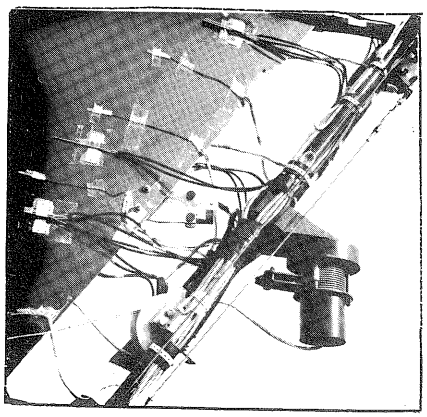

FIG. 8 HELIPOT

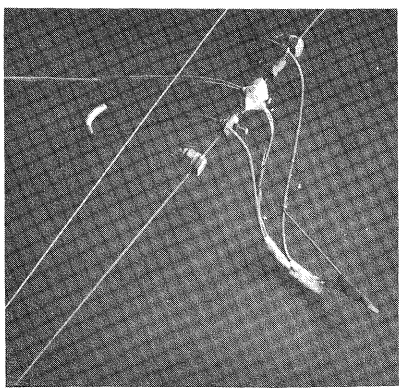

FIG. 9 HOT FILM CARRIAGE - SET FOR FREESTREAM CONDITIONS

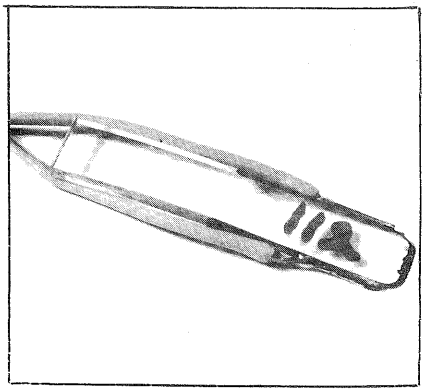

FIG. 10 (a) WEDGE HOT FILM

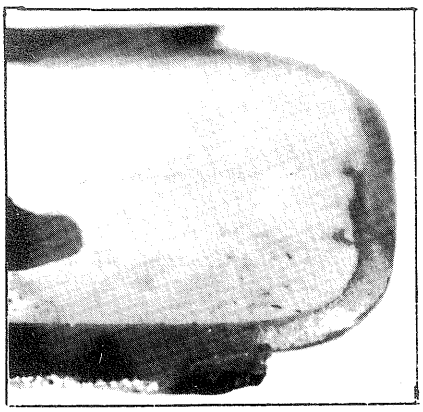

FIG. 10(b) WEDGE HOT FILM - DETAIL OF TIP

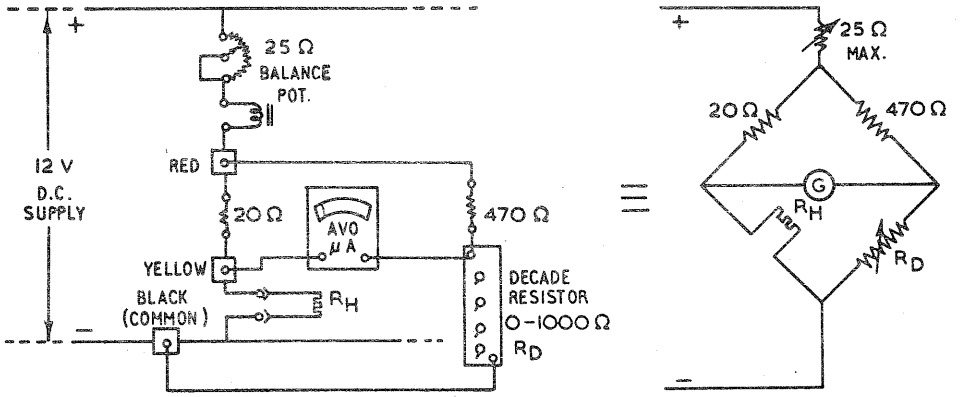

HOT FILM RESISTANCE, $R_H = (\gamma R_c - R_{cable})$, WHERE R_c = COLD FILM RESISTANCE

WHEN BALANCED $R_D = \frac{470}{20} R_H$

γ = OVERHEATING RATIO (1·30)

R_{cable} = FILM CABLE RESISTANCE (USUALLY 1·0 Ω)

TO OBTAIN R_H, SET UP R_D AND INCREASE CURRENT TO FILM VIA 25 Ω BALANCE POT. UNTIL AVO μA READS ZERO.

FIG. 11 HOT FILM BALANCE CIRCUIT

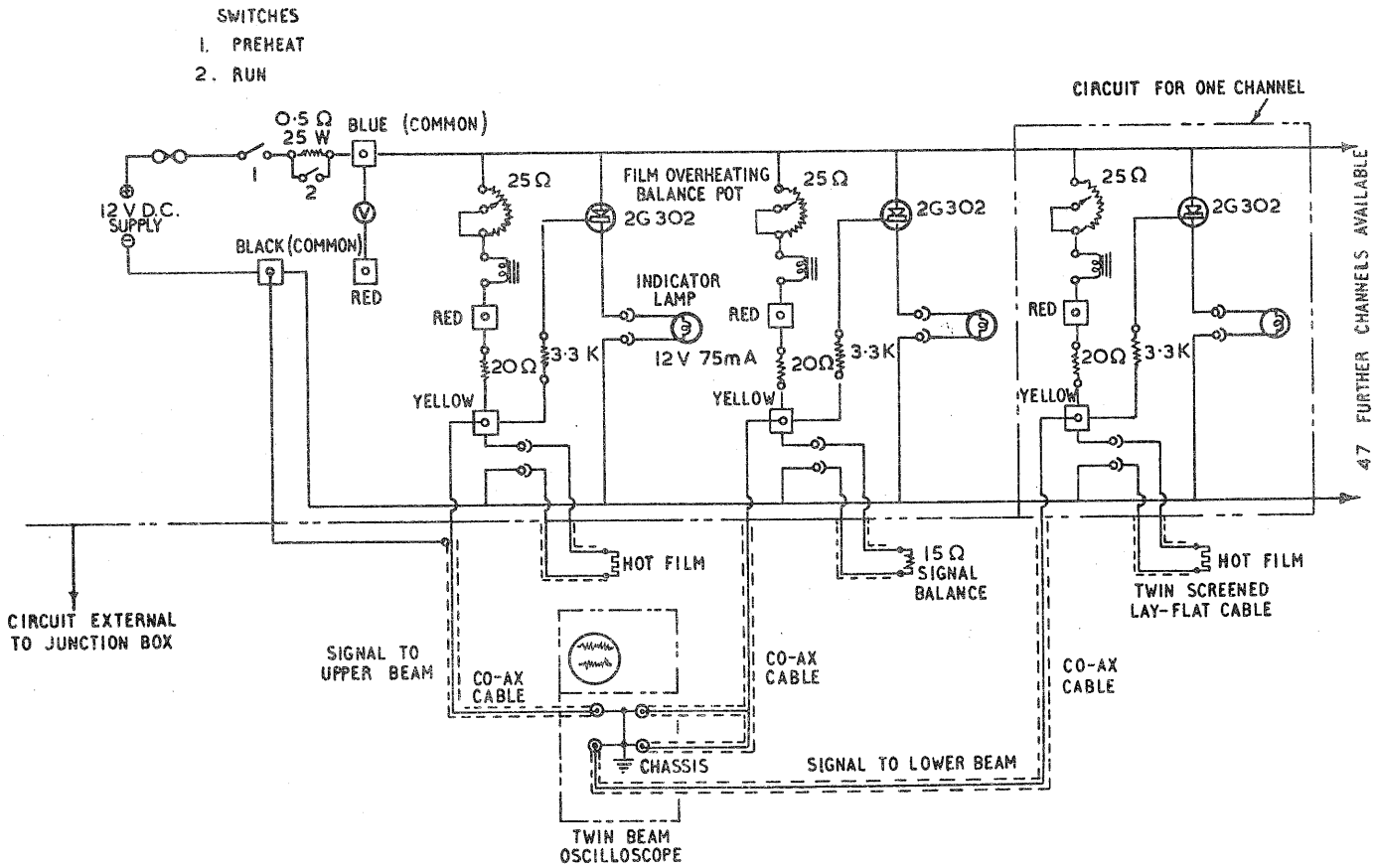

FIG. 12 NORMAL HOT FILM OPERATING CIRCUIT

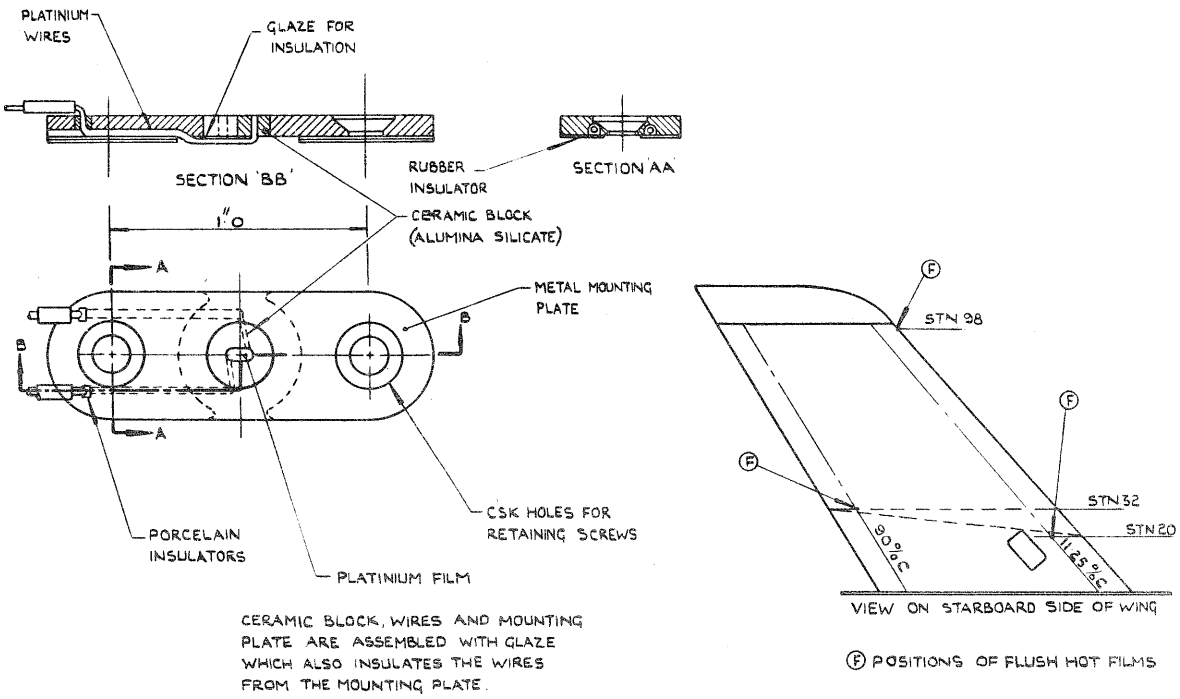

FIG. 13 FLUSH HOT FILM - DETAILS AND INSTALLATION

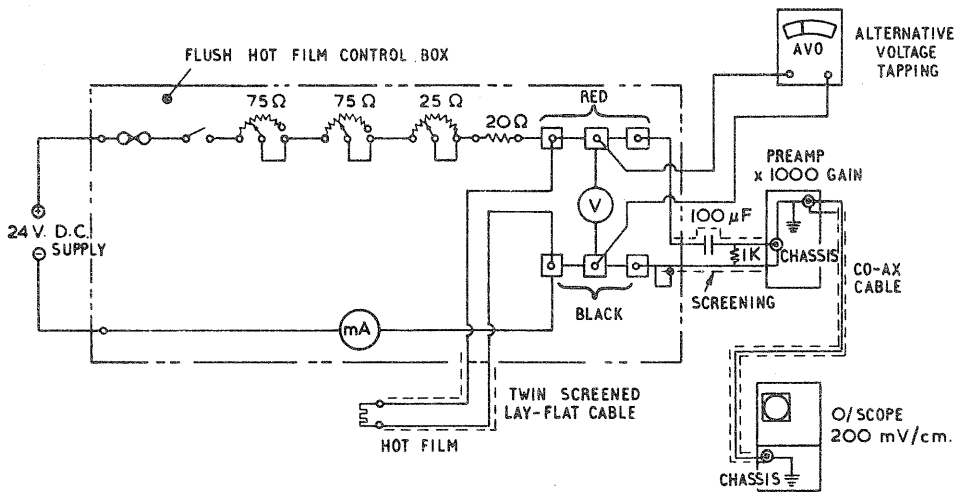

FIG. 14 FLUSH HOT FILM OPERATING CIRCUIT

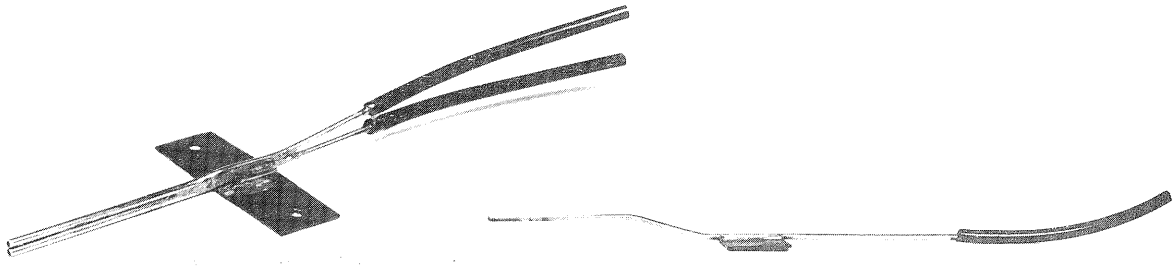

FIG. 15(a) TWIN TUBE PITOT COMB

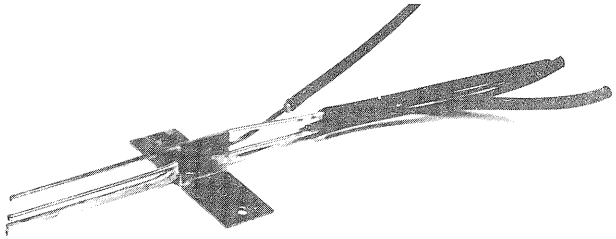

FIG. 15(b) FOUR TUBE PITOT COMB

FIG. 16 STATIC PROBE

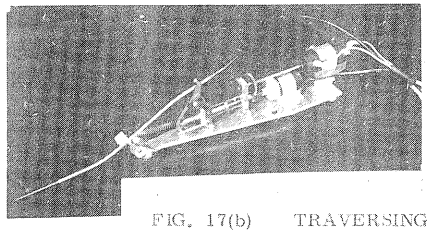

FIG. 17(b) TRAVERSING PITOT

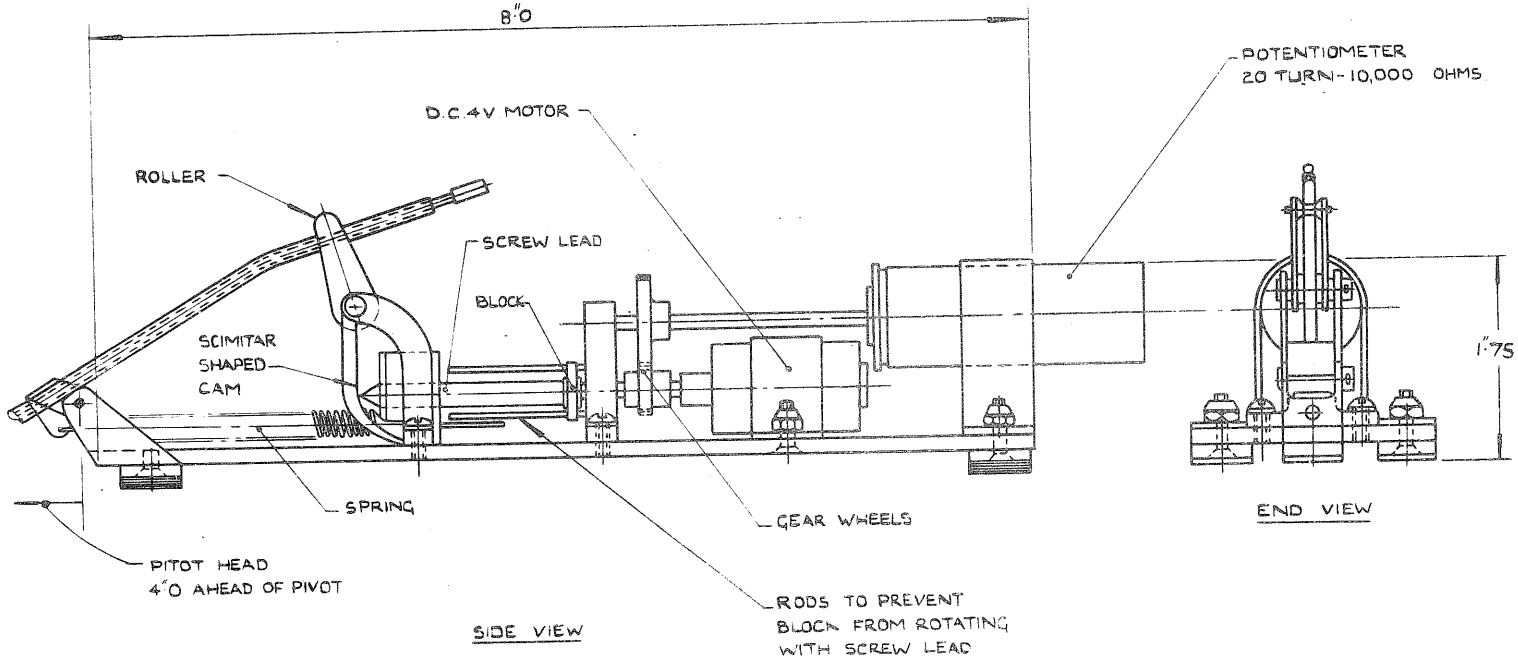

FIG. 17(a) TRAVERSING PITOT - DETAILS

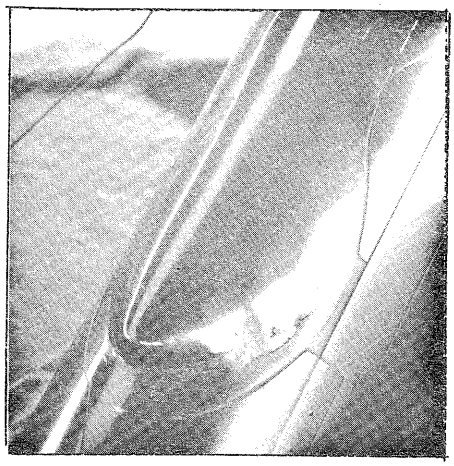

FIG. 18 THE "GASTER" BUMP

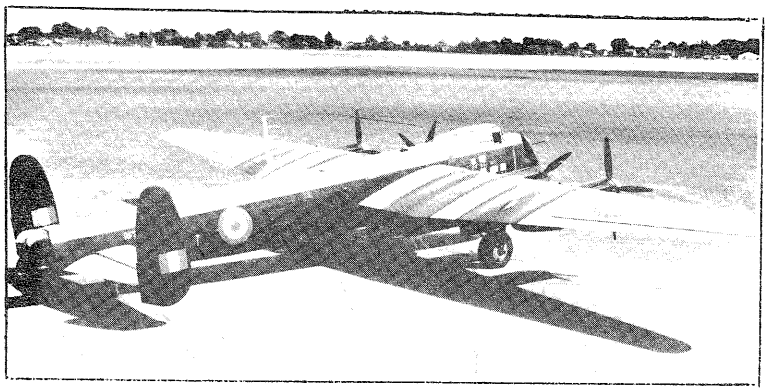

FIG. 20 FLOW FIELD POLE INSTALLATION

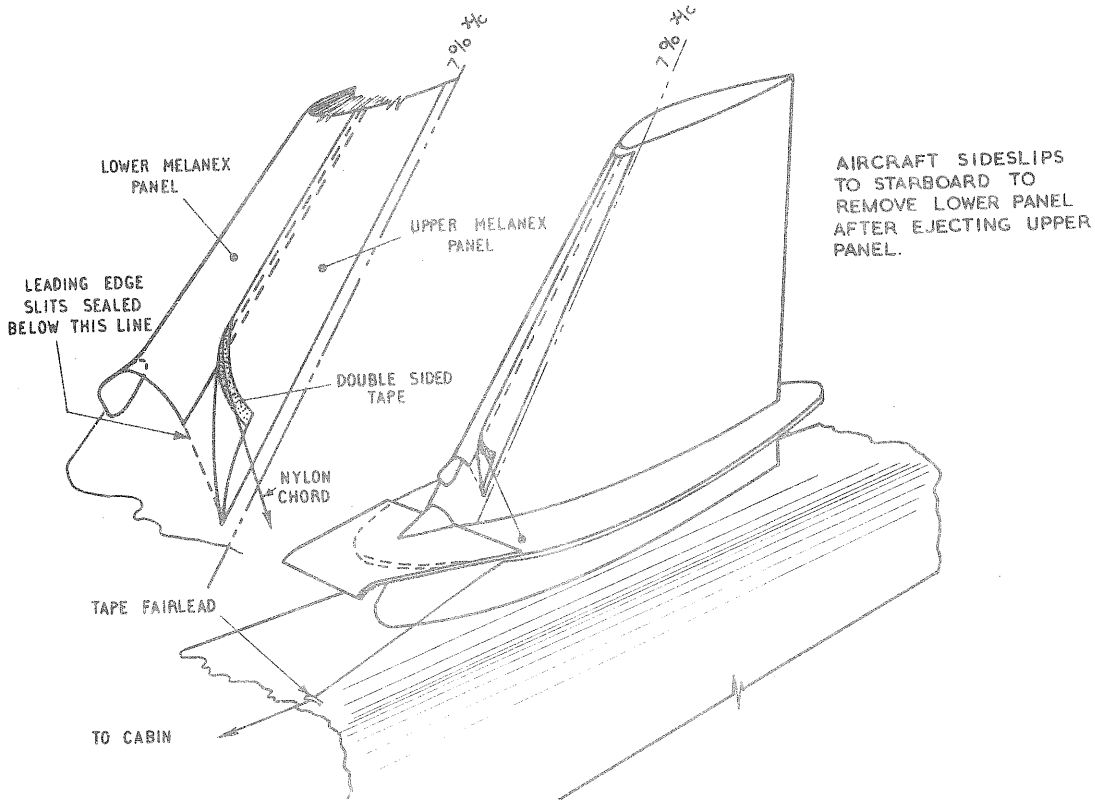

FIG. 19 LEADING EDGE PROTECTION SYSTEM

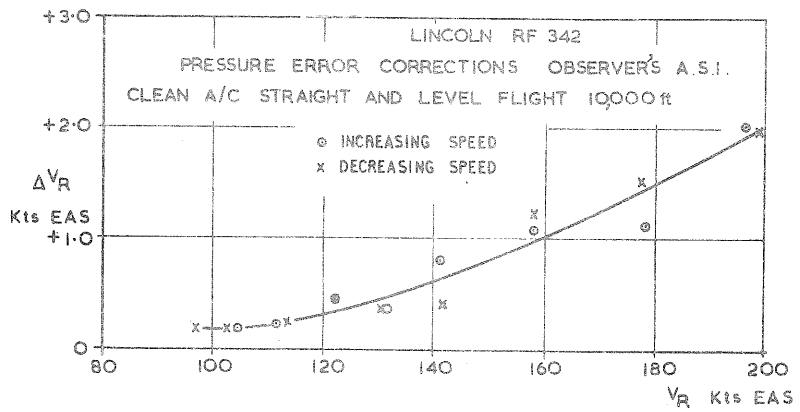

FIG. 21 STATIC PRESSURE ERROR CORRECTION

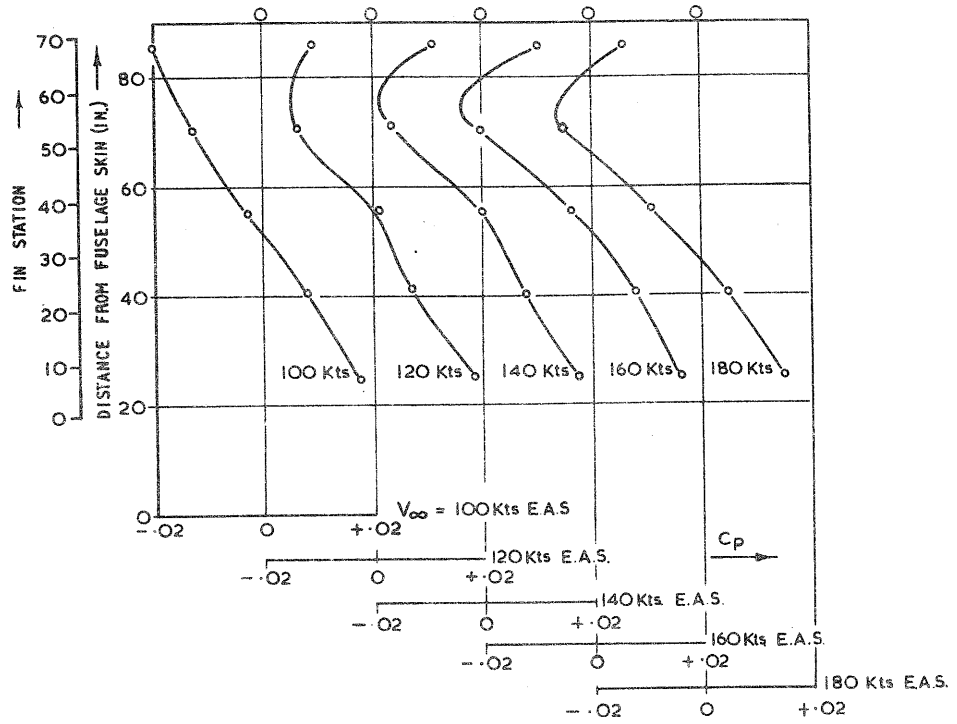

FIG. 22 FREESTREAM STATIC PRESSURE COEFFICIENT VARIATION

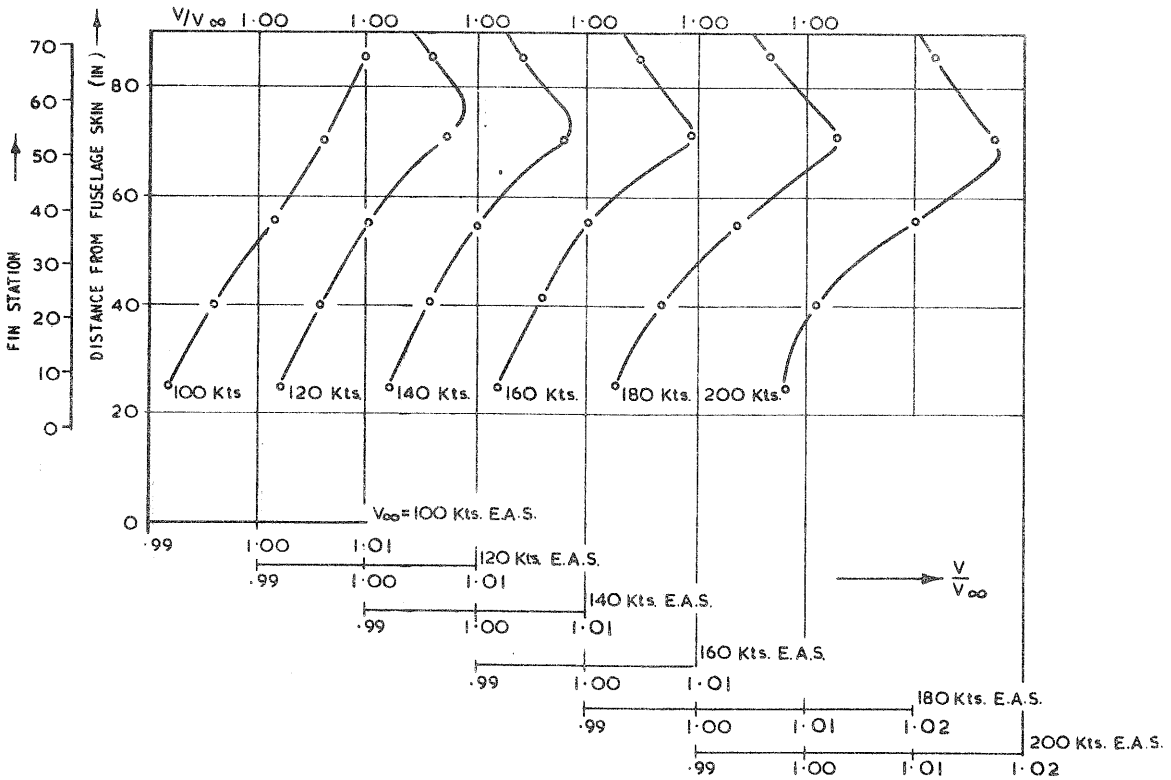

FIG. 23 FREESTREAM VELOCITY DISTRIBUTION VARIATION

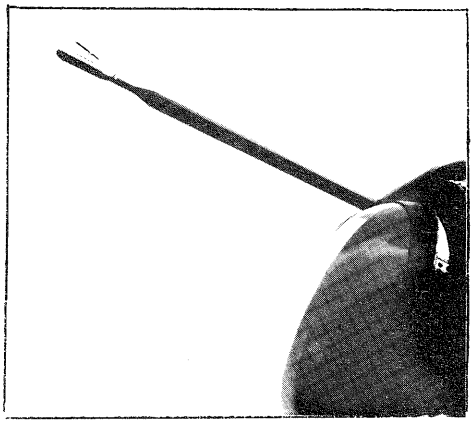

FIG. 24 YAW VANE

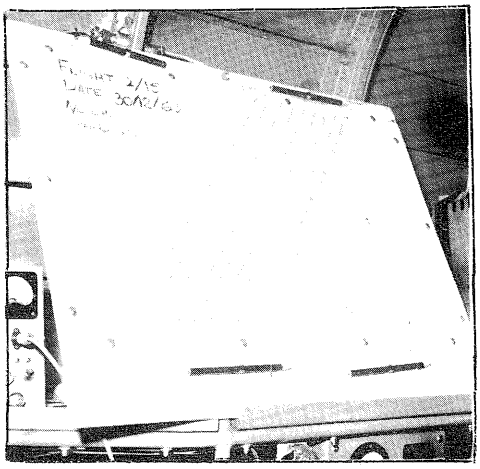

FIG. 25 HOT FILM TRAVERSE CALIBRATION GRID

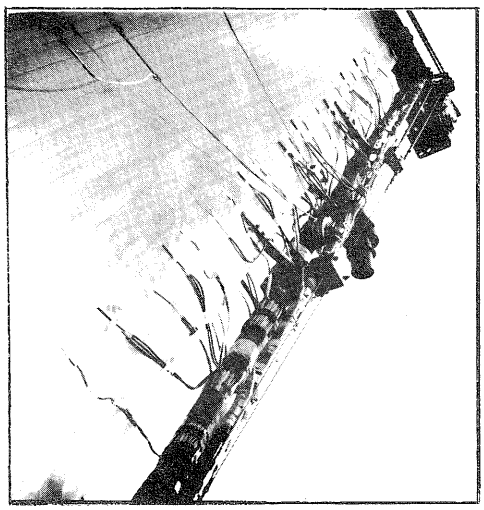

FIG. 26 90% CHORD INSTRUMENTATION

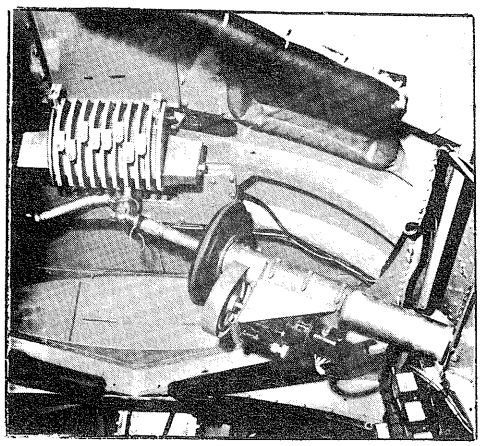

FIG. 27 FIN INCIDENCE ACTUATOR

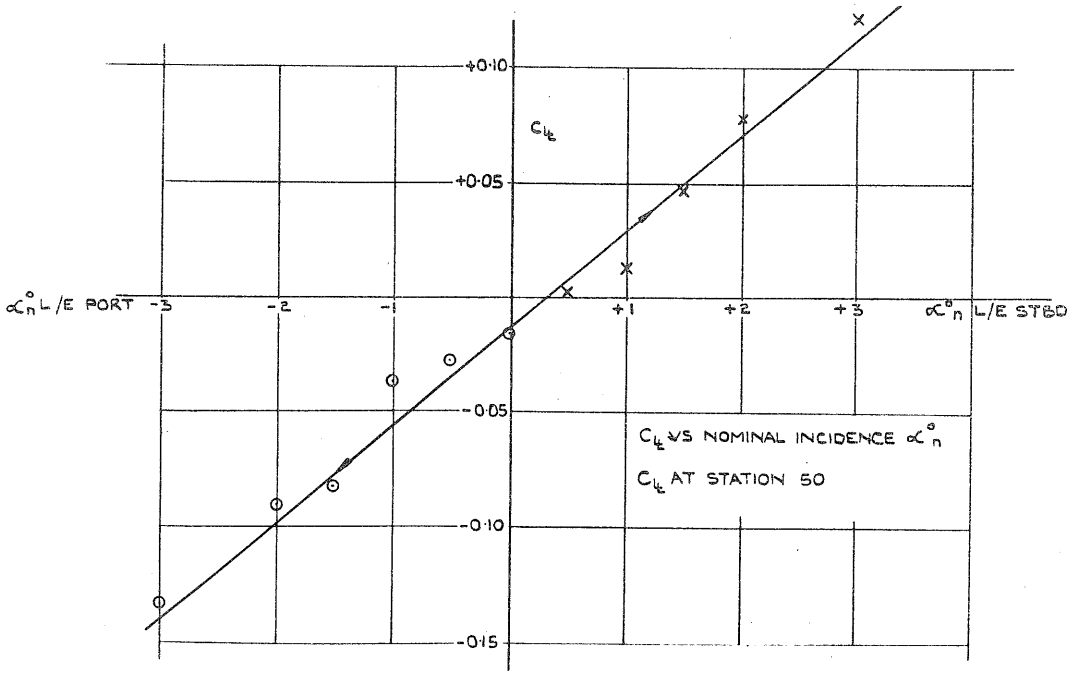

FIG. 28 VARIATION OF LIFT COEFFICIENT WITH NOMINAL INCIDENCE

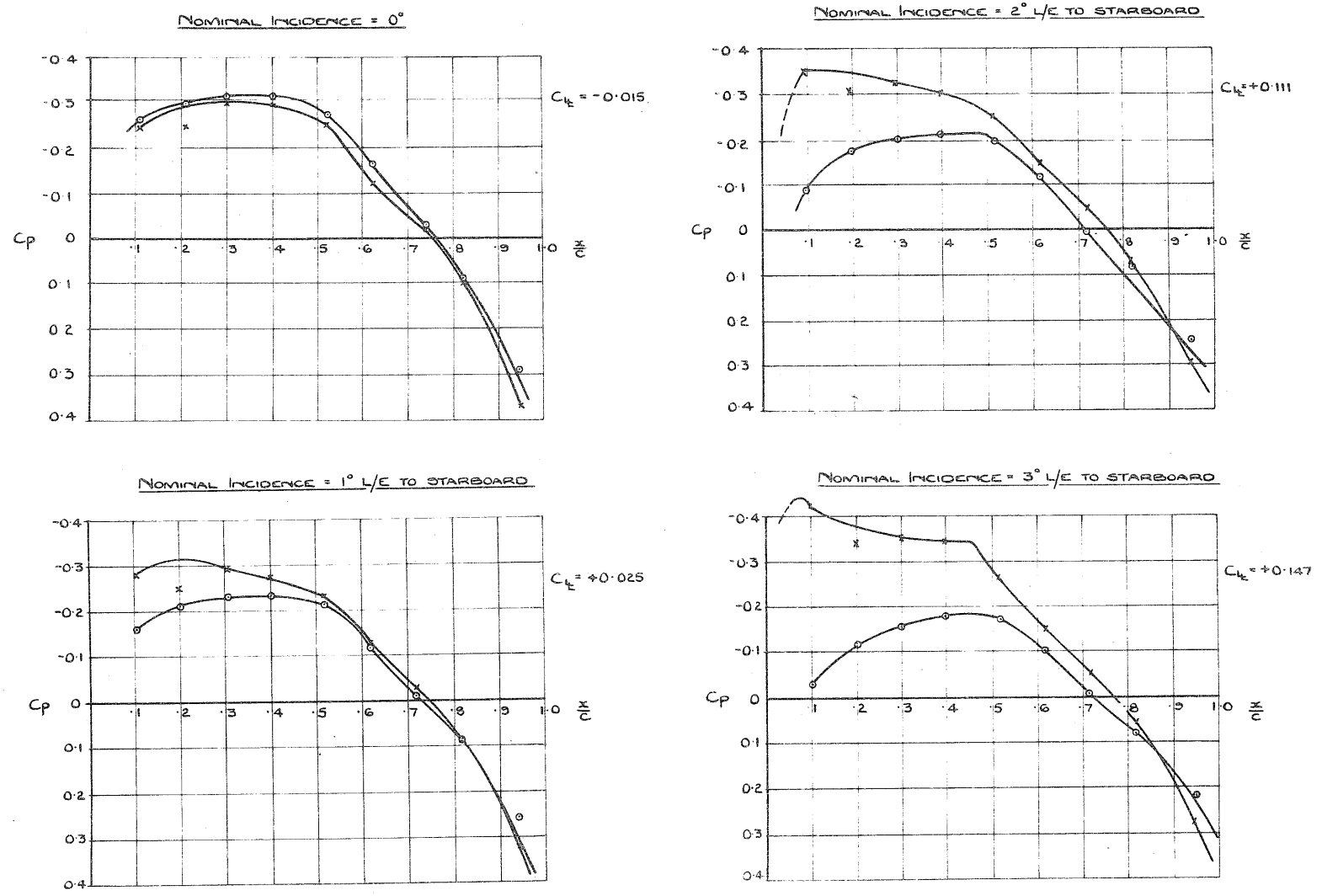

FIG. 29(a), (b), (c), (d) VARIATION OF 50% SPAN CHORDWISE PRESSURE DISTRIBUTION WITH NOMINAL INCIDENCE

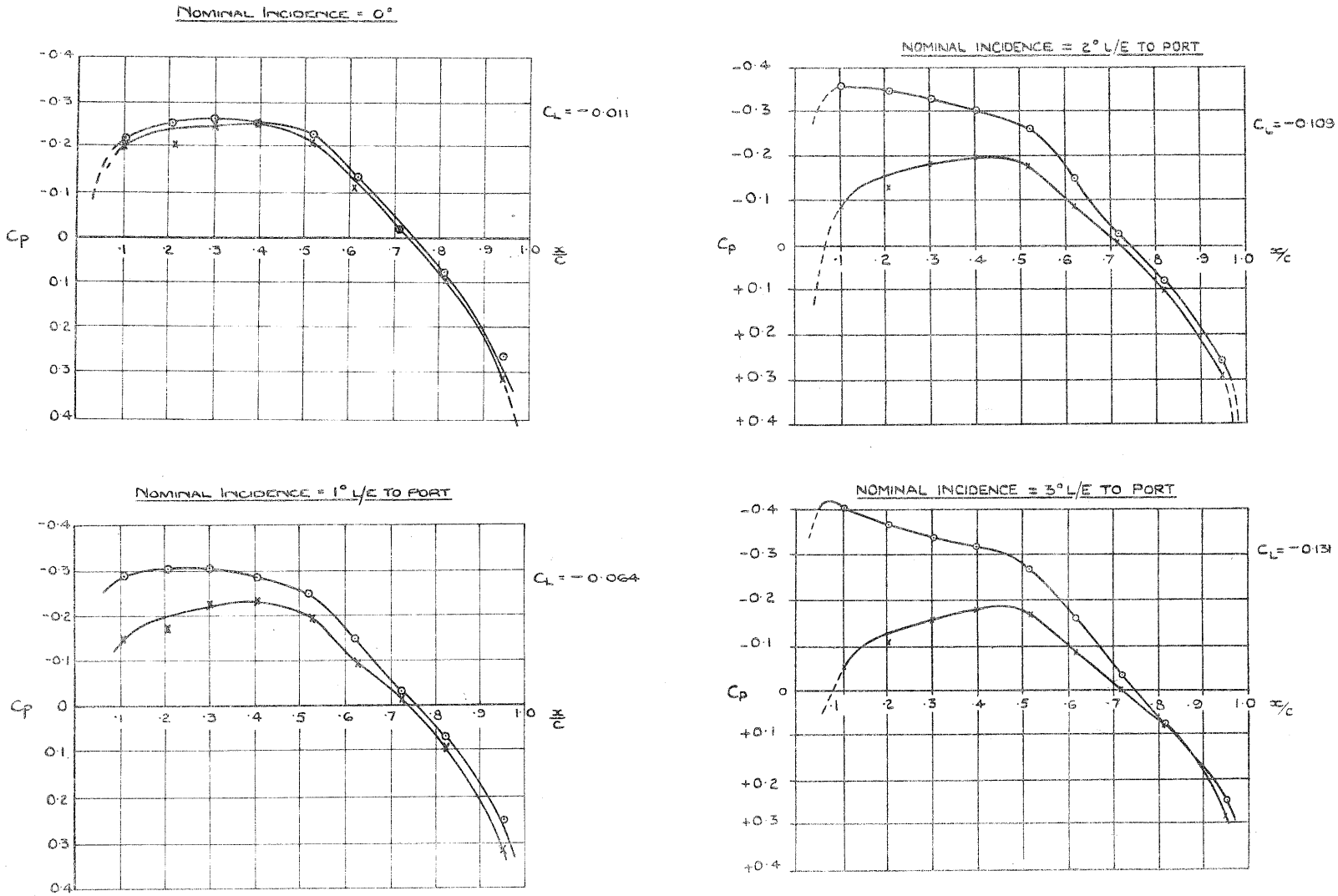

FIG. 29(e), (f), (g), (h) VARIATION OF 50% SPAN CHORDWISE PRESSURE DISTRIBUTION WITH NOMINAL INCIDENCE

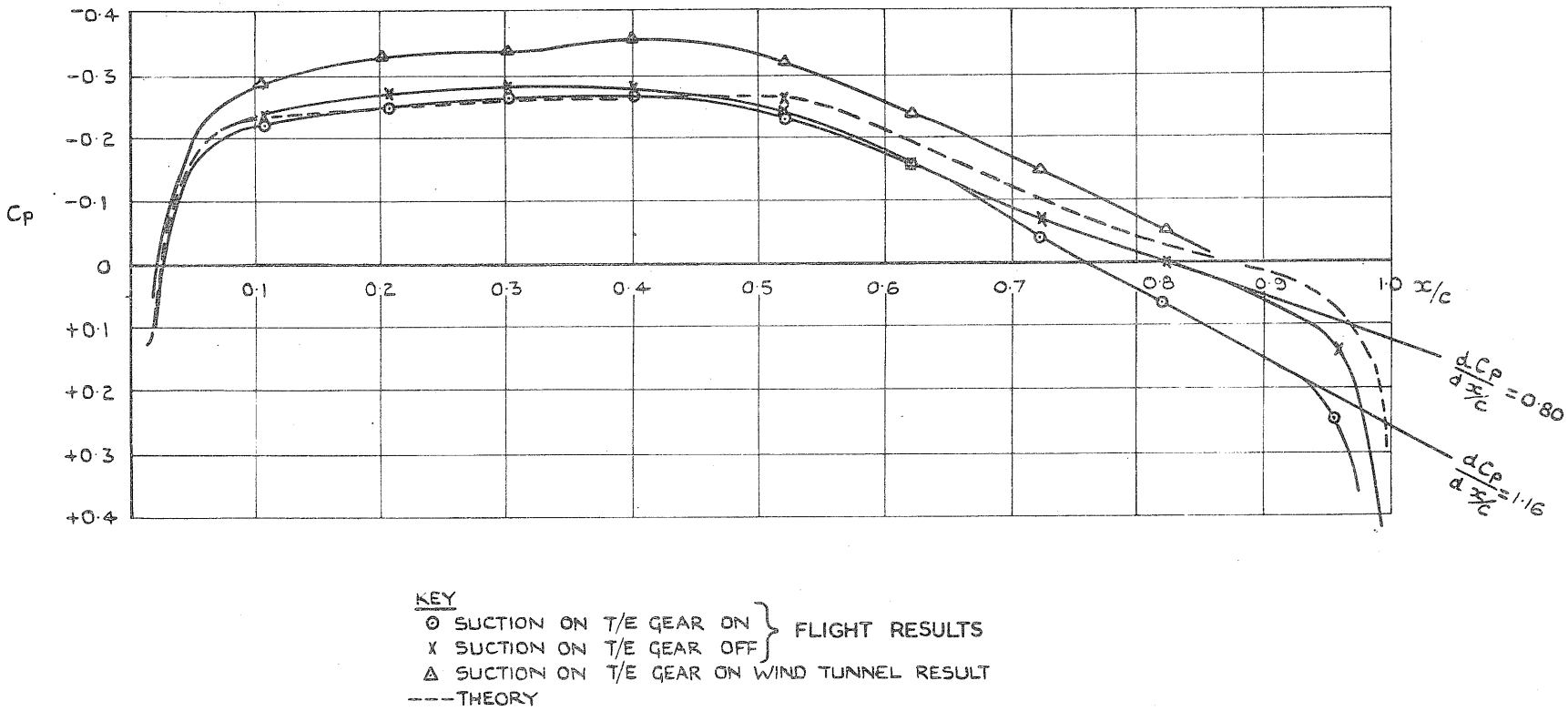

FIG. 30 COMPARISON BETWEEN EXPERIMENTAL AND THEORETICAL CHORDWISE PRESSURE DISTRIBUTION

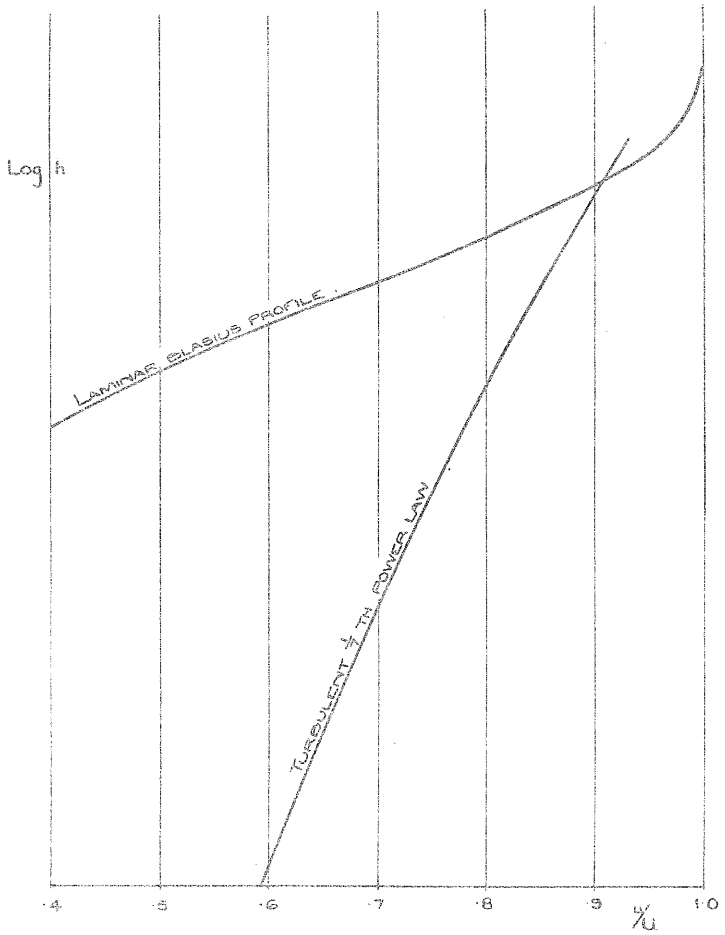

FIG. 31 THEORETICAL BOUNDARY LAYER PROFILES PLOTTED ON A LOG HEIGHT BASIS

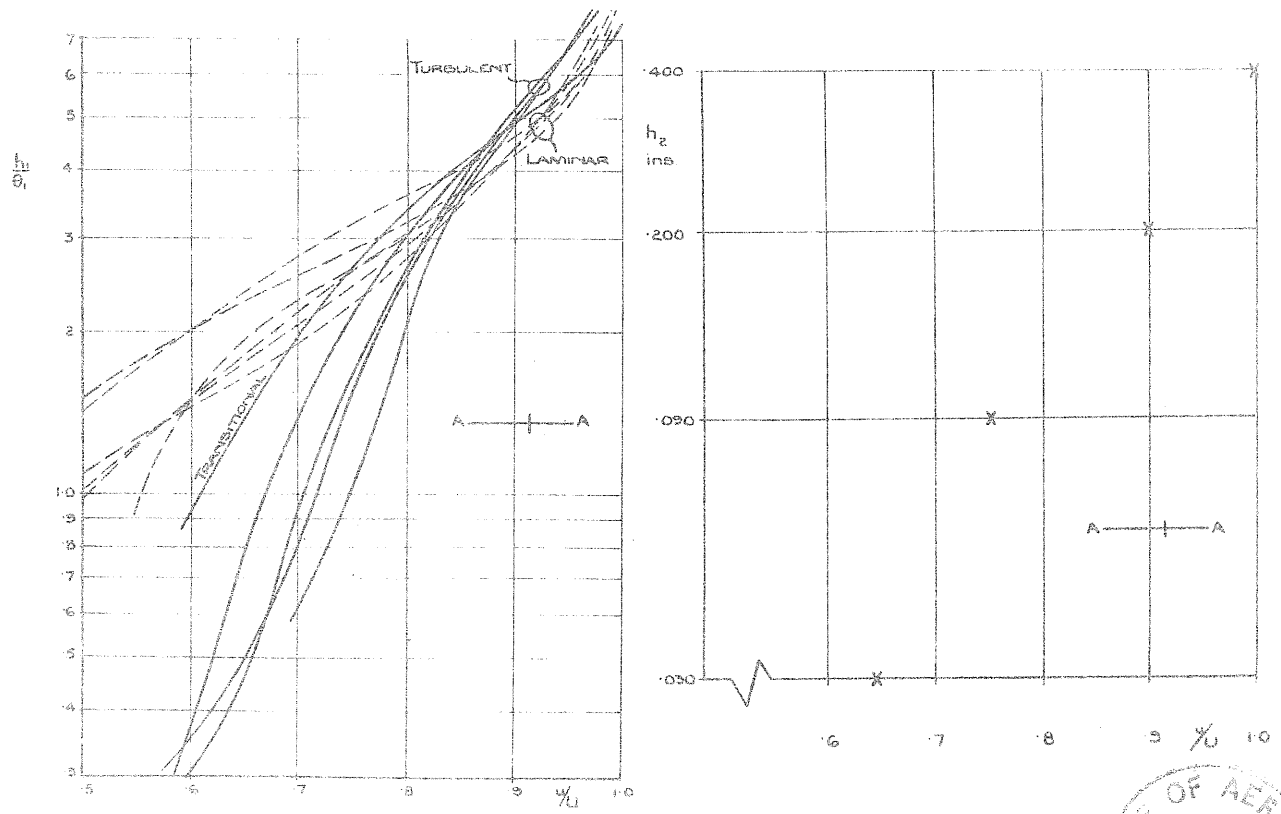

FIG. 32(a) NON DIMENSIONALISED EXPERIMENTAL BOUNDARY LAYER PROFILES

FIG. 32(b) TYPICAL EXAMPLE OF RESULT OBTAINED FROM A FOUR TUBE PITOT COMB

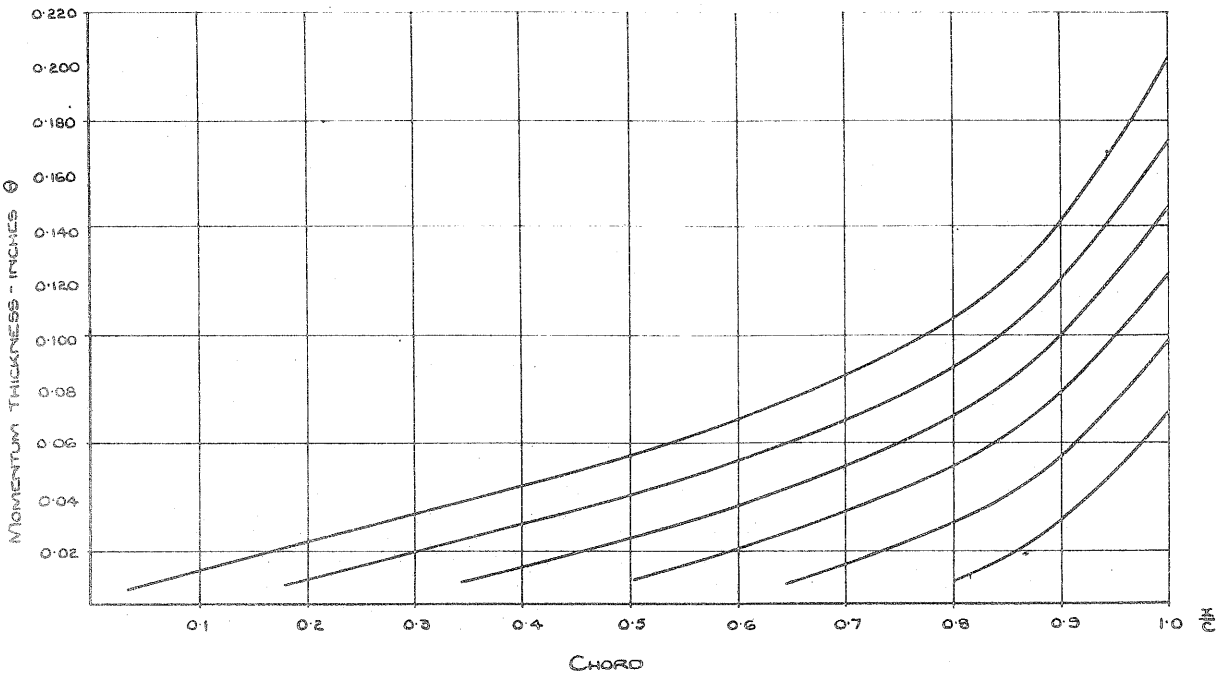

FIG. 33(a) THEORETICAL CHORDWISE GROWTH OF BOUNDARY LAYER MOMENTUM THICKNESS FOR VARIOUS TRANSITION POINTS

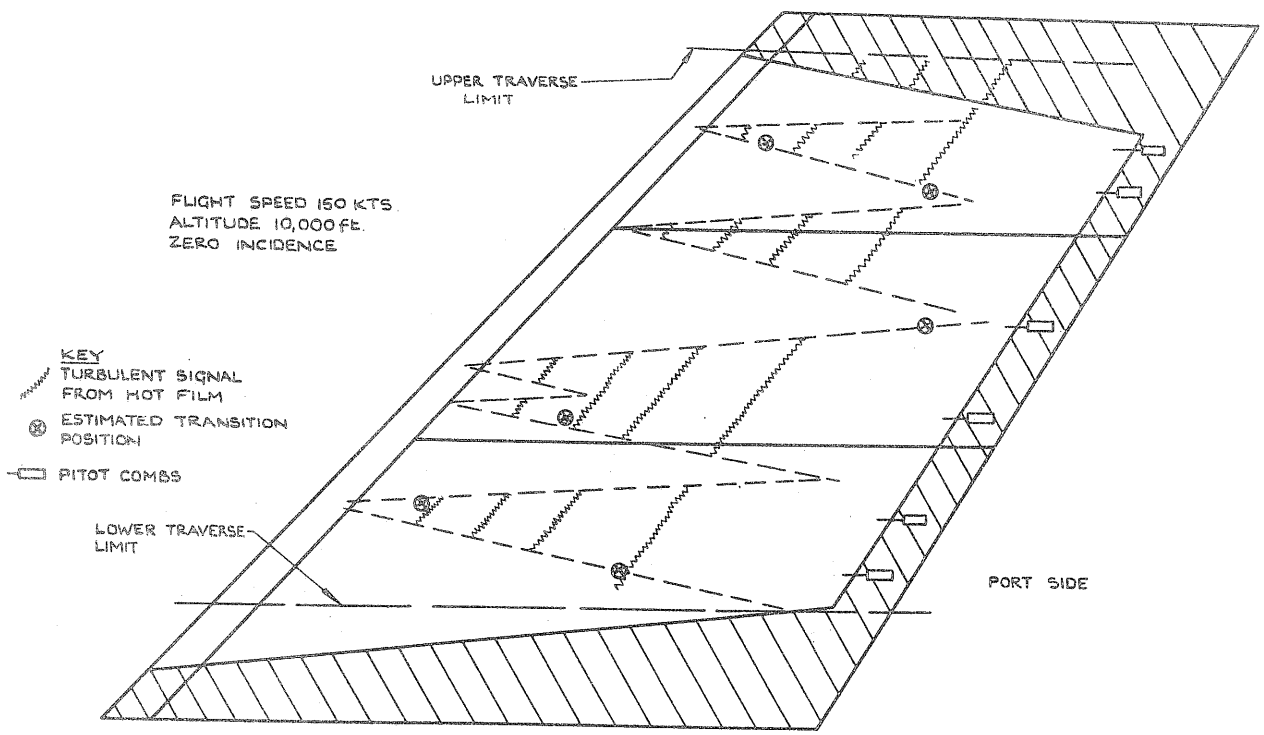

FIG. 33(b) COMPARISON OF TRANSITION PREDICTION FROM 90% CHORD INSTRUMENTATION AND HOT FILM TRAVERSE

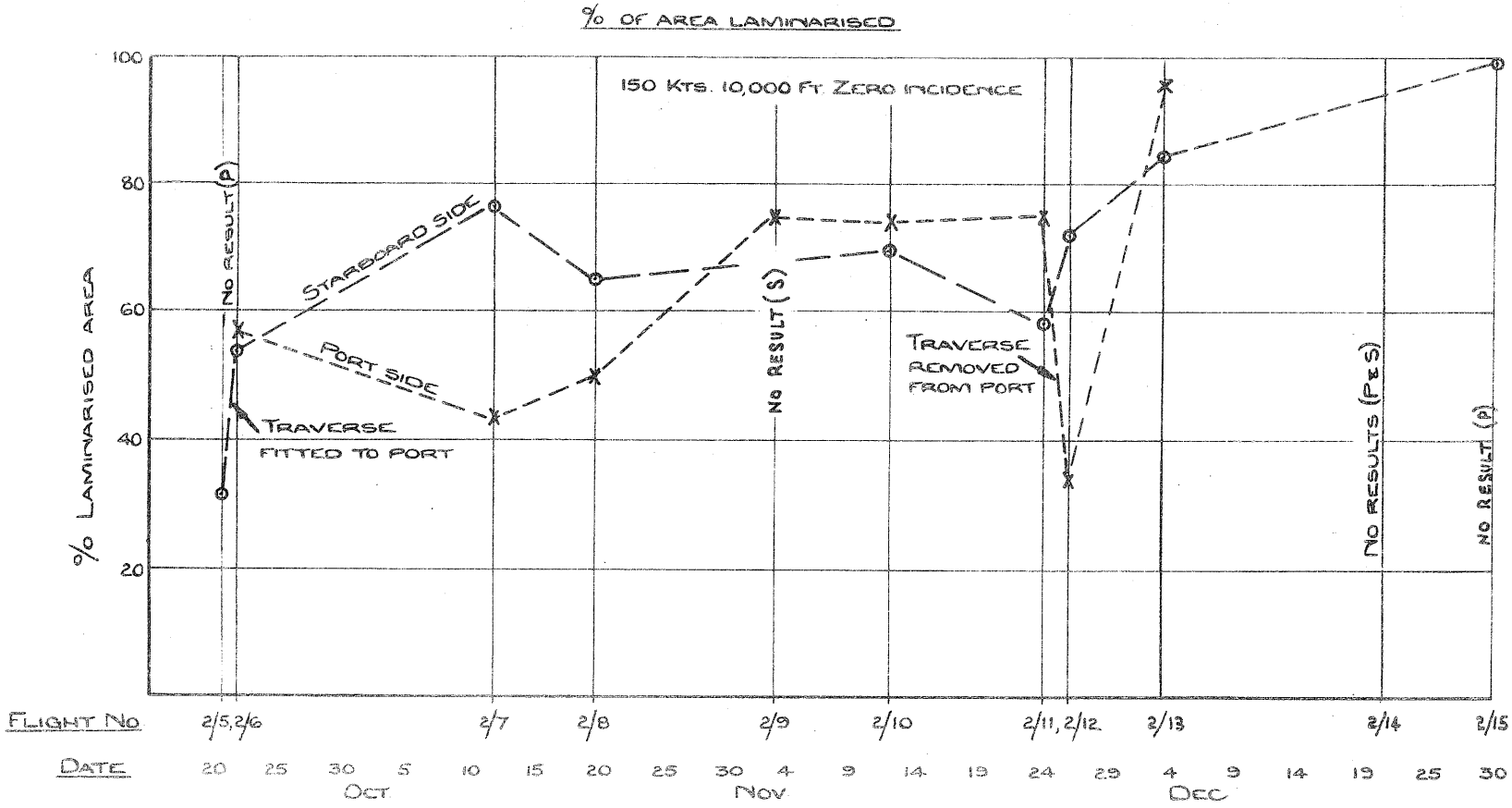

FIG. 34 OPERATIONAL REPEATABILITY

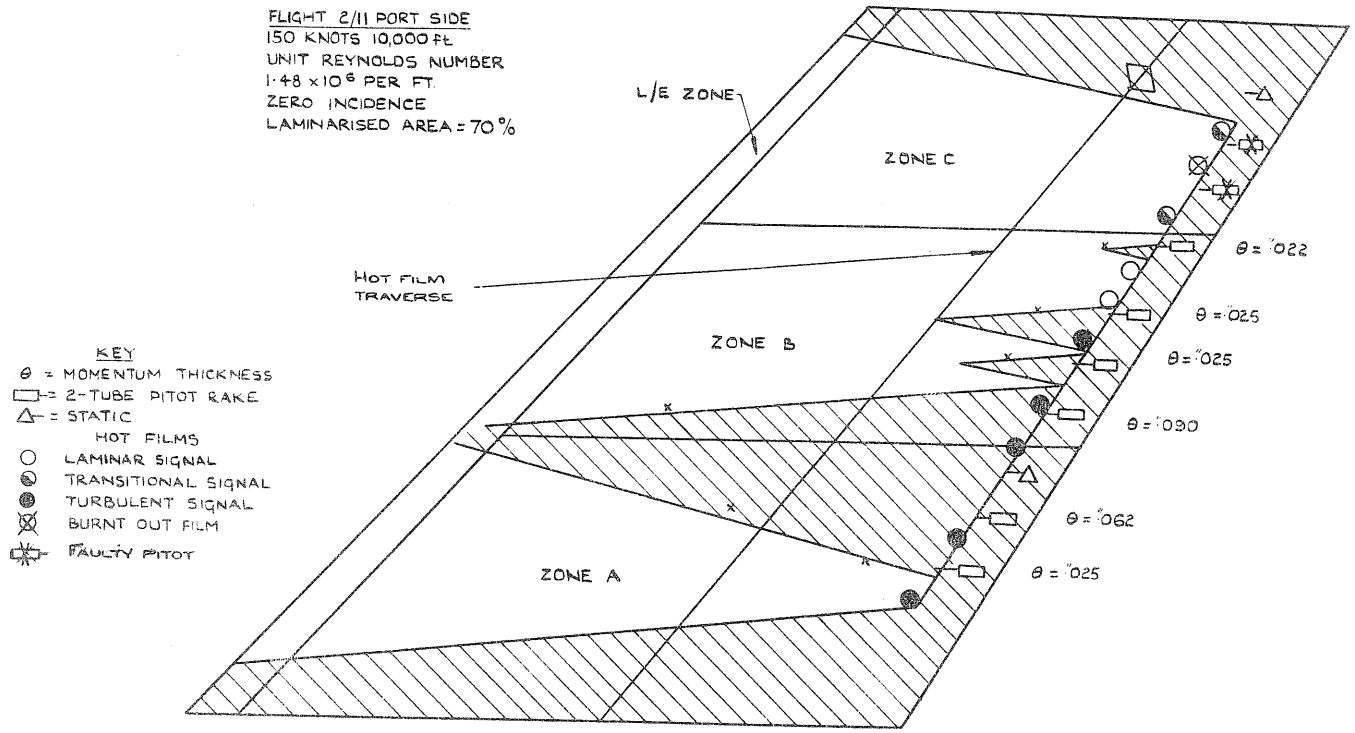

FIG. 35 TYPICAL RESULT FOR PORT SURFACE

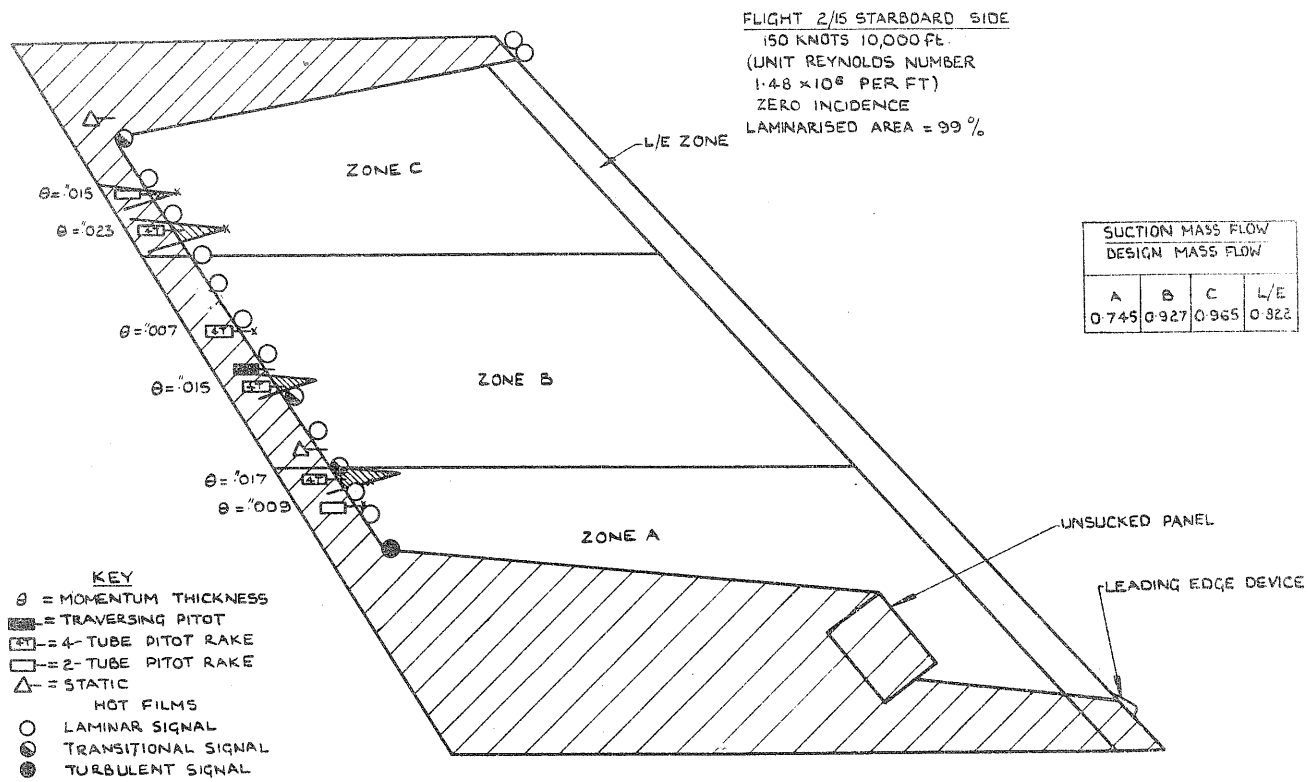

FIG. 36(a) BEST RESULTS OBTAINED ON STARBOARD SURFACE UNIT REYNOLDS NUMBER = 1.48 x 10^6 PER FT.

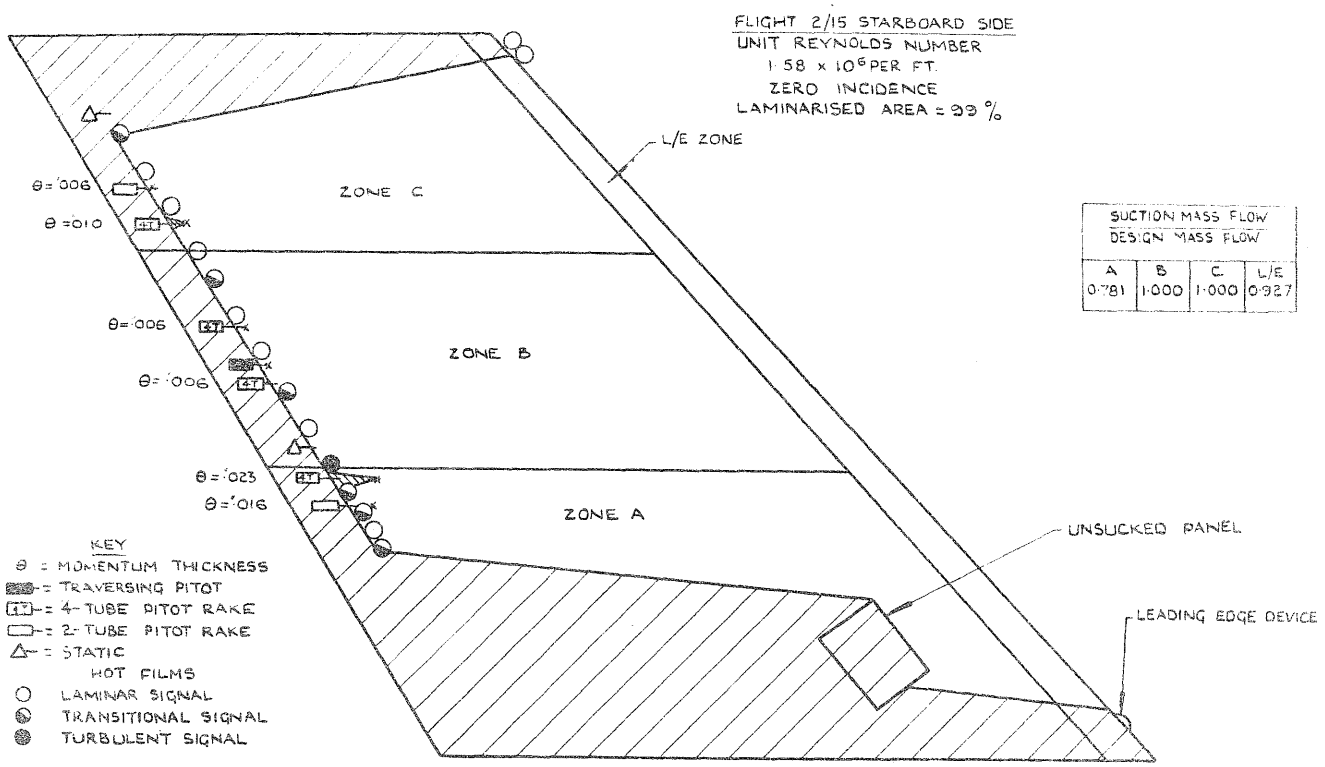

FIG. 36(b) BEST RESULTS OBTAINED ON STARBOARD SURFACE UNIT REYNOLDS NUMBER = 1.58 x 10^6 PER FT.

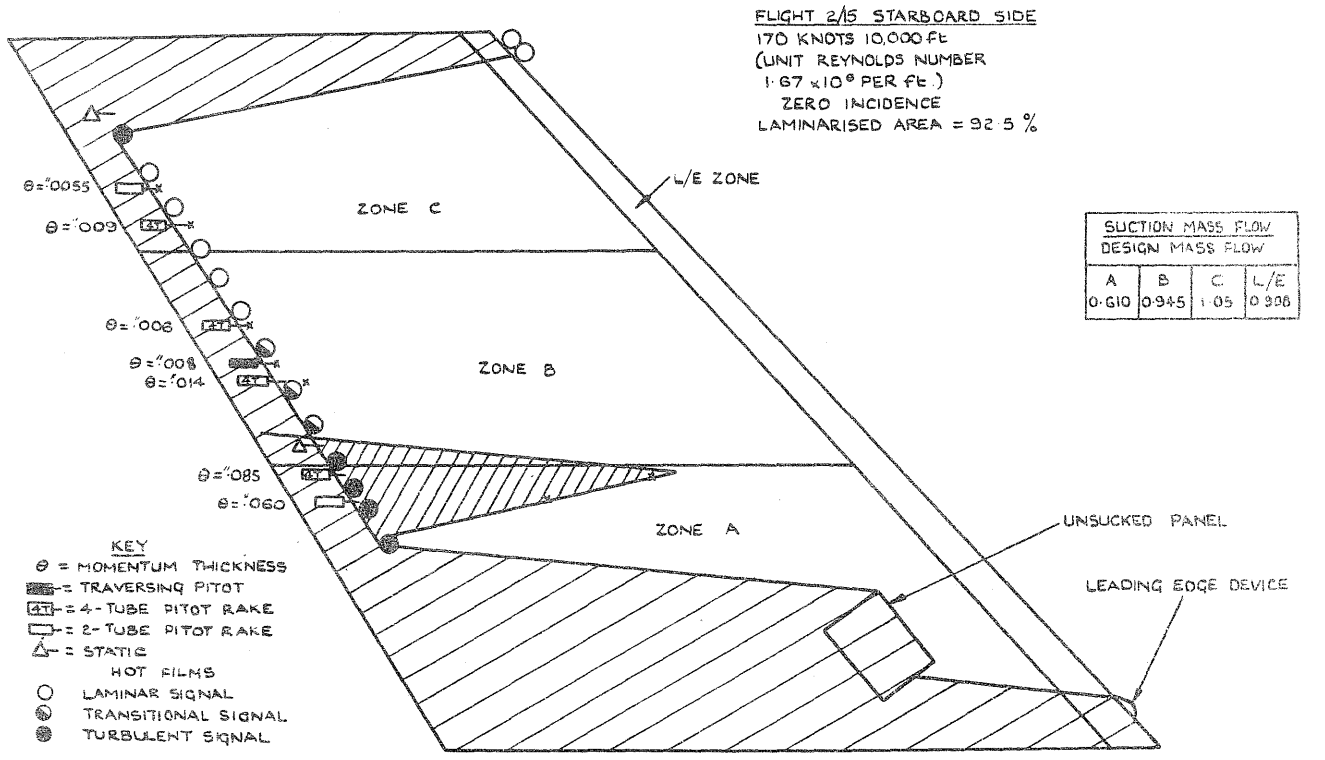

FIG. 36(c) BEST RESULTS OBTAINED ON STARBOARD SURFACE UNIT REYNOLDS NUMBER = 1.67 x 10^6 PER FT.

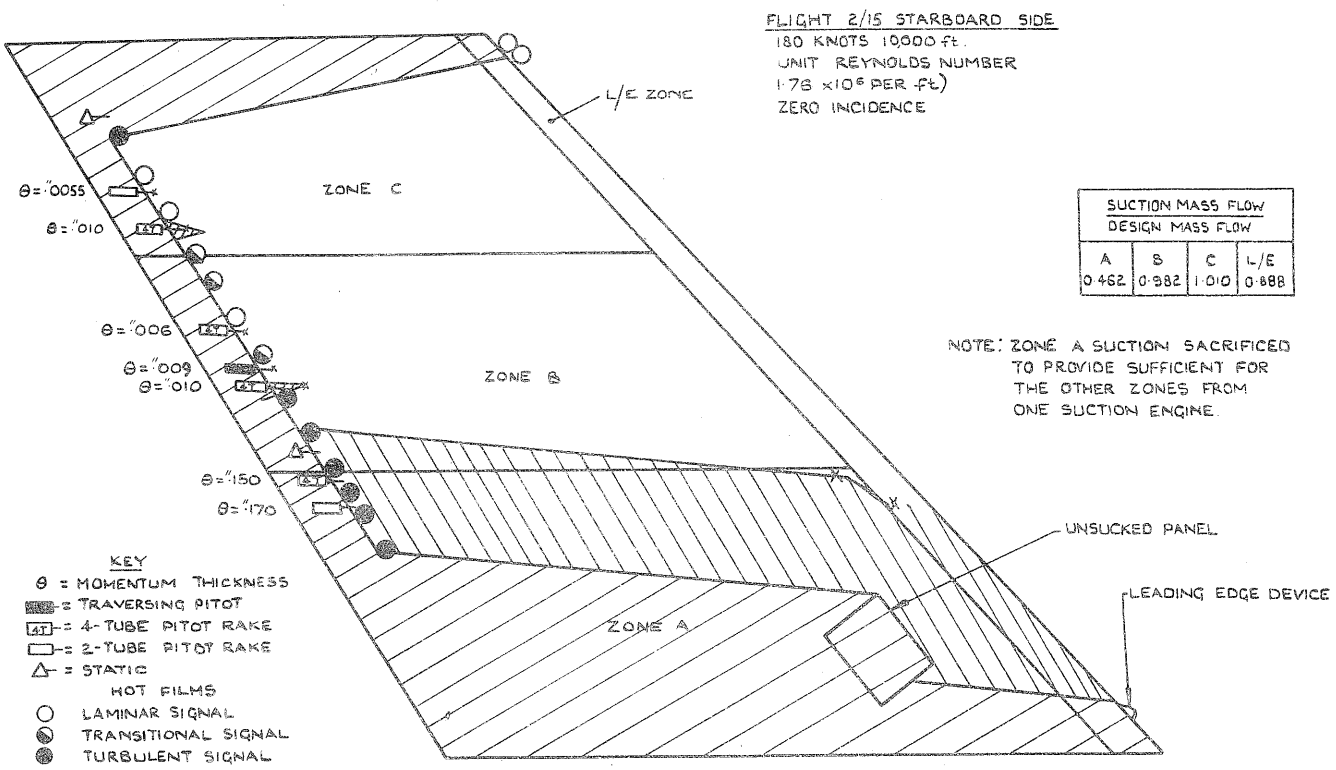

FIG. 36(d) BEST RESULTS OBTAINED ON STARBOARD SURFACE UNIT REYNOLDS NUMBER = 1.76 x 10^6 PER FT.

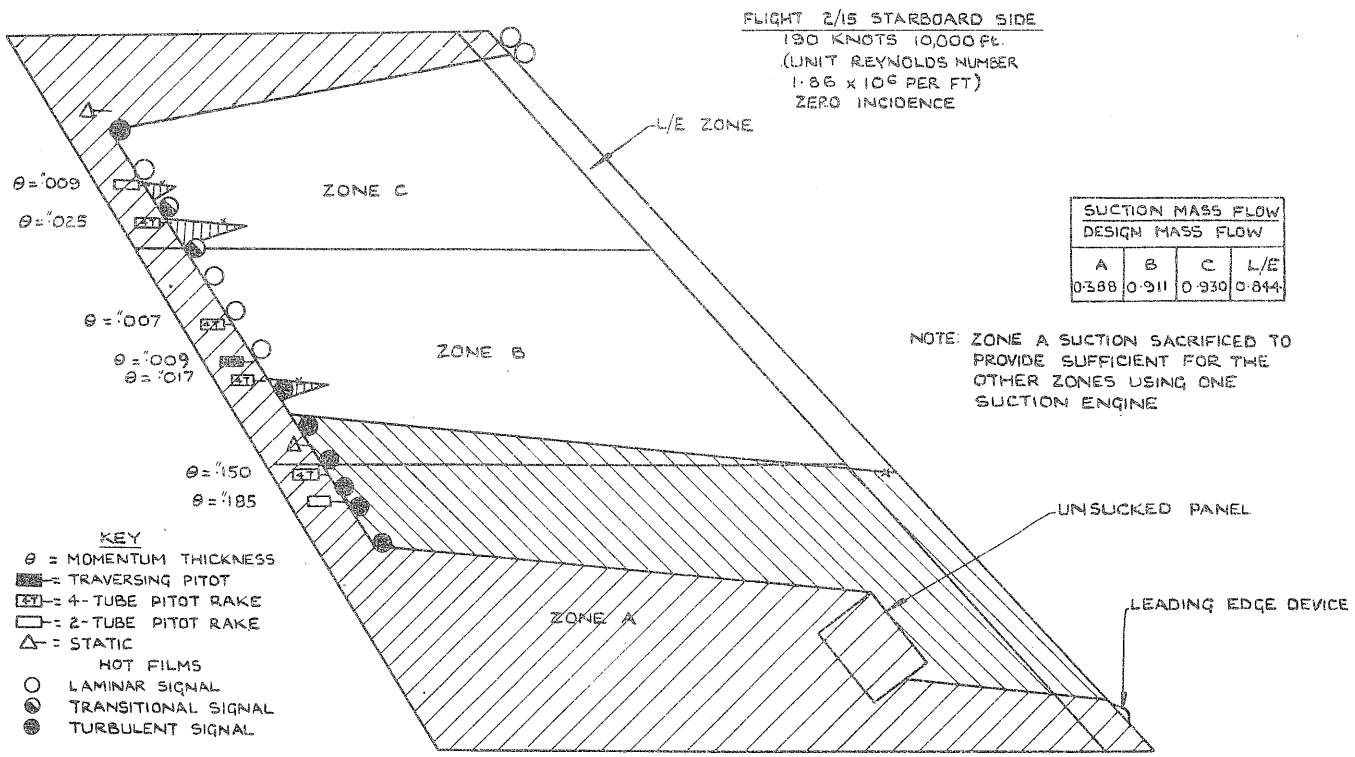

FIG. 36(e) BEST RESULTS OBTAINED ON STARBOARD SURFACE UNIT REYNOLDS NUMBER = 1.86 x 10^6 PER FT.

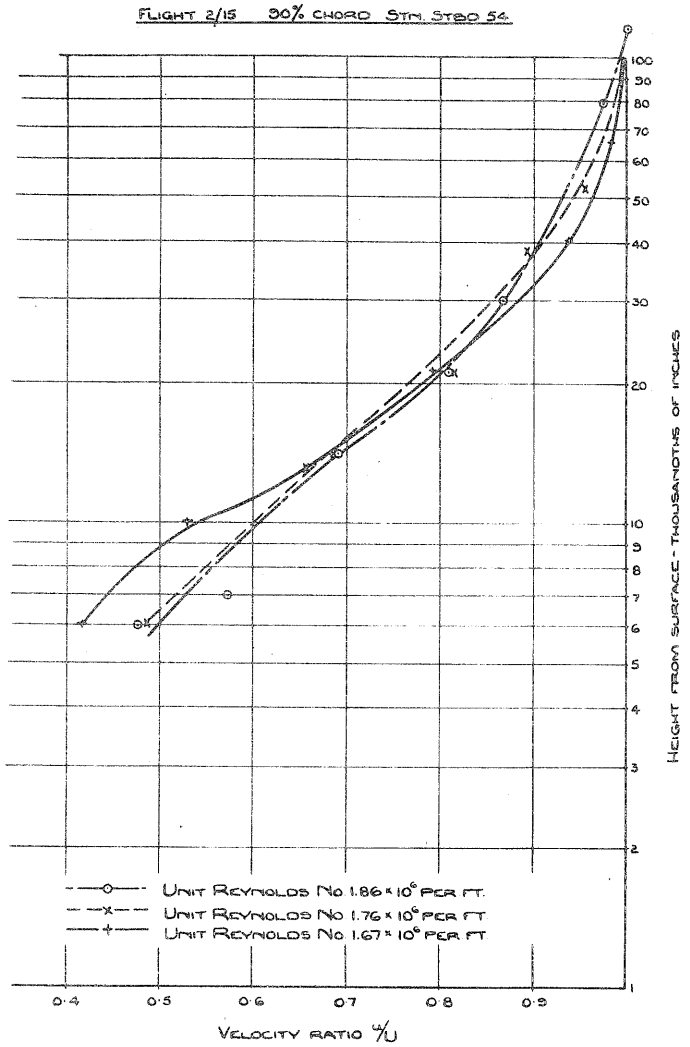

(a) VELOCITY PROFILES

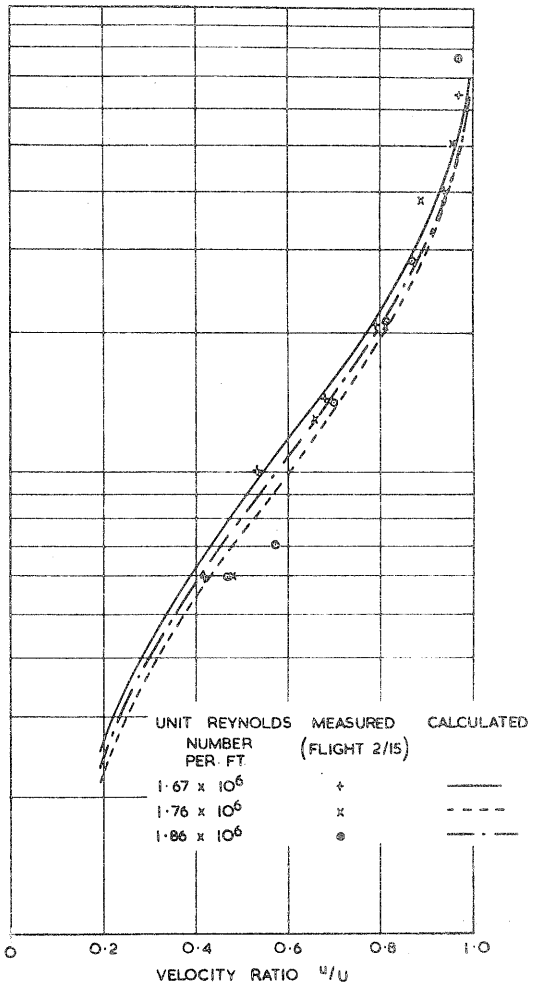

(c) COMPARISON WITH THEORY

FLIGHT 2/15
30% CHORD STARBOARD STN. 554

FLIGHT SPEED KNOTS EAS AT 10,000 FT.	MOMENTUM THICKNESS θ INCHES	UNIT REYNOLDS No u/ν
170	·0077	1·67 × 10⁶
180	·0087	1·76 × 10⁶
190	·0054	1·86 × 10⁶

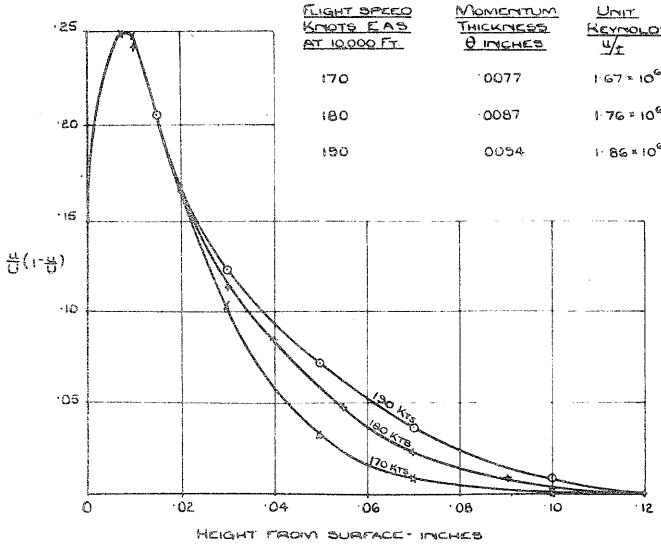

(b) $\frac{u}{U}\left(1-\frac{u}{U}\right)$ PLOTS

FIG. 37 TRAVERSING PITOT RESULTS AT 90% CHORD MID SPAN

FLIGHT 2/13

170 KNOTS E.A.S. 30% CHORD

10,000 Ft

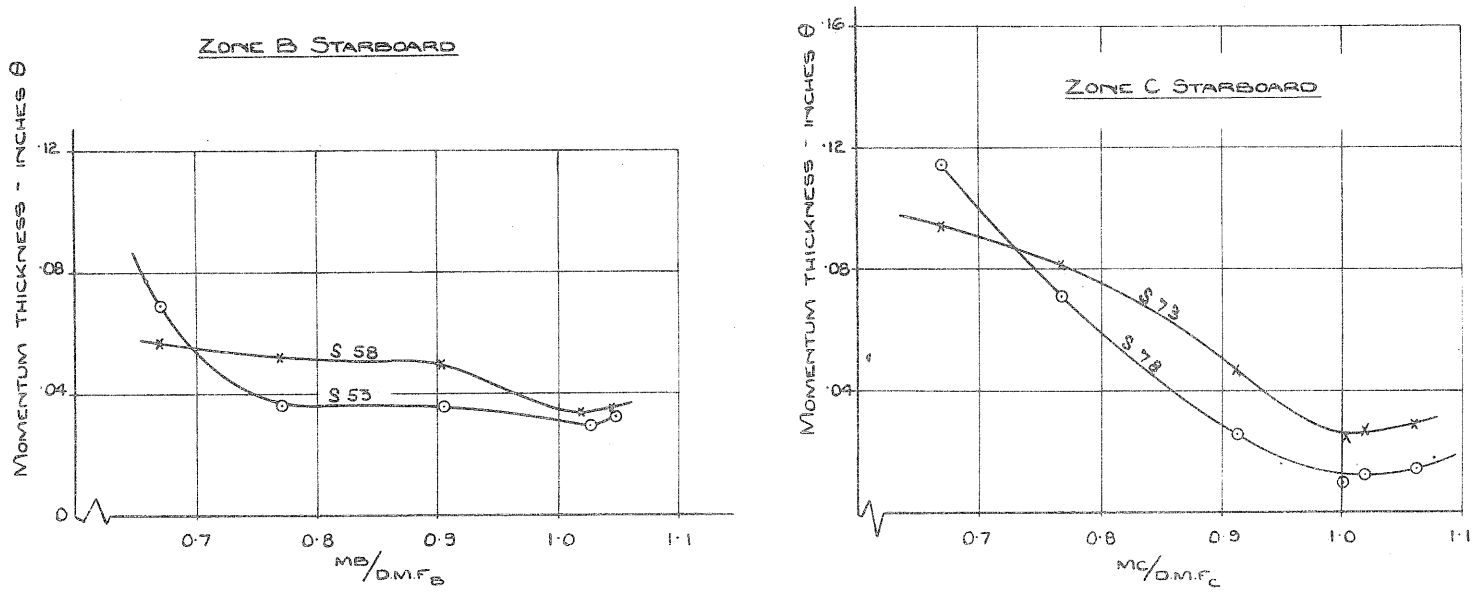

FLIGHT 2/13 170KTS 10000 ft. STARBOARD SIDE α = 0

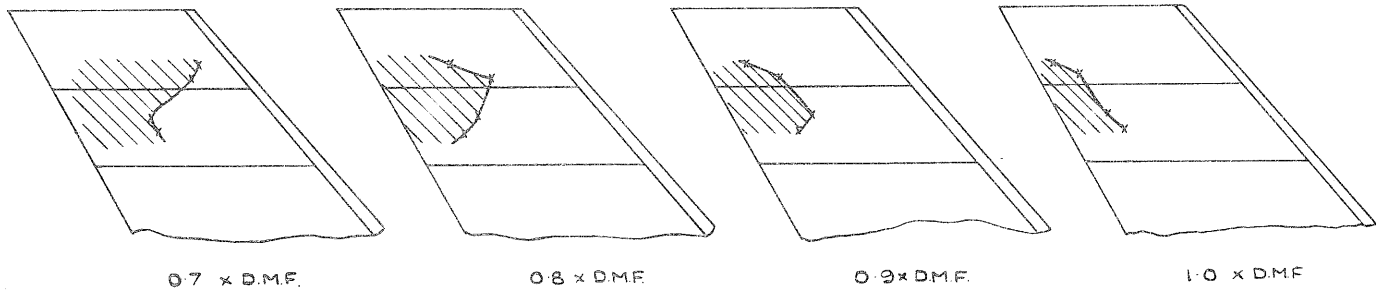

FIG. 38(a), (b), (c) THE EFFECT OF VARYING ZONE SUCTION, AT 170 KTS EAS - STARBOARD SURFACE

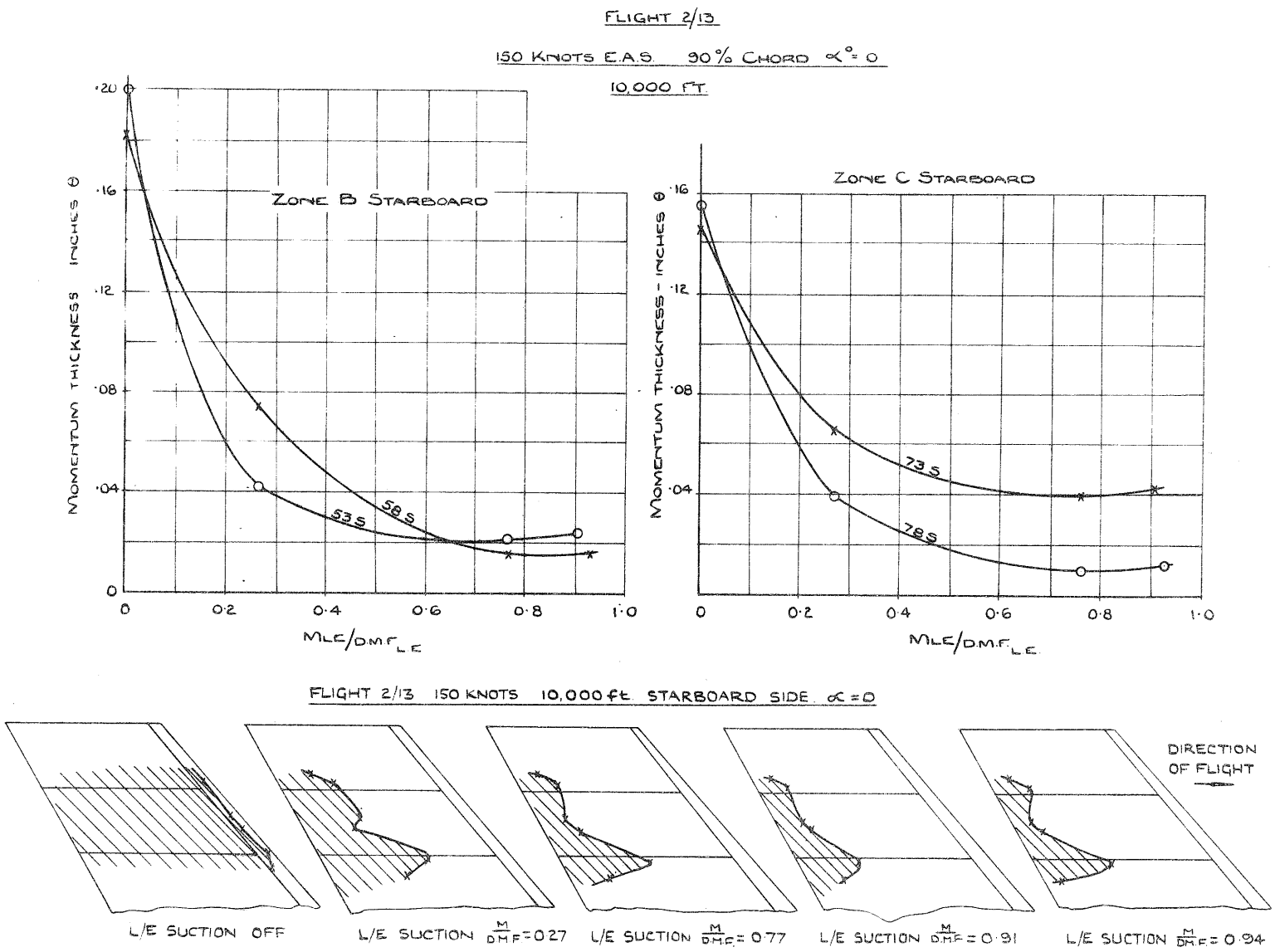

FIG. 39(a), (b), (c) THE EFFECT OF VARYING LEADING EDGE SUCTION AT 150 KTS EAS - STARBOARD SURFACE

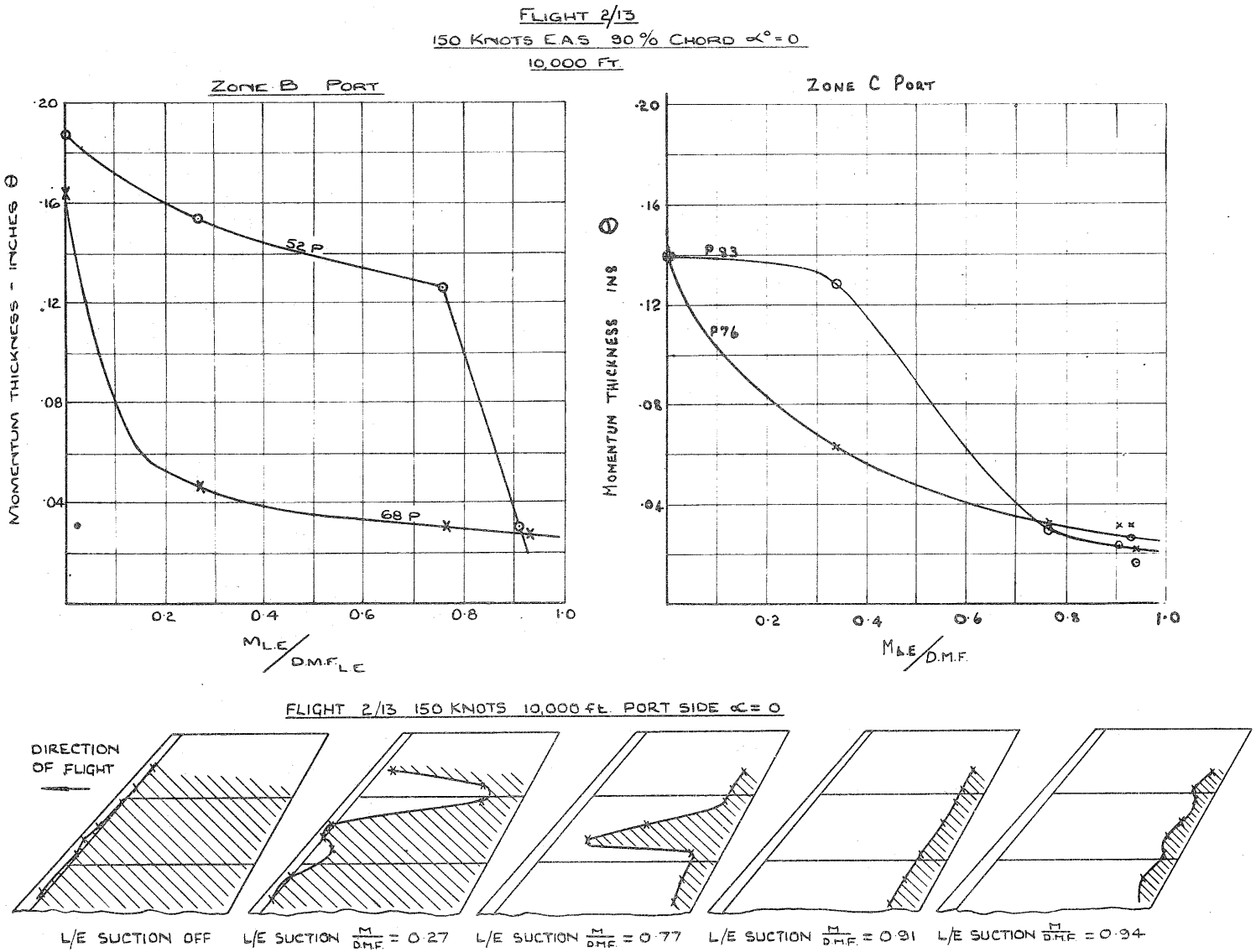

FIG. 40(a), (b), (c) THE EFFECT OF VARYING LEADING EDGE SUCTION AT 150 KTS EAS - PORT SURFACE

FLIGHT 2/10

150 KNOTS E.A.S. 90% CHORD

10,000 FT.

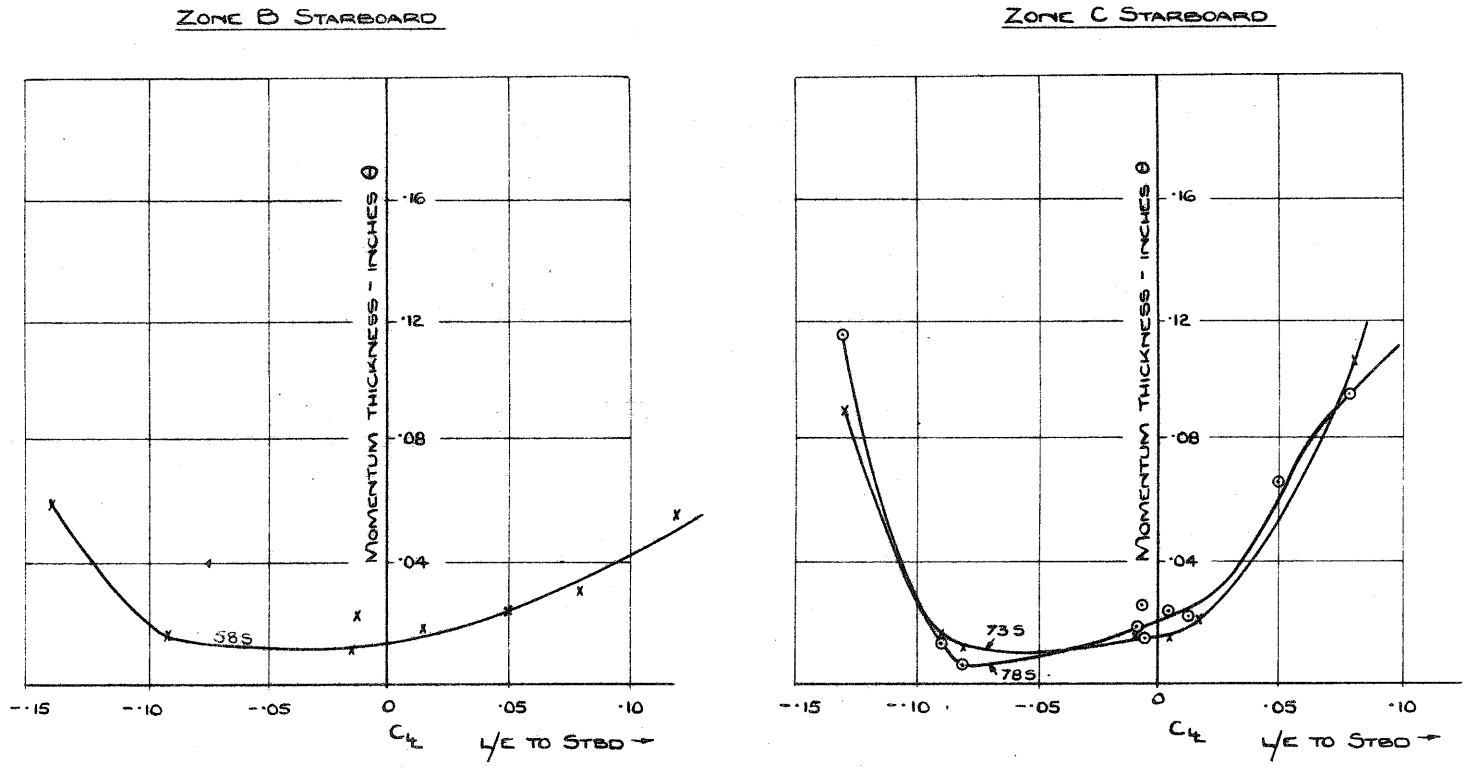

FLIGHT 2/10 150 KNOTS E.A.S. 10,000 FT. CONSTANT C_Q = 0·00059 STARBOARD SIDE

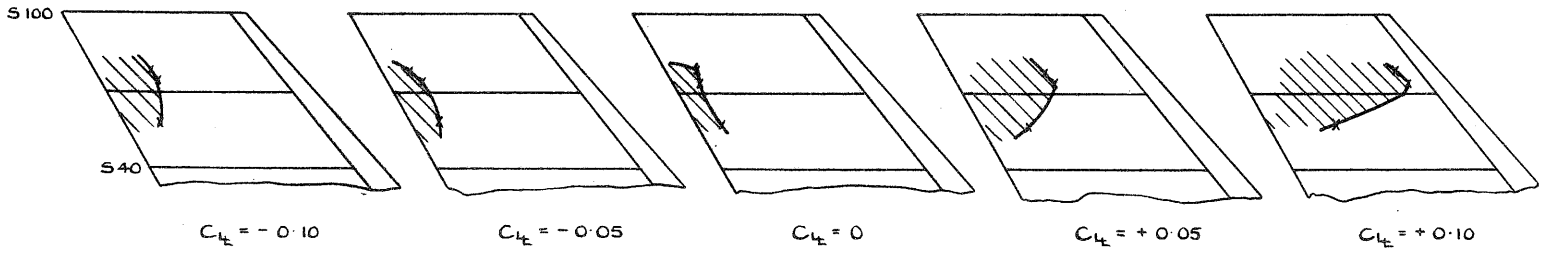

FIG. 41(a), (b), (c) THE EFFECT OF VARYING LIFT COEFFICIENT AT 150KTS EAS - STARBOARD SURFACE

FLIGHT 2/12

160 KNOTS E.A.S 90% CHORD

10,000 FT

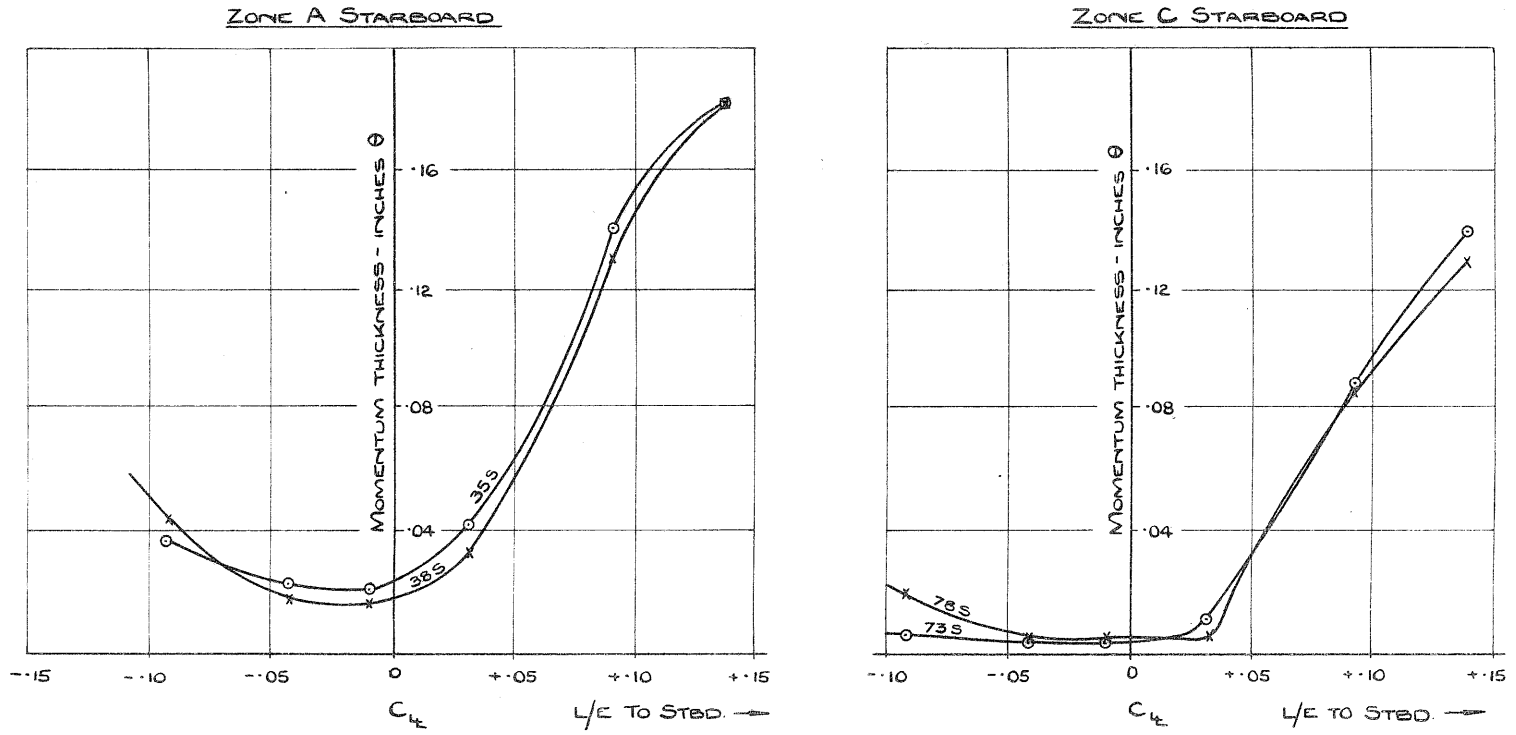

FLIGHT 2/12 160 KNOTS E.A.S. 10,000 FT CONSTANT C_Q = 0·000583 STARBOARD SIDE

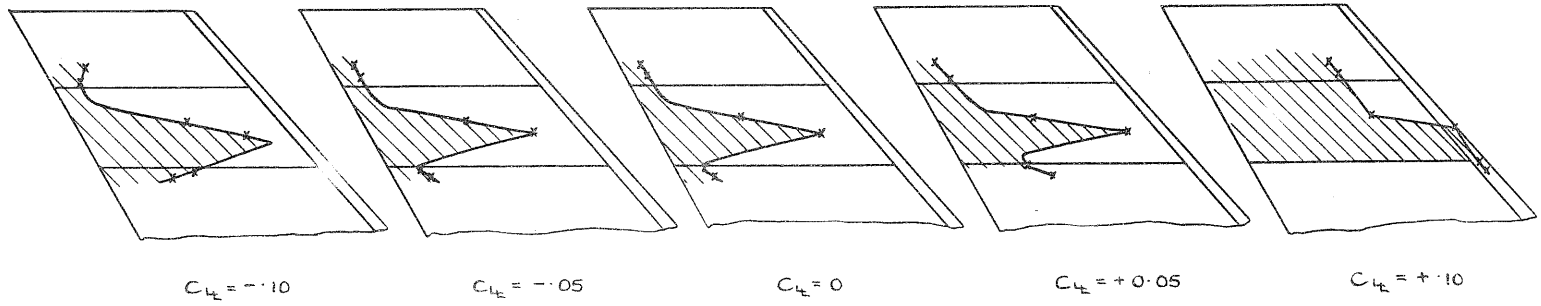

FIG. 42(a), (b), (c) THE EFFECT OF VARYING LIFT COEFFICIENT AT 160KTS EAS - STARBOARD SURFACE

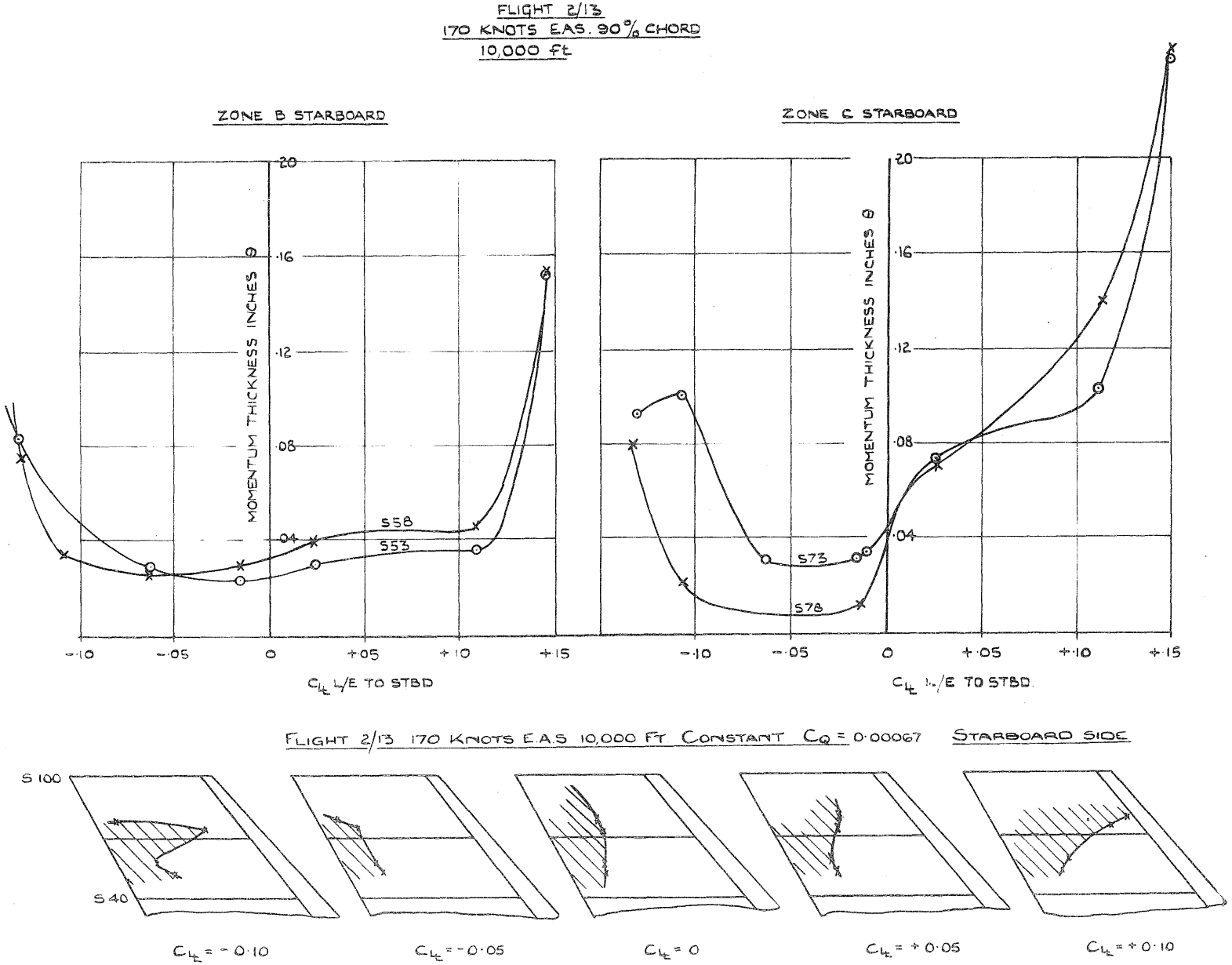

FIG. 43(a), (b), (c) THE EFFECT OF VARYING LIFT COEFFICIENT AT 170KTS EAS - STARBOARD SURFACE

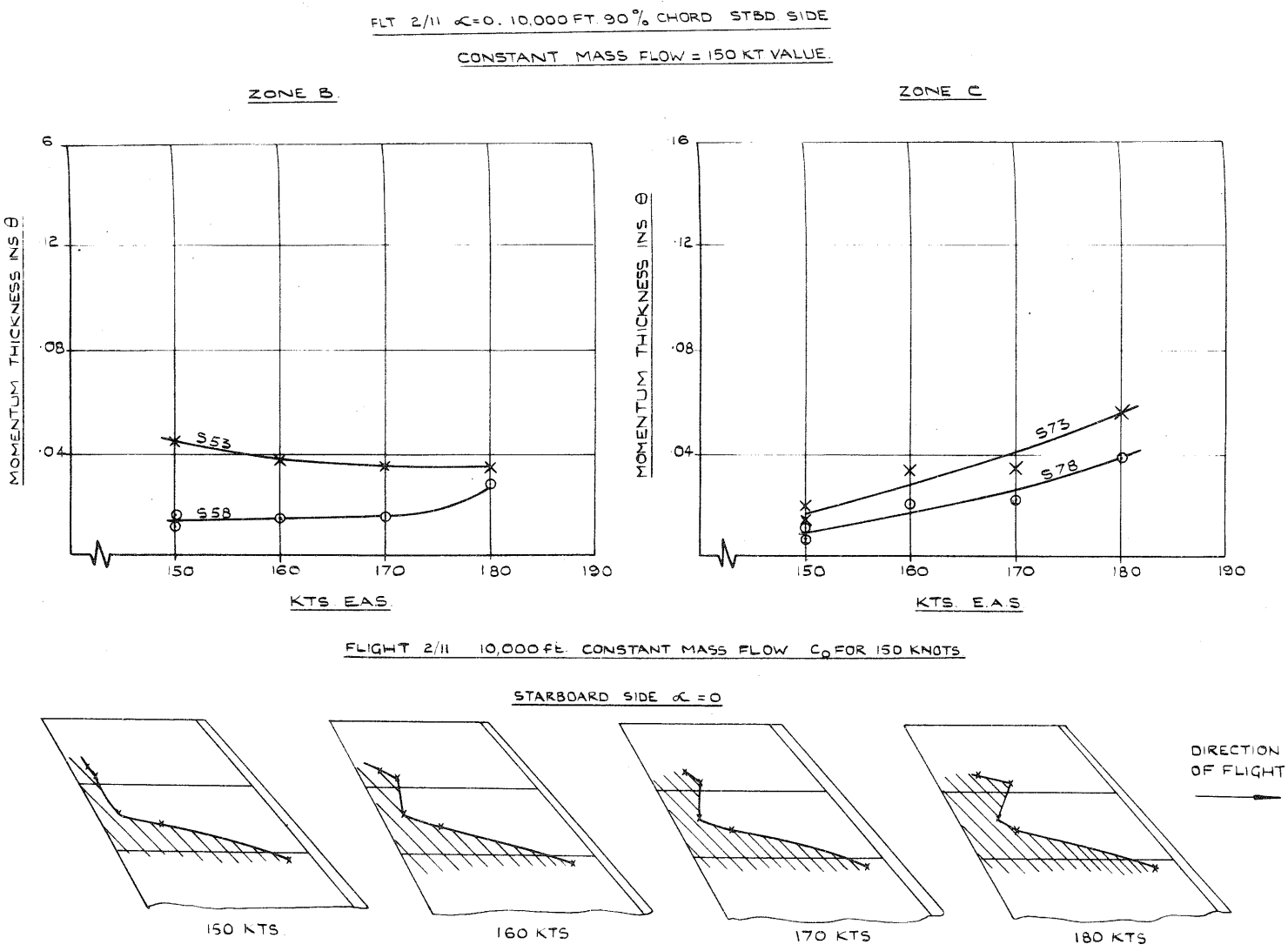

FIG. 44(a), (b), (c) THE EFFECT OF INCREASING SPEED KEEPING ZONE SUCTION CONSTANT - STARBOARD SURFACE

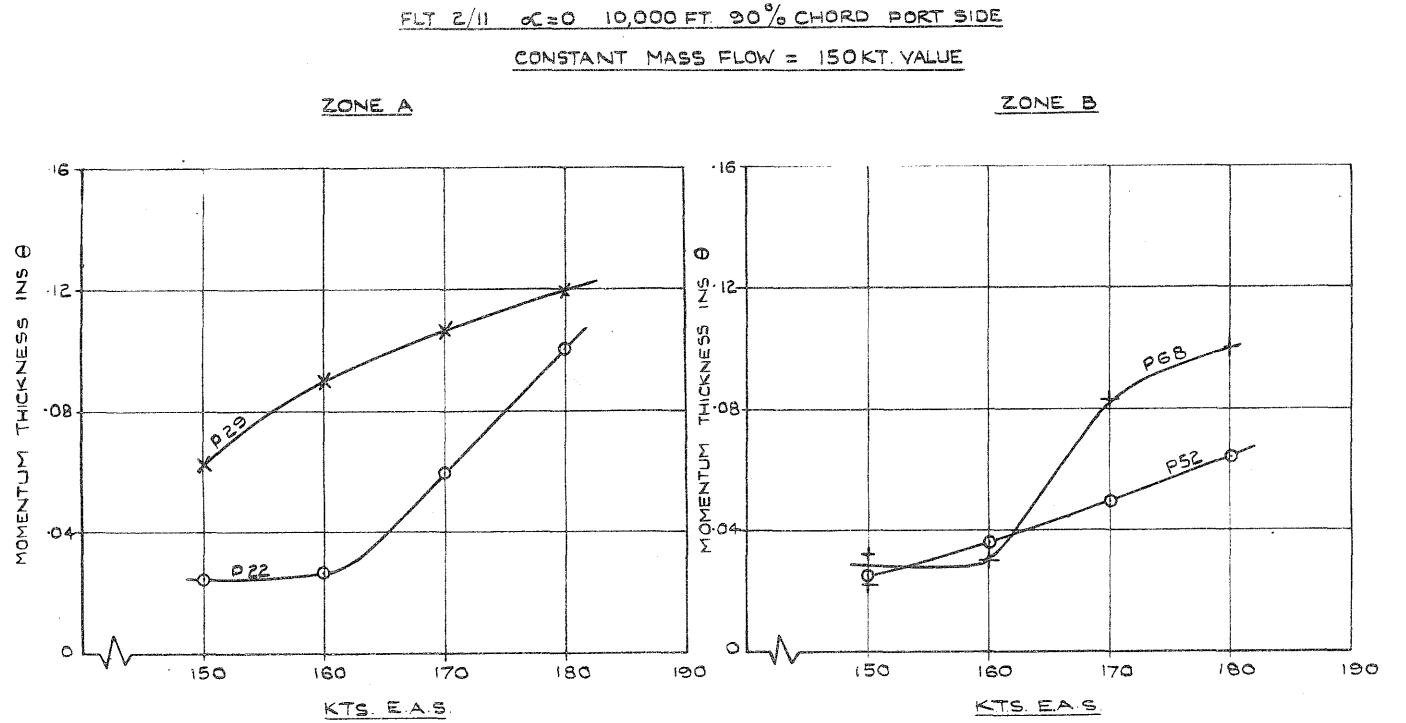

FLIGHT 2/11 10,000FT. CONSTANT MASS FLOW C_Q FOR 150 KNOTS

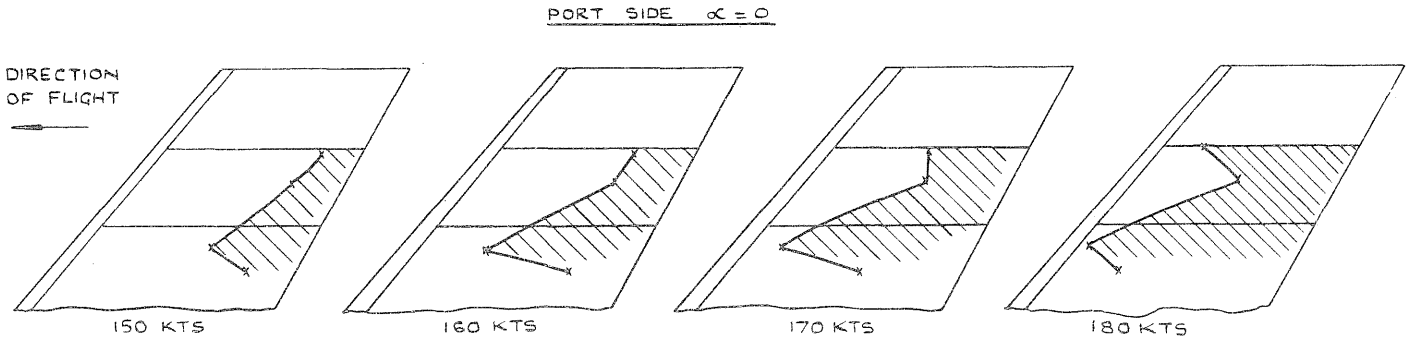

FIG. 45(a), (b), (c) THE EFFECT OF INCREASING SPEED KEEPING ZONE SUCTION CONSTANT - PORT SURFACE

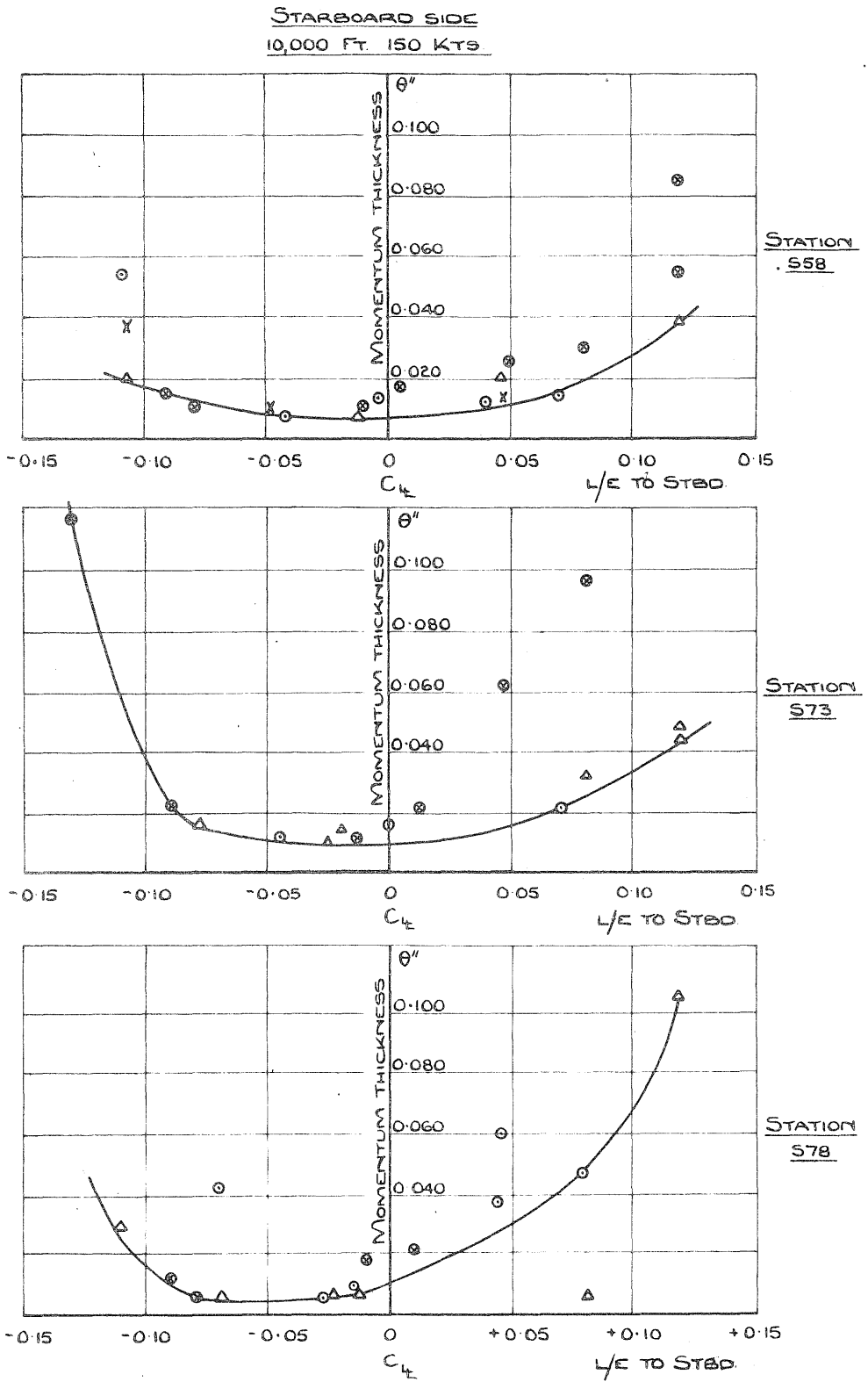

FIG. 46 (a), (b), (c) COMPARISON OF LIFT COEFFICIENT TOLERANCE FOR THREE FLIGHTS

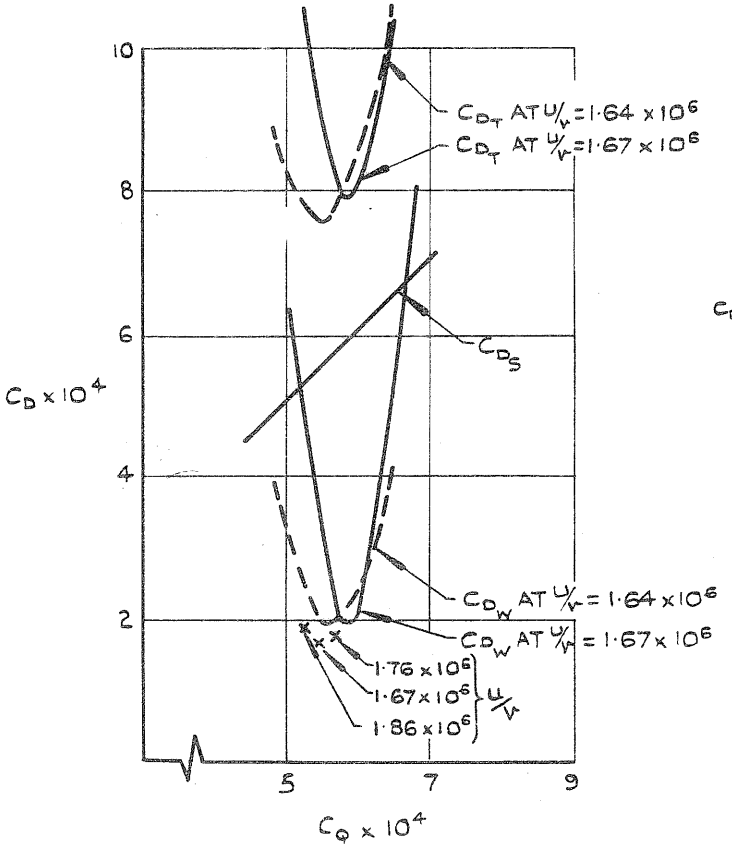

FIG. 47 (a) VARIATION OF DRAG COEFFICIENT WITH SUCTION QUANTITY COEFFICIENT

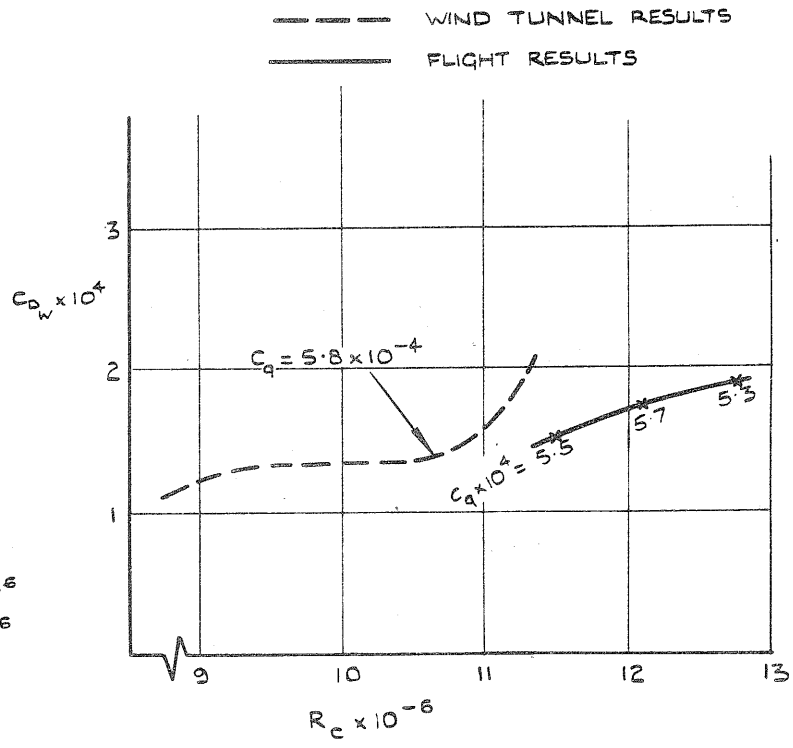

FIG. 47 (b) VARIATION OF DRAG COEFFICIENT WITH CHORD REYNOLDS NUMBER

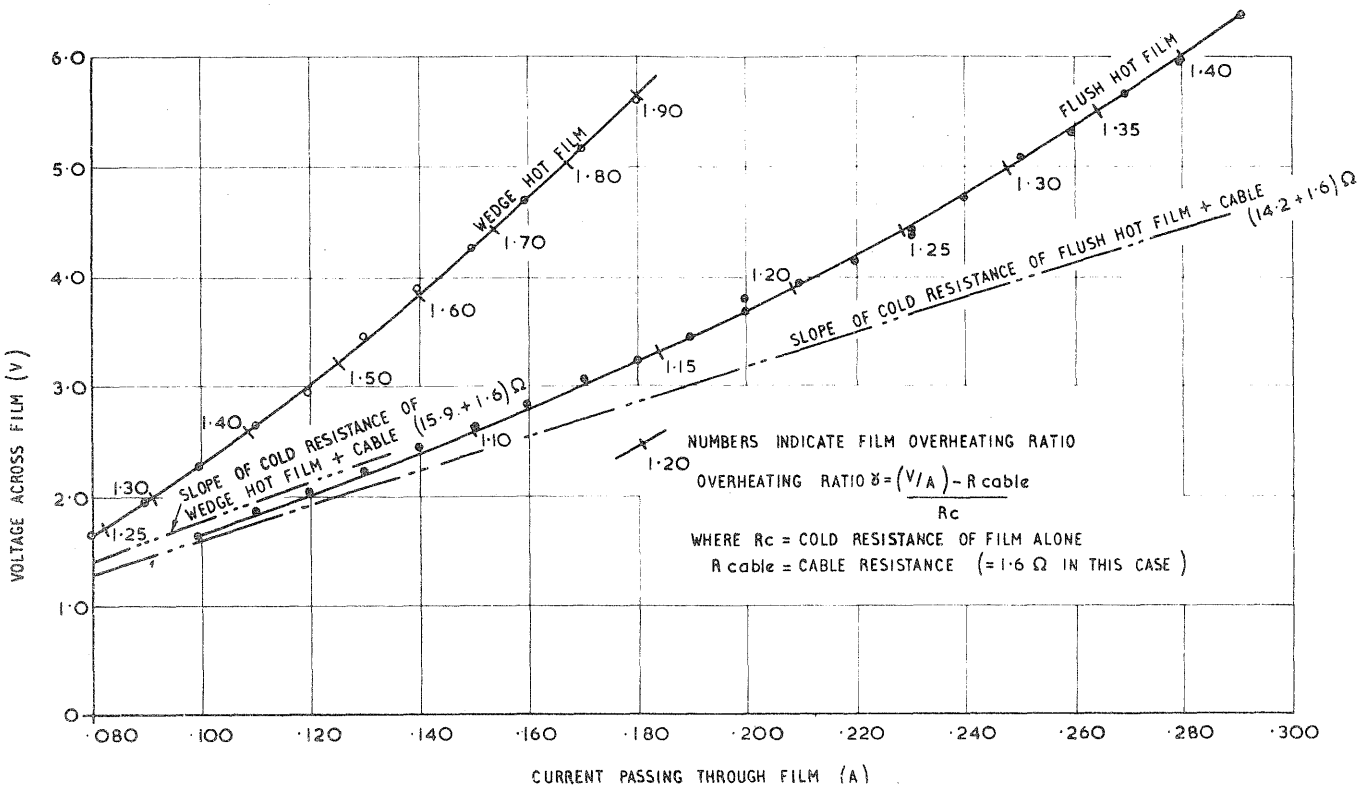

I (1) COMPARISON OF FLUSH AND WEDGE TYPE HOT FILM OPERATING CHARACTERISTICS

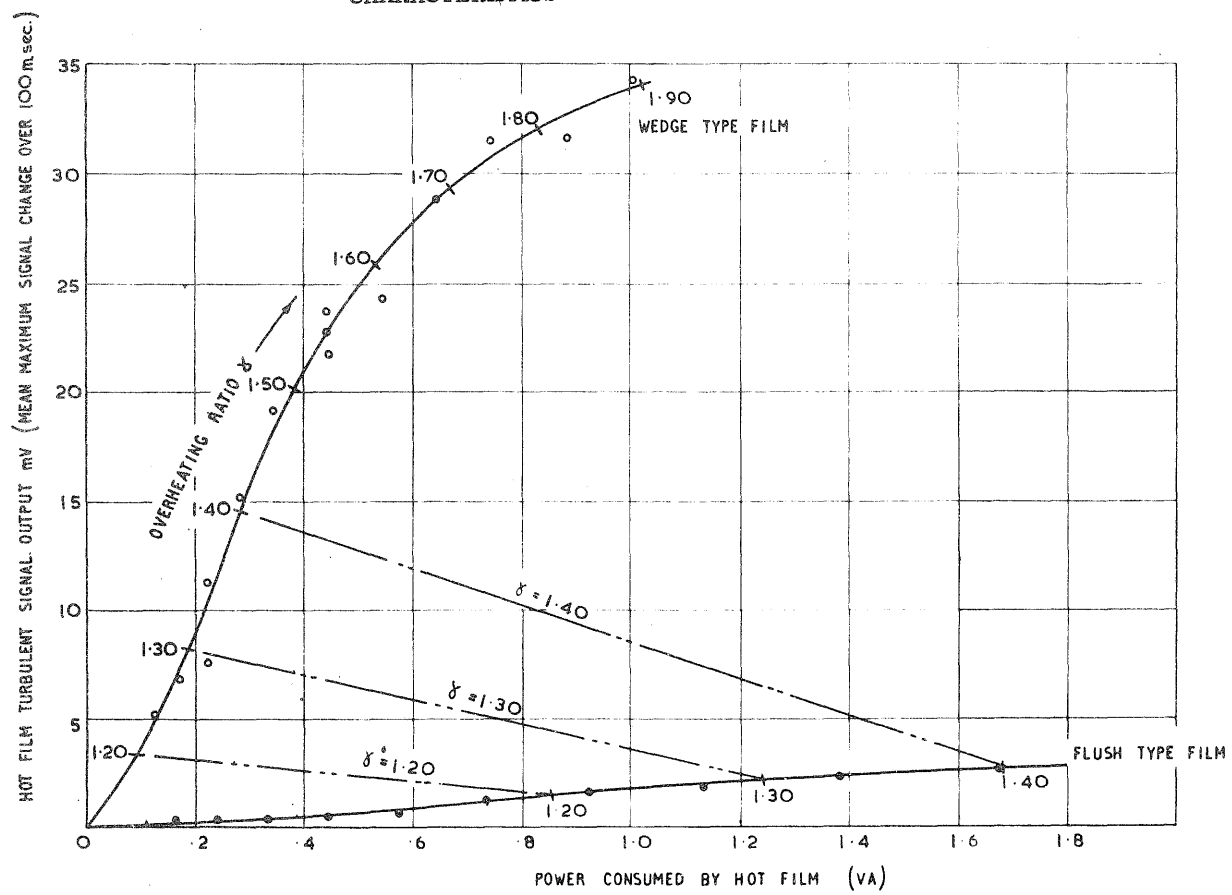

I (2) COMPARISON OF FLUSH AND HOT FILM SIGNAL OUTPUT LEVELS

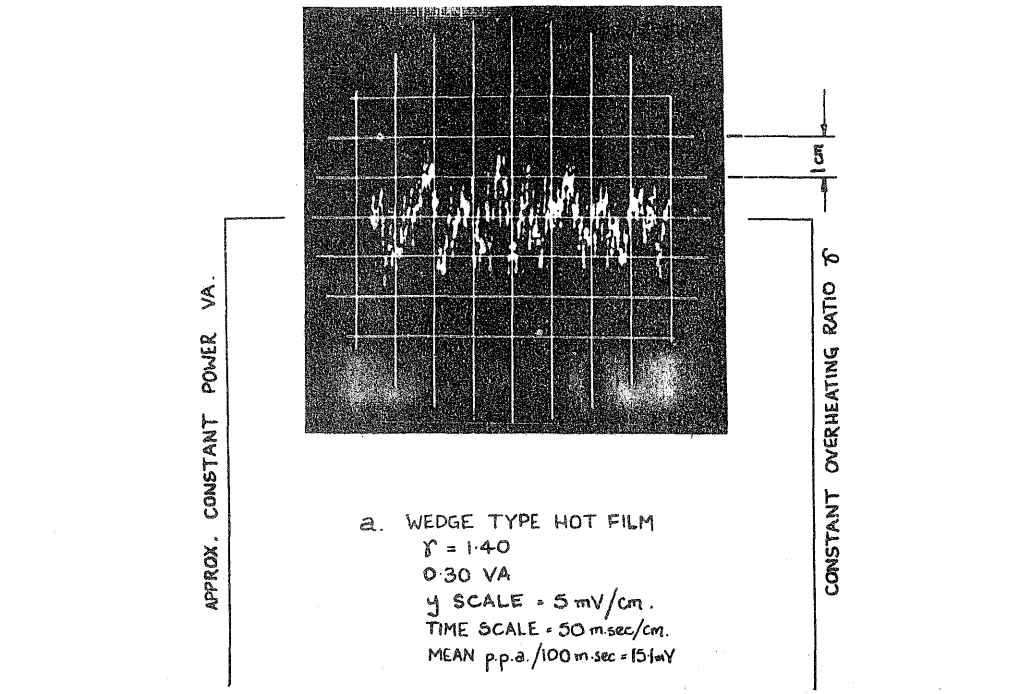

a. WEDGE TYPE HOT FILM
γ = 1·40
0·30 VA
y SCALE = 5 mV/cm.
TIME SCALE = 50 m.sec/cm.
MEAN p.p.a./100 m.sec = 15·1 mV

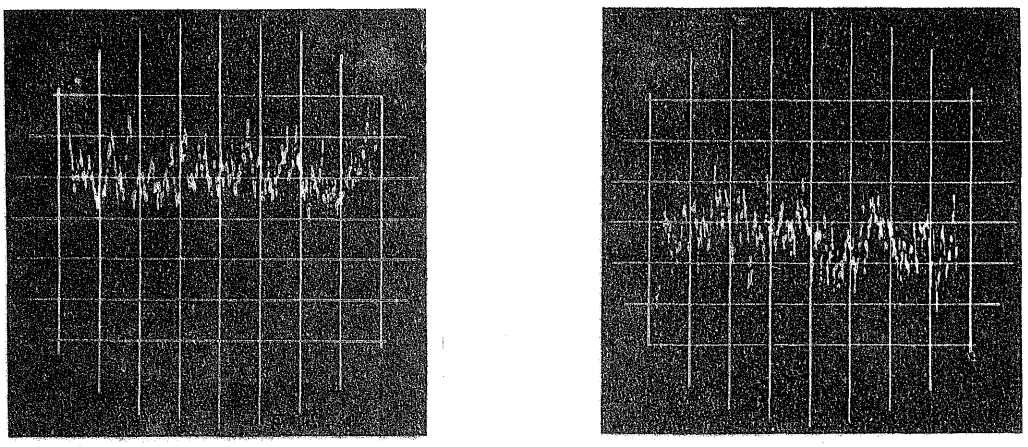

FLUSH TYPE HOT FILM

b. γ = 1·10
0·35 VA
y SCALE = 0·2 mV/cm
TIME SCALE = 50 m.sec/cm
MEAN p.p.a/100 m.sec = 0·46 mV

c. γ = 1·40
1·68 VA
y SCALE = 1 mV/cm
TIME SCALE = 50 m sec/cm.
MEAN p.p.a/100 m sec = 2·81 mV.

I (3) TYPICAL HOT FILM TRACES

APPENDIX II

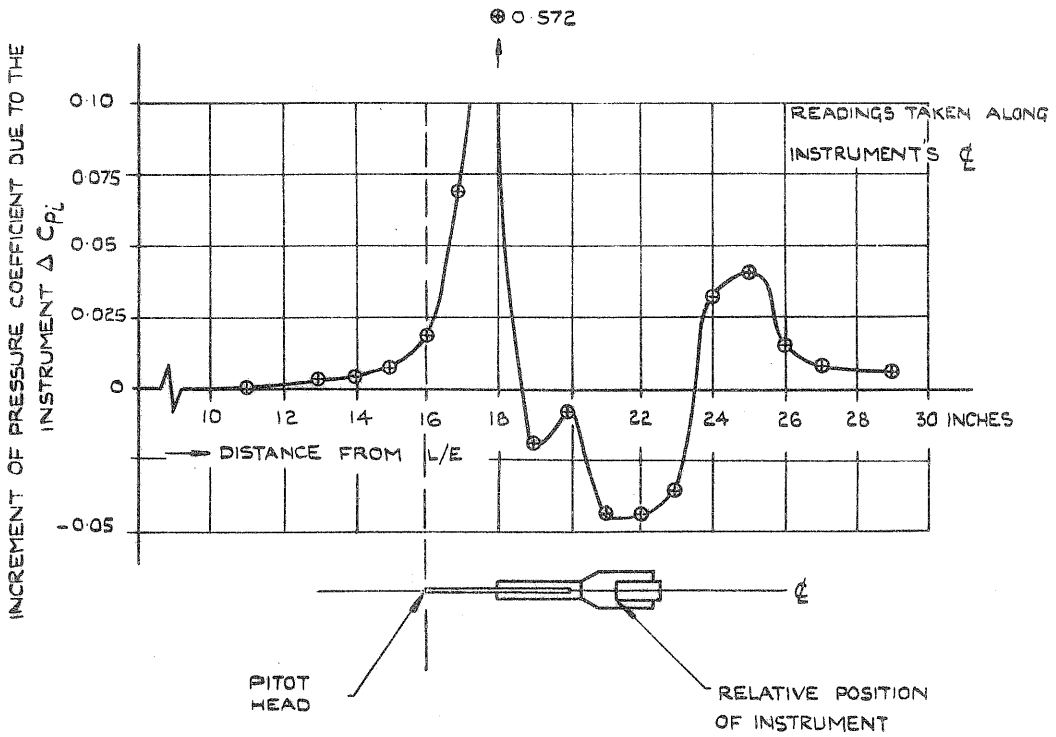

HALF SCALE MOCK-UP OF PITOT TRAVERSING INSTRUMENT MOUNTED ON AN AEROFOIL OF N.A.C.A. 0009 SECTION CHORD 40·0 INCHES

II (1) TRAVERSING PITOT PRESSURE FIELD